OPTIMIZATION OF OVERTOPPING TYPE WAVE ENERGY CONVERTERS ON EXISTING BREAKWATERS

A THESIS SUBMITTED TO
THE GRADUATE SCHOOL OF NATURAL AND APPLIED SCIENCES
OF
MIDDLE EAST TECHNICAL UNIVERSITY

BY

SERIM DOĞAÇ SAYAR

IN PARTIAL FULFILLMENT OF THE REQUIREMENTS
FOR
THE DEGREE OF MASTER OF SCIENCE
IN
CIVIL ENGINEERING

JULY 2022

Approval of the thesis:

OPTIMIZATION OF OVERTOPPING TYPE WAVE ENERGY CONVERTERS ON EXISTING BREAKWATERS

submitted by **SERİM DOĞAÇ SAYAR** in partial fulfillment of the requirements for the degree of **Master of Science** i**n Civil Engineering, Middle East Technical University** by,

Prof. Dr. Halil Kalıpçılar
Dean, Graduate School of **Natural and Applied Sciences** _____

Prof. Dr. Erdem Canbay
Head of the Department, **Civil Engineering** _____

Assist. Prof. Dr. Gülizar Özyurt Tarakcıoğlu
Supervisor, **Civil Engineering, METU** _____

Examining Committee Members:

Assist. Prof. Dr. Cüneyt Baykal
Civil Engineering, METU _____

Assist. Prof. Dr. Gülizar Özyurt Tarakcıoğlu
Civil Engineering, METU _____

Prof. Dr. Ahmet Cevdet Yalçıner
Civil Engineering, METU _____

Assoc. Prof. Dr. Elif Oğuz
Civil Engineering, METU _____

Assist. Prof. Dr. Doğan Kısacık
Civil Engineering, IZTECH _____

Date: 05.07.2022

I hereby declare that all information in this document has been obtained and presented in accordance with academic rules and ethical conduct. I also declare that, as required by these rules and conduct, I have fully cited and referenced all material and results that are not original to this work.

Name Last name : Serim Doğaç Sayar

Signature :

ABSTRACT

OPTIMIZATION OF OVERTOPPING TYPE WAVE ENERGY CONVERTERS ON EXISTING BREAKWATERS

Sayar, Serim Doğaç
Master of Science, Civil Engineering
Supervisor: Assist. Prof. Dr. Gülizar Özyurt Tarakcıoglu

July 2022, 121 pages

Global electricity generation today relies heavily on fossil fuels. Therefore, the need to create innovative and reliable technologies that can consistently generate clean and renewable electricity is of great importance. Generating electricity from wave energy has great potential although, the methods used to convert wave energy has limited applications in real life. Turkey surrounded by different wave conditions is a candidate for such applications. In the literature, there are various studies in which resource evaluation for wave energy is conducted for Turkey Seas. However, studies on WEC type selection, design performance as well as the applicability of such device is very limited. Thus, in this study, overtopping type WEC optimizations were performed for the breakwaters of the four pilot sites (mainly fisheries) on the Black Sea Coast of Turkey. In order to optimize the WECs in the breakwaters, wave analyzes were performed for selected sites along the Black Sea coast. Then, the dimensions that the overtopping type WECs would be most efficient were determined by the developed optimization algorithm. The energy that can be produced by the optimized WECs was determined and significant factors were

discussed affecting the energy production and WEC optimization processes for the selected sites.

Keywords: Wave Energy Converter, Breakwater, Black Sea, OBREC

ÖZ

AŞMA TİPİ DALGA ENERJİ DÖNÜŞTÜRÜCÜLERİNİN MEVCUT DALGAKIRANLARA OPTİMİZASYONU

Sayar, Serim Doğaç
Yüksek Lisans, İnşaat Mühendisliği
Tez Yöneticisi: Dr. Öğr. Üyesi Gülizar Özyurt Tarakcıoğlu

Temmuz 2022, 121 sayfa

Küresel elektik üretimi günümüzde büyük ölçüde fosil yakıtlara dayanmaktadır. Bu nedenle, sürekli olarak temiz ve yenilenebilir elektrik üretebilen yenilikçi ve güvenilir teknolojiler yaratma ihtiyacı büyük önem taşımaktadır. Dalga enerjisinden elektrik üretmek büyük bir potansiyele sahip olsa da dalga enerjisini dönüştürmek için kullanılan yöntemlerin gerçek hayatta uygulamaları sınırlıdır. Farklı dalga koşullarıyla çevrili Türkiye bu tür uygulamalara adaydır. Literatürde Türkiye Denizlerinde dalga enerjisi için kaynak değerlendirmesinin yapıldığı çeşitli çalışmalar bulunmaktadır. Ancak dalga enerji dönüştürücüsü (DED) tipi seçimi olan çalışmalar, tasarım performansı ve bu tür bir cihazın uygulanabilirliği için ise oldukça sınırlıdır. Bu nedenle, bu çalışmada, Türkiye'nin Karadeniz kıyısındaki dört pilot bölgenin (çoğunlukla balıkçı barınakları) dalgakıranları için aşma tipi DED optimizasyonları gerçekleştirilmiştir. Dalgakıranlardaki DED'leri optimize etmek için Karadeniz kıyısı boyunca seçilen bölgeler için dalga analizleri yapılmıştır. Daha sonra geliştirilen optimizasyon algoritması ile aşma tipi DED'lerin en verimli olacağı boyutlar belirlenmiştir. Optimize edilmiş DED'ler tarafından üretilebilecek enerji

belirlenmiş ve seçilen sahalar için enerji üretimi ve DED optimizasyon süreçlerini etkileyen önemli faktörler tartışılmıştır.

Anahtar Kelimeler: Dalga Enerji Dönüştürücüsü, Dalgakıran, Karadeniz, OBREC

To my father

ACKNOWLEDGMENTS

I would like to express my gratitude to my supervisor Assist. Prof. Dr. Gülizar Özyurt Tarakcıoğlu for her continuous support and advice. She always helped me during my thesis studies. She always solved the problems and shared her knowledge with me. This thesis was completed under favour of her guidance and support.

I would also express my appreciation to Prof Dr. Ahmet Cevdet Yalçıner for his support and encouragement on my future career as a mentor.

I would like to express my sincere thanks to Dr. Işıkhan Güler, Assist. Prof. Dr. Cüneyt Baykal, Dr. Hasan Gökhan Güler, Prof. Dr. Ayşen Ergin and Gözde Güney Doğan Bingöl for their guidance and supportive attitude.

I would like to state my sincere feelings to my precious wife, the one and only Gözde Yılmaz Sayar. She is my biggest supporter during all the times with her unconditional love.

I would like to express my gratitude to my mother Dürdane Sayar and my brother Mutlu Sayar. I would not be successful in my life without their lasting support.

I am very grateful to my father Yücel Sayar and I would like to honor his memory to always remember his endless support, encouragement for me, and his great personality.

I would like to thank Arda Çiçek, Akdeniz İnce, Barış Ufuk Şentürk, Berkay Akyol, Berkay Erler, Bilge Karakütük, Cem Sevindik, Egemen Ander Balas, Elif Ayşe Öztürk, Furkan Demir, Günay Gazaloğlu, for their sincere friendship and together having good time in the Coastal and Ocean Laboratory at METU.

My special thanks to Burak Kuyumcu for his perfect fellowship and his continuous support. I also wish to thank Ahmet Bedirhan Işık, Alperen Kuzu and Hasan Ödemiş

for their friendship, support during my hard times and the memories of lots of training sessions and tournaments.

I would also like to thank to Işıl Servetoğlu for supporting me all the times for many years.

I wish to thank Berke Ertuğrul, Can Güneş, Demirhan Sever, Halil Şibil, Nazlı Saltoğlu, Oğuzhan Yılmaz, Osman Karaoğlu, Satuk Buğrahan Sari and Yavuz Özden for their friendship and support in the METU Civil Engineering Department.

I would also like to thank Feyza Yavuz, Sahra Akgün, Suna Ekin Kali since they are more than teammates with their great friendship.

TABLE OF CONTENTS

ABSTRACT…… ……..v

ÖZ…….....vii

ACKNOWLEDGMENTS.....x

TABLE OF CONTENTS xii

LIST OF TABLES xiv

LIST OF FIGURES.....xvi

LIST OF ABBREVIATIONS xix

LIST OF SYMBOLS.....xx

1 INTRODUCTION.....1

2 LITERATURE REVIEW.....5

2.1 Information about Wave Energy 5

2.1.1 Wave Energy Potential of Turkey 6

2.1.2 Wave Energy Converter (WEC) Types.....10

2.2 Breakwater Integrated WECs.....17

2.2.1 Overtopping Type Breakwater Integrated WECs.....20

2.2.2 The Overtopping Breakwater for Energy Conversion (OBREC).....21

3 METHODOLOGY 31

3.1 Selection of Pilot Sites.....32

3.2 Wave Climate Study for SWAN Wave Model.....34

3.2.1 Nearshore Bathymetry at The Selected Sites 41

3.3 Overtopping Type WEC Optimization Algorithm.....41

4 RESULTS AND DISCUSSION.....51

4.1 Cayeli Fishery.....53

4.2 Cide Fishery 60
4.3 Amasra Port 67
4.4 Kiyikoy Fishery 76
5 CONCLUSION 83
REFERENCES 87
APPENDICES……95
A. Cayeli Small Domain, Wave Heights in SWAN Model Results 95
B. Cide Small Domain, Wave Heights in SWAN Model Results 99
C. Amasra Small Domain, Wave Heights in SWAN Model Results ...105
D. Kiyikoy Small Domain, Wave Heights in SWAN Model Results ..110
E. Cide Seasonal Wave Distribution 114
F. Overtopping WEC Design Algorithm 119

LIST OF TABLES

TABLES

Table 3.1 Properties of the Large Domains 37
Table 3.2 Properties of the Intermediate Domains 37
Table 3.3 Properties of the Small Domains 38
Table 4.1 Structural and Intensity Criterias for Cayeli Fishery (FCSSNAR,2011) 54
Table 4.2 Cayeli Wave Frequency Table (%) (East Directions) 55
Table 4.3 Cayeli Wave Frequency Table (%) (West Directions) 55
Table 4.4 Cayeli Wave Height at Deep Water and Toe of the Breakwater 57
Table 4.5 Cayeli Overtopping WEC Optimization and Energy Results 58
Table 4.6 Structural and Intensity Criteria for Cide Fishery (FCSSNAR,2011) 61
Table 4.7 Cide Wave Frequency Table (%) (East Directions) 62
Table 4.8 Cide Wave Frequency Table (%) (West Directions) 62
Table 4.9 Cide Wave Height at Deep Water and Toe of the Breakwater 63
Table 4.10 Cide Overtopping WEC Optimization and Energy Results 64
Table 4.11 Seasonal Energy Production of WEC Optimization for Cide Breakwater 67
Table 4.12 Structural and Intensity Criteria for Amasra Port (FCSSNAR,2011) ... 68
Table 4.13 Amasra Wave Frequency Table (%) (East Directions) 69
Table 4.14 Amasra Wave Frequency Table (%) (West Directions) 70
Table 4.15 Amasra Wave Height at Deep Water and Toe of the Breakwater 71
Table 4.16 Amasra Overtopping WEC Optimization and Energy Results 72
Table 4.17 Wave Height Values at the depths 7m, 9m and 12m at the Toe of Amasra Breakwater 74
Table 4.18 Energy Output at the Depths 7m, 9m, and 12m at the Toe of Amasra Breakwater 75
Table 4.19 Structural and Intensity Criteria for Kiyikoy Fishery (FCSSNAR,2011) 77
Table 4.20 Kiyikoy Wave Frequency Table (%) (East Directions) 78

Table 4.21 Kiyikoy Wave Frequency Table (%) (West Directions)..... 78
Table 4.22 Kiyikoy Wave Height at Deep Water and Toe of the Breakwater 79
Table 4.23 Kiyikoy Overtopping WEC Optimization and Energy Results 80
Table 4.24 Working Hours Percent and Annual Energy Production for Kiyikoy Breakwater WEC Optimization 82
Table E. 1 Wave Height Distribution in Winter Seasons for 16 Directions in Hours, Cide (East Directions)…….....114
Table E. 2 Wave Height Distribution in Winter Seasons for 16 Directions in Hours, Cide (West Directions) 115
Table E. 3 Wave Height Distribution in Spring Seasons for 16 Directions in Hours, Cide (East Directions)..... 115
Table E. 4 Wave Height Distribution in Spring Seasons for 16 Directions in Hours, Cide (West Directions) 116
Table E. 5 Wave Height Distribution in Summer Seasons for 16 Directions in Hours, Cide (East Directions) 116
Table E. 6 Wave Height Distribution in Summer Seasons for 16 Directions in Hours, Cide (West Directions)..... 117
Table E. 7 Wave Height Distribution in Fall Seasons for 16 Directions in Hours, Cide (East Directions)..... 117
Table E. 8 Wave Height Distribution in Fall Seasons for 16 Directions in Hours, Cide (West Directions) 118

LIST OF FIGURES

FIGURES

Figure 2.1 Maximum Significant Wave Height and Wave Period Distribution over 1979-2009 in Black Sea (Akpınar et al.,2016) 8
Figure 2.2 Spatial distribution of mean annual averaged wave power flux for all years based on 15-year SWAN hind cast results in the Black Sea (Akpinar & Komurcu, 2013) 8
Figure 2.3 Spatial distribution of mean annual averaged significant wave height for all years based on 15-year SWAN hind cast results in the Black Sea (Akpinar and Komurcu, 2013) 9
Figure 2.4 Classification of Wave Energy Converters according to Location and Working Principles of Primary and Secondary Conversion Systems (Wang et al., 2018) 11
Figure 2.5 Wave Power Representation according to the Location of the Wave Energy Converters (Blackledge et al., 2013) 12
Figure 2.6 The Working Principle of The Limpet, an OWC Type WEC (Harada, 2009) 13
Figure 2.7. The working principles of Point Absorber and Attenuator (Linear Absorber) WABs (Mohd Yusop et al., 2020) 14
Figure 2.8 The Working Principle of Overtopping WEC (Soares et.al., 2012) 15
Figure 2.9 Stages of Energy Conversion by WECs (López et al., 2013) 15
Figure 2.10 Pelton turbine, Kaplan turbine, and Francis Turbine, respectively, Hydro Turbines for WECs (Lopez et. al., 2013) 16
Figure 2.11 Overtopping Type WEC integration to a Rubble Mound Breakwater (Mustapa et al., 2017) 18
Figure 2.12 OWC Type WEC in Sakata Port (constructed as vertical caisson) (Vicinanza et al., 2014) 19
Figure 2.13 Mutriku Wave Power Plant, OWC type WEC integration to a Rubble Mound Breakwater (Villate, 2016) 20

Figure 2.14 Comparison of Dimensionless Average Overtopping Discharge Results of Experimental Tests and Numerical Simulation (Iuppa et al.,2018)..... 24
Figure 2.15 The Experimental, Numerical, and Theoretical Overtopping Results for Normal Wave Conditions (Palma, 2019)..... 25
Figure 2.16 Cross Sections of Two Different Geometric Configuration in OBREC (Contestabile et al., 2017). 27
Figure 2.17 OBREC Prototype Integrated in San Vincenzo Breakwater in Naples (Contestabile et al., 2017). 28
Figure 2.18 (a) The traditional rubble mound breakwater, (**b**) the OBREC physical model and (**c**) the OBREC numerical model (adapted from Vicinanza 2014) (Palma, 2019)..... 29
Figure 3.1 Flowchart for The Methodology of The Study..... 31
Figure 3.2 Pilot Sites in the Black Sea (Google Earth, 2022)..... 33
Figure 3.3 Kiyikoy Wave Data Points and Model Domains (Google Earth, 2022) 35
Figure 3.4 Amasra and Cide Wave Data Points and Model Domains (Google Earth, 2022) 35
Figure 3.5 Cayeli Wave Data Points and Model Domains (Google Earth, 2022) .. 36
Figure 3.6 Bathymetry of Kiyikoy in 3 Domains 39
Figure 3.7 Bathymetry of Amasra in 3 Domains..... 39
Figure 3.8 Bathymetry of Cide in 3 Domains..... 40
Figure 3.9 Bathymetry of Cayeli in 3 Domains..... 40
Figure 3.10 The Inputs, Equations and Outputs of Optimization Algorithm 43
Figure 3.11 The Flowchart of Optimization Algorithm..... 45
Figure 3.12 The cross-section of Optimized Overtopping WEC..... 46
Figure 3.13 Presentation of Overtopping Type WEC Integrated into a Rubble Mound Breakwater (Iuppa et al.,2016)..... 47
Figure 4.1 The Breakwater of Cayeli Fishery (Google Earth, 2022)..... 53
Figure 4.2 Efficiency Curve for Cayeli Breakwater Overtopping WEC Optimization 59
Figure 4.3 The Breakwater of Cide Fishery (Google Earth, 2022)..... 60

Figure 4.4 Efficiency Curve for Cide Breakwater Overtopping WEC Optimization 65
Figure 4.5 Seasonal Exceedance Probability for Cide Region 66
Figure 4.6 The Breakwater of Amasra Port (Google Earth, 2022) 68
Figure 4.7 Efficiency Curve for Amasra Breakwater Overtopping WEC Optimization 73
Figure 4.8 The Breakwater of Kiyikoy Fishery (Google Earth, 2022) 76
Figure 4.9 Efficiency Curve for Kiyikoy Breakwater Overtopping WEC Optimization 81
Figure A. 1 Cayeli Small Domain Model N direction 95
Figure A. 2 Cayeli Small Domain Model NNW Direction 96
Figure A. 3 Cayeli Small Domain Model NW Direction 97
Figure A. 4 Cayeli Small Domain Model WNW Direction 98
Figure B. 1 Cide Small Domain Model N Direction 99
Figure B. 2 Cide Small Domain Model NNW Direction 100
Figure B. 3 Cide Small Domain Model WNW Direction 101
Figure B. 4 Cide Small Domain Model W Direction 102
Figure B. 5 Cide Small Domain Model NNE Direction 103
Figure B. 6 Cide Small Domain Model NW Direction 104
Figure C. 1 Amasra Small Domain Model N Direction 105
Figure C. 2 Amasra Small Domain Model NNW Direction 106
Figure C. 3 Amasra Small Domain Model NNE Direction 107
Figure C. 4 Amasra Small Domain Model NW Direction 108
Figure C. 5 Amasra Small Domain Model NE Direction 109
Figure D. 1 Kiyikoy Small Domain Model E Direction 110
Figure D. 2 Kiyikoy Small Domain Model ENE Direction 111
Figure D. 3 Kiyikoy Small Domain Model NNE Direction 112
Figure D. 4 Kiyikoy Small Domain Model NE Direction 113

LIST OF ABBREVIATIONS

ABBREVIATIONS

CFSR : Climate Forecast System Reanalysis

DTM : Digital Terrain Model

EMODNET : European Marine Observation and Data Network

ERA – 5 : Fifth Generation ECMWF Atmospheric Reanalysis of the Global Climate

FCSSNAR : Fishery and Coastal Structures Situation and Needs Analysis Report

GW : Giga-watt

MW : Mega-watt

OBREC : The Overtopping Breakwater for Energy Conversion

OWC : Oscillating Water Column

PTO : Power Take Off

TW : Tera-watt

WAB : Wave Activated Bodies

WEC : Wave Energy Converter

Wh : Watt-Hour

LIST OF SYMBOLS

SYMBOLS

$P_{collected}$: Collected Wave Power

P_{wave} : Wave Power

B : Reservoir Width

E_{annual} : Annual Energy Production

f : Frequency of Waves

g : Gravitational Acceleration

h_1 : Reservoir Head

h_s : Water Column Inside The Pipe Above Turbine

Hs : Significant Wave Height

n_1 : Total Number of Calculated Rc Values

n_2 : Total Number of Wave Conditions

n_{gen} : Efficiency of Second Conversion

n_{hydro} : Hydrodynamic Efficiency

P_t : The Power of the Water Turbine

q : Overtopping Through Reservoir of Overtopping WEC

R_c : Reservoir Crest Height

s : Steepness

T : Wave Period

tan(α) : Slope of Front Face of the Optimized Overtopping WEC

γ_f : Influence Factor for Roughness Elements

γ_v : Influence Factor for Wave Wall

γ_β : Influence Factor for Oblique Wave Attack

CHAPTER 1

INTRODUCTION

Most of the electricity production in the world is still provided by fossil fuels. Therefore, new technologies that can produce clean and renewable electricity are becoming increasingly significant. According to the European Commission, sea waves have a great potential as renewable energy source. In this context, the demand for electrical energy generation from wave energy is increasing. However, wave energy has not yet reached a level of applicability that can compete with other renewable energy sources.

World energy demand in 2040 is expected to be roughly 30% greater than in 2010. Energy production will account for more than 40% of world energy consumption by 2040 (Exxonmobil, 2012). Gunn and Stock-Williams estimated the total global wave power potential occurring on ocean-facing coasts at about 2.1 TW, equivalent to 18500 TWh per year, almost 80% of world electricity consumption in 2018. Technically, wave energy generated by wave energy converters (WECs) is a huge resource that, if efficiently converted, could provide a significant portion of the world's electricity demand. However, electricity generation from wave energy is still negligible (Cabral et al., 2020).

Since its density (2–3 kW/m2) is larger than wind and solar energy, wave energy power is enormous and more predictable than some other renewable energy sources like solar and wind energy (0.4–0.6 kW/m2 for wind and 0.1–0.2 kW/m2 for solar) (Czech & Bauer, 2012). Other benefits of wave energy include the ability to move long distances with minimum energy loss, also the ability of wave energy converters to create electricity up to 90% of a year which is 20–30% for solar and wind power devices. Its predictive capacity is even significantly better than that of wind power.

Since roughly 37% of the world's population lives within 90 kilometers of the coastline, wave energy has a favorable correlation between supply and demand.

Wave energy converters are the device systems that transform wave energy into electrical energy. With such a large resource capacity, a variety of technologies for harvesting ocean energy have been invented Numerous types of WECs can be classified according to their location and working principles. One of the most studied types of WEC is overtopping type wave energy converter. Overtopping Breakwater for Energy Conversion (OBREC) is the first completely breakwater integrated overtopping wave energy converter in the world. The full-scale prototype was constructed in Naples Harbour, with a reservoir capable of capturing overtopping waves to generate power (Contestabile, 2016).

Several European nations have set out to create commercially operational wave energy conversion technologies in the medium to long future, as a result of numerous government and privately supported research initiatives. Turkey's coastline, excluding the Marmara area, is roughly 8210 kilometers long. Due to fishing, tourism, and other coastal operations, about 1/5 of all this can be used for energy production. The wave energy potential given by this proportion of Turkish coastlines is projected to be 18.5 billion kWh. This accounts for around a third of Turkey's total energy consumption (Keskin Citiroglu & Okur, 2014).

Along the Turkish seas, the Black Sea shoreline is the most energetic location in terms of wave climate. Because Turkish shores are highly inhabited, wave power generators could be positioned where electricity is used when wave energy generation becomes common in Turkey. This would result in significant reductions in energy transmission expenses. The regional electrical system can be interconnected to wave generation facilities. Although numerous studies were conducted about deep water wave energy resource assessment and WEC site selection. There is not any breakwater integrated WEC optimization study for the Black Sea Coasts of Turkey in the literature.

This thesis study researches the optimization and demonstration of OBREC type wave energy converters into the existing breakwaters by conducting a wave model and an optimization tool. The wave transformation model was used to provide nearshore wave characteristics in front of the selected breakwaters by using wave data from deep water regions. Then, the optimization of overtopping WEC and energy outputs were obtained by the optimization tool. Through this research process, the thesis answers the research question "How does efficiency and optimization of overtopping type wave energy converters to the existing breakwaters in the Black Sea coast of Turkey is affected by marine and structural conditions of the breakwater based on 4 cases? " by investigating the optimized cases and discussing the energy outputs.

In chapter two, information is provided about global and regional wave energy, wave energy converter types and their working principles, optimization of overtopping type wave energy converters, and site selection criteria for targeted breakwaters. This literature review shows the effective variables and the availability of breakwaters for the optimization of overtopping type WECs.

In chapter three, the method of the study is explained with criteria for the selection of breakwaters, nearshore wave characteristics modeling, and optimization algorithm of OBREC type WECs. The bathymetry and wave data used in the study are included in this chapter.

In chapter four, results of the optimization algorithm, optimized section for overtopping WEC optimization and the theoretical energy produced for selected breakwaters are presented in the Black Sea Coast of Turkey. Finally, the significant factors for the optimization of OBREC section are discussed using site specific wave information. Lastly, the conclusions, limitations, and possible further studies are mentioned in chapter five.

CHAPTER 2

LITERATURE REVIEW

2.1 Information about Wave Energy

Scientific research on wave energy has been done since the 1970s, and the presentation of the very first energy conversion systems began in the mid-1980s with test on numerous prototypes being performed in the ocean with the number of prototypes growing significantly in the past decade. It can be currently stated that wave energy is in the pre-commercial stage, and significant work is being done to assess the wave energy potential and characterize this major renewable energy resource in great depth.

The sources of wave energy can be characterized in a variety of ways. The theoretical source is the first and foremost the real hydrodynamic power inherent in ocean waves. In the early stages, Isaacs and Seymour (1973) estimated the worldwide wave power potential to be on the scale of 1-10 TW, which was close to the same amount as global electrical energy use.

The idea of using the waves to generate electricity started at early times. As early as 1799, a patent for a wave energy converter (WEC) was submitted, and by the late 20th century, there were hundreds of trademarks covering this technology (Aderinto & Li, 2018). When Masuda employed ocean waves to power navigation buoys, it was the first time that wave energy had been exploited in a practical way. The oil crises of 1973 contributed to a new era in wave energy technology because they made governments and policymakers more conscious of the temporal and geographical characteristics of fossil fuel deposits. Authorities and intergovernmental organizations, therefore, led many research and innovation

projects. The fact that fossil fuels, particularly those derived from petroleum, are considered as a contributor to global warming as well as other negative environmental consequences by releasing harmful gases like carbon dioxide into the atmosphere (Aderinto & Li, 2018).

The intensity and consistency of wind velocity are strongly connected to the energy profile of a wave, taking into consideration the scale of the effective fetch distance where the wind blows from. The most appealing locations in terms of energy are located between 30 and 60 degrees' latitude in both hemispheres, with an overall energy source of roughly 32000 TWh/yr (Edenhofer et al., 2011).

The productivity of wave energy conversion is not sufficiently high yet. Thus, forecasting the development of the wave energy sector is difficult because; the chances are growing as technology advances. By 2050, effective wave technological advancement in the European wave sector might provide 188 GW which is 10 of Europe's power demands (Wave Roller, 2020). This would need the effective construction and operation of new and more developed systems. Existing projects' research has produced information on how to reduce the price of upcoming wave innovations. Developments in the next phase of wave technologies may cut the price of power take-off by 22%, construction cost by 18%, operation and maintenance costs by 17%, foundation and mooring cost by 6%, and grid connection cost by 5% (Ocean Energy Europe, 2017).

2.1.1 Wave Energy Potential of Turkey

Turkey is a country surrounded by seas on three sides and provides the majority of its electricity generation from fossil fuel sources. It is important to use renewable energy technologies in Turkey in line with the goals of reducing foreign dependency on energy production and use and reducing carbon dioxide emissions in energy production. Therefore, wave energy is of great significance for energy production in Turkey in the near future because Turkey has a wave energy potential of total 10TWh

per year and the best places envisioned for generating wave energy are: the west of the Black Sea, the north of the Bosphorus and the southwest coast of the Aegean Sea. It is considered that these waters are suitable for initial trials according to Altas and Sahin (2019). Also, According to Uygur et al (2006), the amount of wave energy that can be produced technically by using one-fifth of Turkey's coastline is 18.5 TWh. Furthermore, in the Black Sea Coasts of Turkey, the wave energy potential is significantly higher with respect to the Aegean and Mediterranean Coasts of Turkey as mentioned in the same study. Furthermore, Bozgeyik's (2019) study was conducted to identify appropriate sites for WECs in Turkey's coastal areas using a combination of expert and researcher-recognized criteria. In this study, the wave energy potential of Turkish Coasts was evaluated, wave energy potential of the Western Black Sea is considered that it has the greatest wave energy potential along Black Sea, and Mediterranean Sea Coasts of Turkey. Thus, the focus area of this thesis study is specified as the Black Sea Region.

Scientific studies have been carried out to investigate the wave energy potential of the Black Sea Region. Wave energy potential was investigated based on the 15-year numerical data of the Black Sea in Akpinar and Komurcu (2013). It has been determined that the western regions of the Black Sea have more energetic waves than the eastern regions. In addition, the annual average wave energy source is determined as up to 3 kW/m in the southwest of the Black Sea. In Figure 2.1, maximum wave heights during 1979-2009 in the Black Sea concerning the wave model and study conducted by Akpınar et al. (2016) and in Figure 2.2, the spatial distribution of yearly mean averaged wave power flux based on 15-year SWAN hind cast results in the Black Sea is presented by Akpinar and Komurcu (2013) are given.

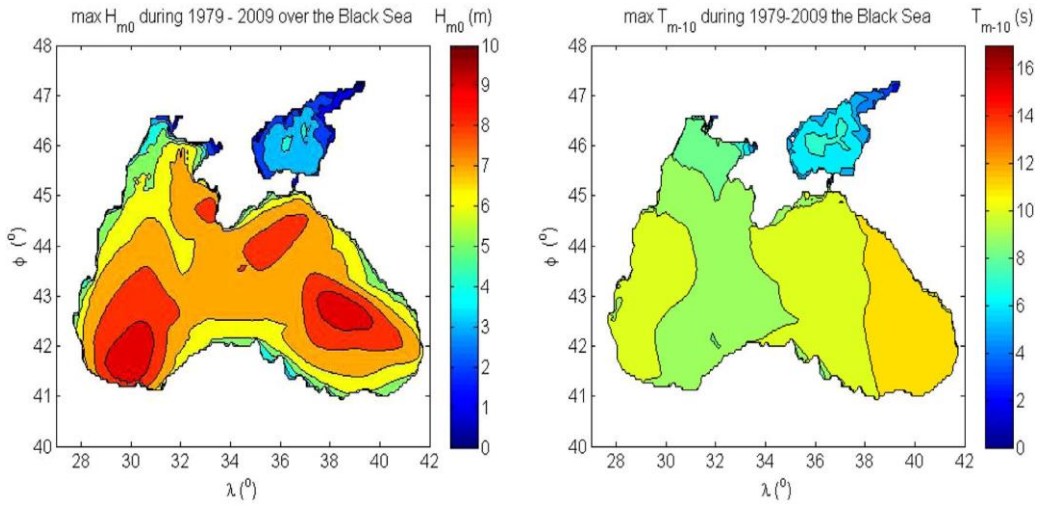

Figure 2.1 Maximum Significant Wave Height and Wave Period Distribution over 1979-2009 in Black Sea (Akpınar et al.,2016)

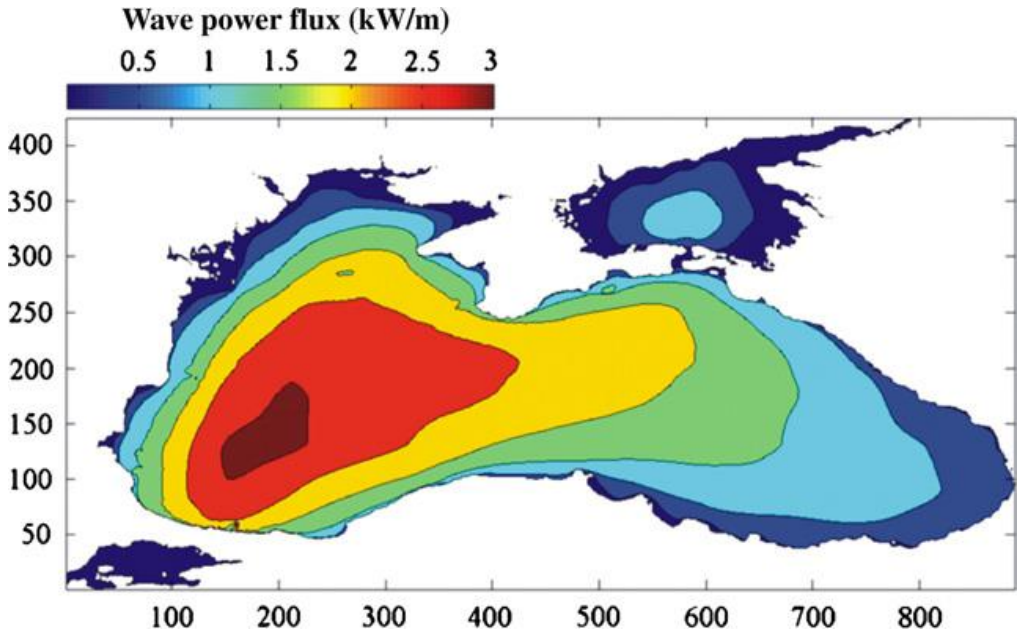

Figure 2.2 Spatial distribution of mean annual averaged wave power flux for all years based on 15-year SWAN hind cast results in the Black Sea (Akpinar & Komurcu, 2013)

In the study conducted by Aydogan et al. (2013). 13 years of wind data belonging to the Black Sea Region were analyzed with the 3rd generation spectral wave model

and it was determined that the wave energy potential is higher in the west part of the Black Sea coasts of Turkey rather than the east part. According to this study, the largest average wave power in the Southwest part of the Black Sea is about 7 kW/m and the average wave power is about 3 kW/m in the eastern part. According to the study conducted by Akpinar and Komurcu (2012), the wave energy potential of the southeast coast of the Black Sea is given. In this study, Sinop was the province with the highest wave power flux of 10 MWh/m. It is stated that the annual wave energy potential of other coastline provinces (Samsun, Ordu, Giresun, Trabzon, Rize, and Hopa) is about 6 MWh/m and this potential is formed by waves with significant wave heights of 0.5-2 m and wave periods of 2-5 s.

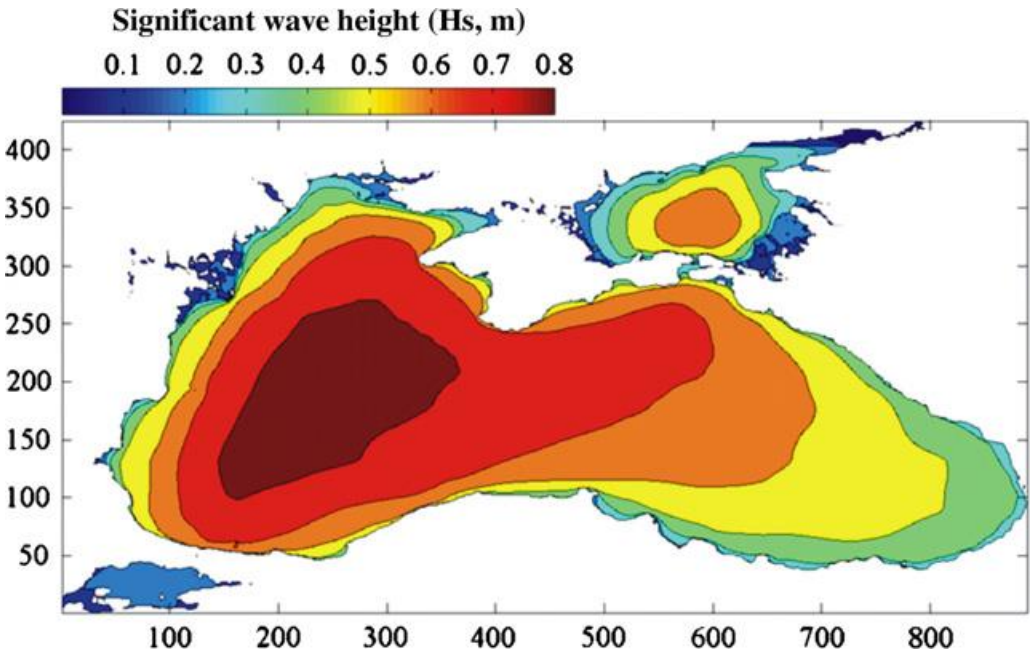

Figure 2.3 Spatial distribution of mean annual averaged significant wave height for all years based on 15-year SWAN hind cast results in the Black Sea (Akpinar and Komurcu, 2013)

The Black Sea coasts of Turkey have a high average significant wave height which is key for an overtopping type of WEC optimization as seen in Figure 2.2. In the study, when the average significant wave heights values in the West and Middle

Black Sea are close to each other, it is a little lower in the East Black Sea Coasts. However, all of the Turkey coastlines are appropriate for the several types of wave energy converters including the overtopping type.

All the mentioned studies were conducted for deep-sea regions in Turkey to evaluate the wave energy in deep water in the coasts of Turkey. The wave energy potential in the Black Sea was investigated for offshore areas in previous studies. However, in this thesis study, a nearshore breakwater integrated WEC optimization is performed distinctly.

2.1.2 Wave Energy Converter (WEC) Types

WECs can be classified in a variety of ways. However, main classifications are performed based on the location of WEC and working principles of wave capture systems and Power Takeoff Systems. The classification scheme of the wave energy converters which is followed in this study is given in Figure 2.4.

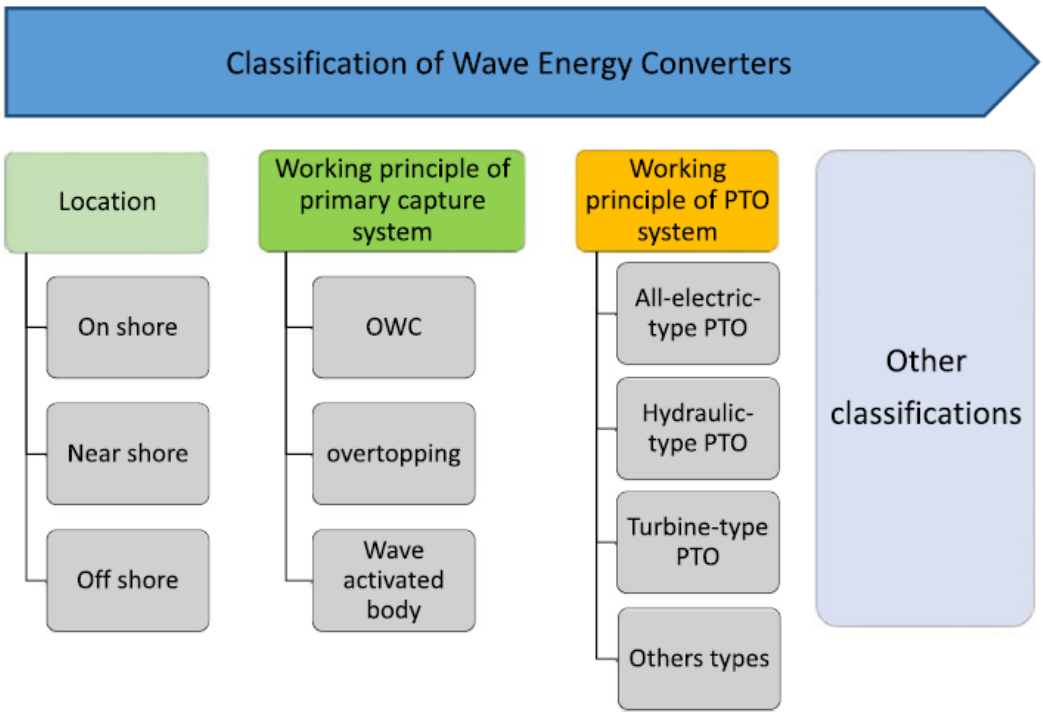

Figure 2.4 Classification of Wave Energy Converters according to Location and Working Principles of Primary and Secondary Conversion Systems (Wang et al., 2018)

2.1.2.1 According to Location

Onshore converters offer the advantages of becoming close to the power grid, being simple to maintain, and having a lower risk of being destroyed in storm conditions since waves are weakened as they travel over shallow water. Another of the drawbacks of onshore devices is that shallow water results in lesser wave power (Sorensen, 2011).

Nearshore converters are those which are located in or close to shallow water. Nearshore converters are frequently anchored to the seafloor, providing a stable basis for an oscillating device to be able to operate. A problem, similar to onshore devices, seems to be that shallow water causes weaker waves, reducing the amount of harvestable energy.

The majority of the offshore converters are located in deep water. The benefit of putting the device in deep water is that it can gather more energy since deep ocean waves have a larger energy output. Offshore WECs, on the other hand, are harder to build and operate and they must be constructed to withstand more extreme circumstances due to the higher wave height in the waves, contributing to the expense of installation. Although the challenges of deep water, it is believed that floating WECs in deep water could have higher efficiency with higher waves (Korde, 2000). Representation of the wave power according to the location of the wave energy converters is shown in the Figure 2.5. The maximum, average and exploitable wave energy amounts are compared among onshore, nearshore and offshore areas in the study performed by Blackledge et al. (2013).

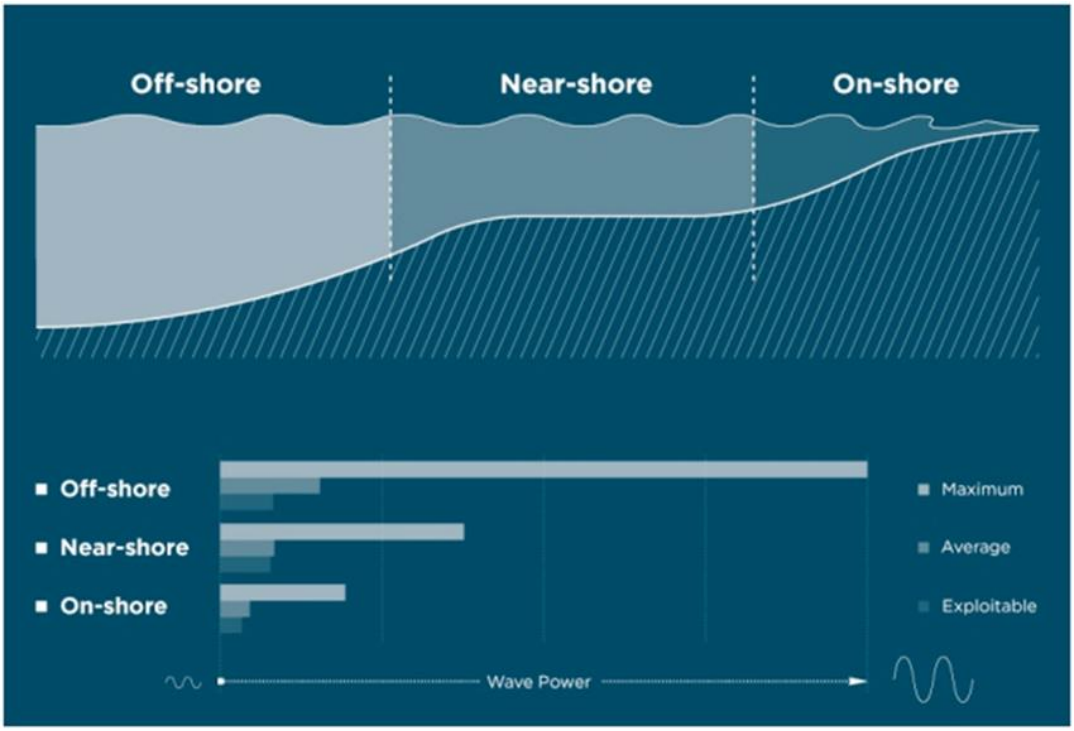

Figure 2.5 Wave Power Representation according to the Location of the Wave Energy Converters (Blackledge et al., 2013)

2.1.2.2 According to Primary Conversion System

WECs may be grouped into three types based on the operating concept of the primary conversion system. These three types are oscillating-water columns (OWC), wave-activated bodies (WAB) and overtopping WEC (Sarmento &Falcão, 1985).

An OWC is a chamber having an entrance to the sea below the water surface. Water is driven into the chamber when waves hit the device, exerting pressure on the air inside the chamber. Using a turbine, the air is released into the atmosphere. The air is pulled in through the turbine when the water fades away. A low-pressure Wells turbines are commonly applied in this operation since they rotate in the same orientation regardless of inflow (Drew et al., 2009).

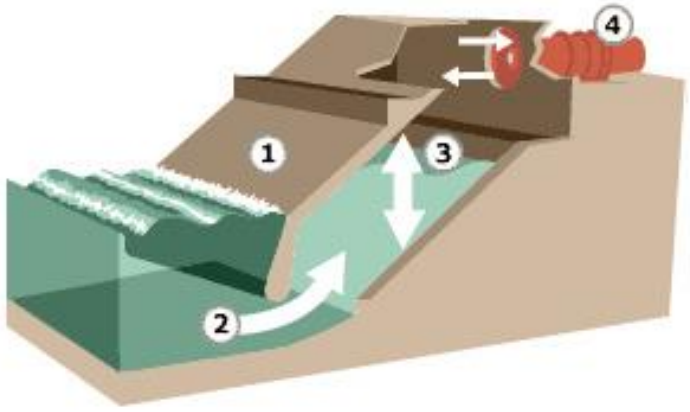

1. Wave capture chamber set into rock face
2. Tidal power forces water into chamber
3. Air alternately compresssed and decompressed by "oscillating water column"
4. Rushes of air drive the Wells Turbine, creating power

Figure 2.6 The Working Principle of The Limpet, an OWC Type WEC (Harada, 2009)

Wave Activated Body WECs could be categorized as point absorbers, attenuators, or terminators according to the absorber size and its relationship to the incident

wave's direction. A point absorber is an absorber that is significantly shorter compared to the wavelength. The WEC is called a terminator if the major wave propagation orientation is perpendicular to the structural extension of the WEC. Whereas, attenuators are lengthy devices similar to terminators, but their long parts are parallel to the direction of waves (Wang et al., 2018).

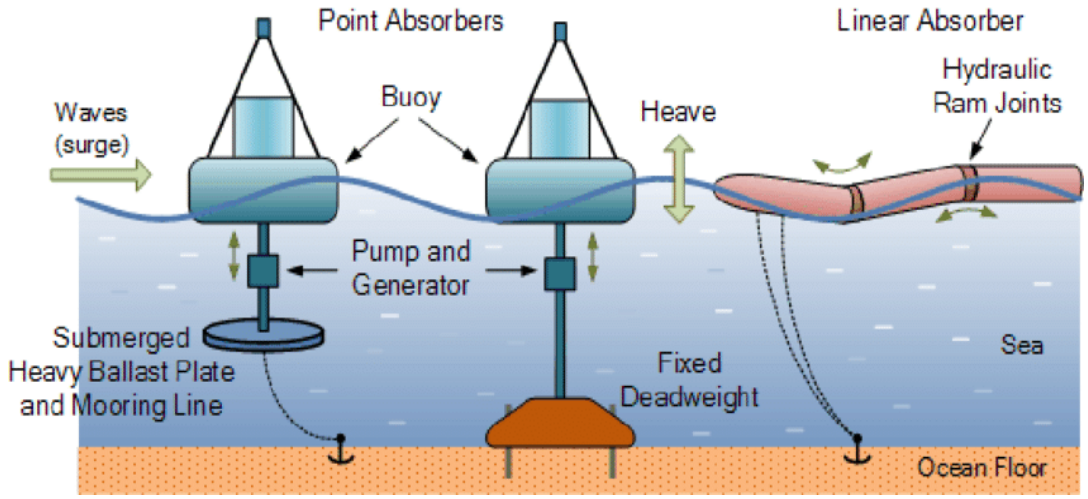

Figure 2.7. The working principles of Point Absorber and Attenuator (Linear Absorber) WABs (Mohd Yusop et al., 2020)

The working principle of Overtopping WECs is capturing the water from incoming waves. The waves overtop the WEC's surface and are accumulated in the reservoir of the WEC above sea level. Then, the water is released to the ocean from the reservoir using low head turbines to generate energy. Thus, overtopping devices primarily utilize well-organized systems which lower the improvement risks and costs; the only moving parts are the turbines, and any other components do not move with the waves. This working method reduces failure risks, as well as the structural and mooring requirements. They're easy to scale and don't require any re-calibration (Soares et.al., 2012).

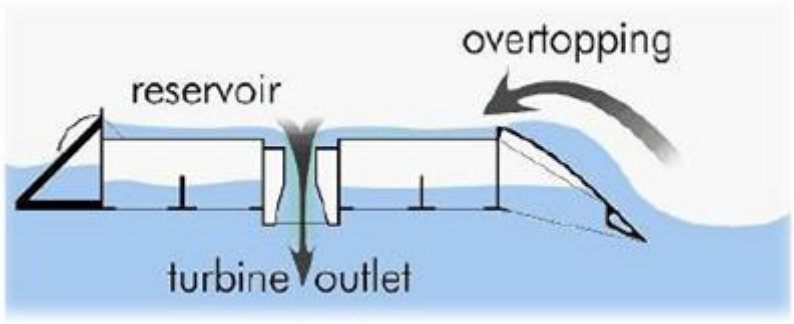

Figure 2.8 The Working Principle of Overtopping WEC (Soares et.al., 2012)

2.1.2.3 According to Secondary Conversion System

The secondary conversion step includes converting energy from the fluid created during the first conversion into usable energy. Three types of turbines are utilized for this process which are air turbines, hydraulic turbines, and hydraulic motors. In addition, direct conversion is another method that includes both primary and secondary conversions.

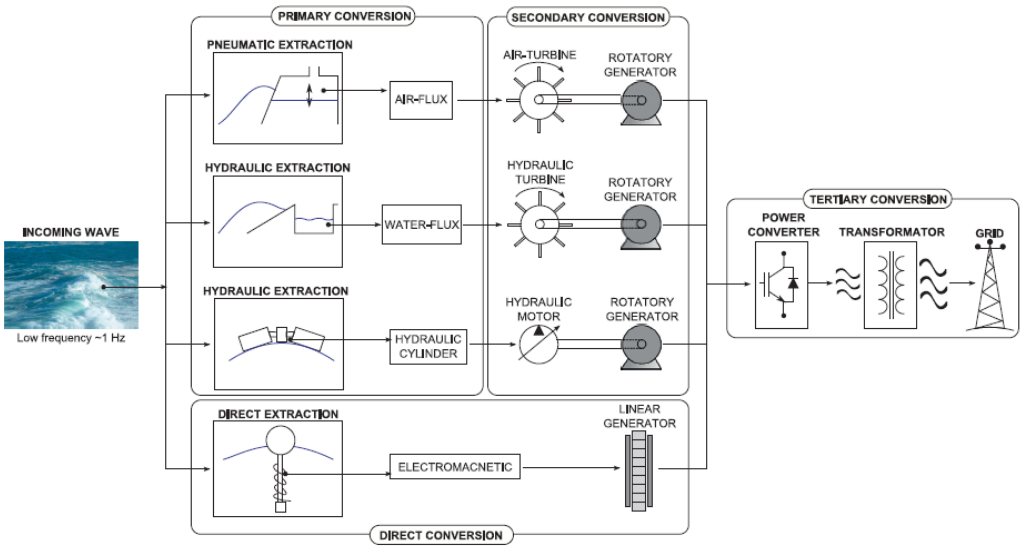

Figure 2.9 Stages of Energy Conversion by WECs (López et al., 2013)

Air and hydraulic turbines refer to systems in which a turbine is driven by the movement of air or water and is connected to a generator. The usage of seawater turbines has the substantial benefit of not causing any ecological issues due to fluid escape. Seawater, on the other hand, is a complicated fluid with a variety of unexpected elements. Particles might also harm seals and valves in onshore equipment. If the turbine is in shallow water, cavitation might be a concern due to positive pressure (Drew et al., 2009).

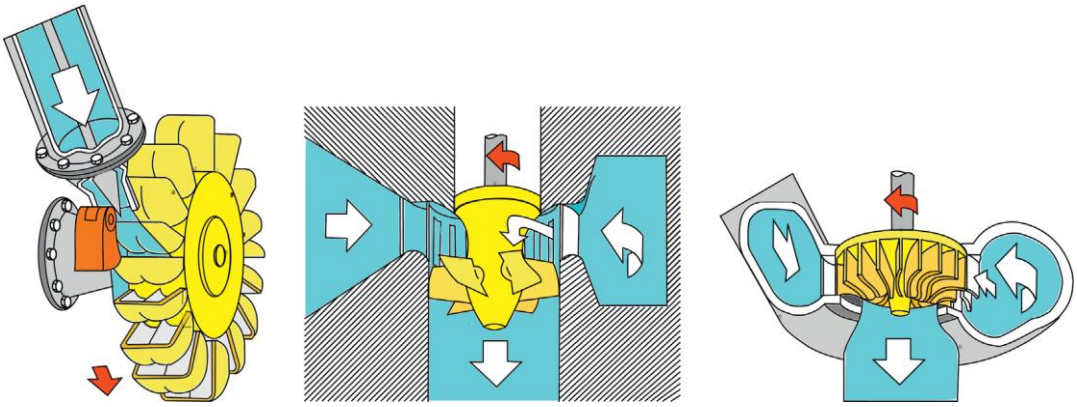

Figure 2.10 Pelton turbine, Kaplan turbine, and Francis Turbine, respectively, Hydro Turbines for WECs (Lopez et. al., 2013)

Fan-type turbines are frequently utilized in low-pressure circumstances, as seen in overtopping devices like OBREC. The benefit of using air as the fluid is that it allows you to convert slower wave velocities into a higher airflow rate. The most common air turbine design is the Wells turbine since it has the capability to operate in the same orientation regardless of airflow. Therefore, Wells turbines are utilized in Limpet Oscillating Water Column Type WECs (The Queen's University of Belfast, 2002).

The use of hydraulic cylinders is also another way to transform energy. Slow oscillating devices, such as Aquabuoy, commonly employ these techniques. A series of hydraulic cylinders convert body movement to hydraulic energy. A conventional electrical generator is used to transform hydrodynamic energy into electrical energy, which is powered by a rapid hydraulic motor. There among the motor and the

cylinder, there is normally an oil or gas storage system used to store energy across some wave periods to maintain a consistent inflow to the hydraulic motor to provide consistent output power (Falcao, 2010).

A linear generator's simple concept is to provide a translator about interchanging polarity magnets are attached vertically combined to a heaving buoy, with the stator containing windings attached in a relatively stationary structural system which is generally fixed to the sea bottom (Drew et al., 2009).

The last step of the energy conversion, tertiary conversion is where the energy is transformed into the required signals that are transmitted to the grid. Power electronics converters with diverse designs that were conceived and built for particular applications are employed at this level. This technique is significant since it may be used in a wide variety of systems. Tertiary conversion offers the interaction between the wave energy system and the grid for WECs (Prasad et al., 2022).

2.2 Breakwater Integrated WECs

WECs placed in breakwaters are going to provide a renewable resource especially in the coastal regions, helping to reduce pollution levels. The innovative system might possibly offer a feasible alternative to fossil fuels.

Several types of WECs are appropriate to be integrated with the coastal structures. The structure of the breakwater and WEC can cause some physical or technical limitations. Therefore the structural properties of the breakwaters are crucial for the integration of WECs.

As a result, breakwater integrated WECs require a design optimization in order to operate in various wave climates.

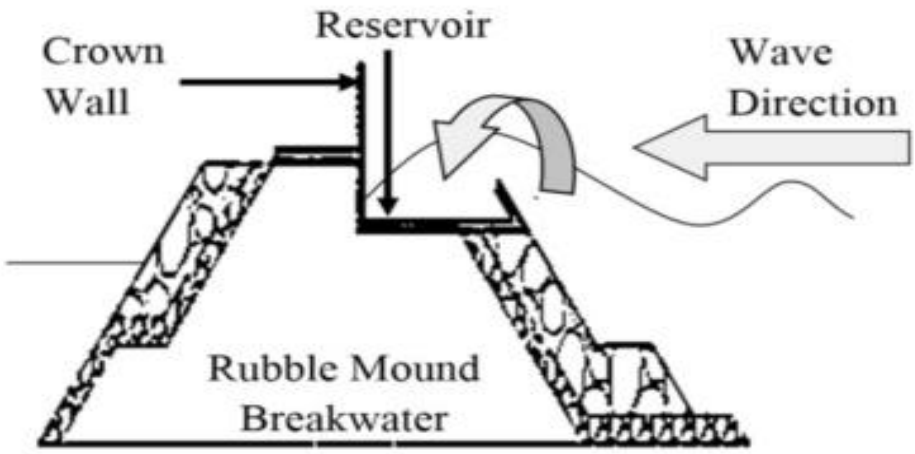

Figure 2.11 Overtopping Type WEC integration to a Rubble Mound Breakwater (Mustapa et al., 2017)

Because the Oscillating Water Column type WECs have a box-like front part to use air pressure caused by the waves, they are more convenient for the integration to vertical caisson type breakwaters. An example of this kind of an OWC WECs is given in the Figure 2.12. However, there is an application of OWC type WEC integration to a rubble mound breakwater in Mitruki Power Plant which is the only breakwater integrated WEC in commercial use as can be seen in Figure 2.13.

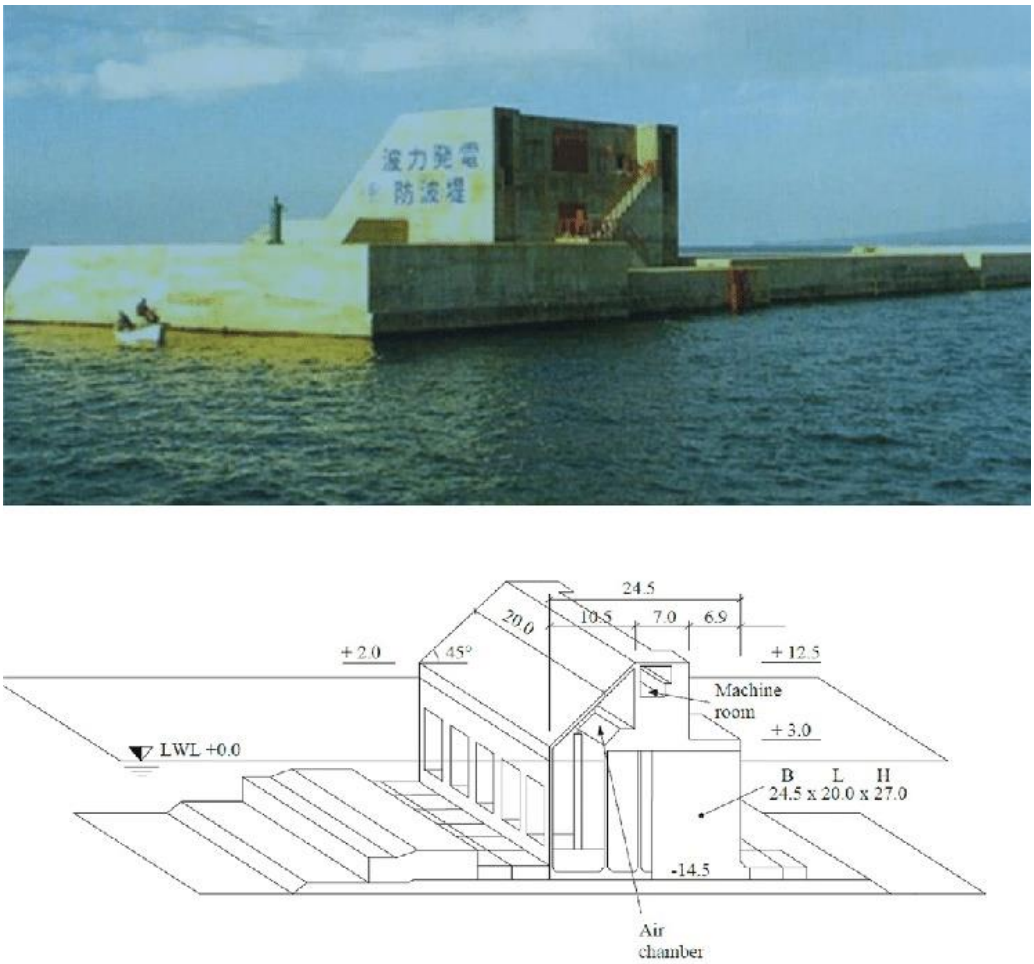

Figure 2.12 OWC Type WEC in Sakata Port (constructed as vertical caisson) (Vicinanza et al., 2014)

Figure 2.13 Mutriku Wave Power Plant, OWC type WEC integration to a Rubble Mound Breakwater (Villate, 2016)

2.2.1 Overtopping Type Breakwater Integrated WECs

Overtopping WECs feature several benefits that set them apart from other type wave energy converters. To begin with, the electricity generated by these WECs has very minimal variations since the transformation occurs in steady conditions in the storage in which the water is initially held. As a result, putting these converters in place is linked to a better degree of financial viability. It is feasible to integrate them with other constructions in coasts, like traditional breakwaters. Furthermore, because calm circumstances have been maintained behind the breakwater integrated WECs, this region may be used to expand some activities such as fisheries. In addition, while generating energy, the water released through the turbines could be recycled back to enhance the aquatic environment. Moreover, the use of a ramp that concentrates

water into the reservoir allows the water to overtop the slope and accumulate in the reservoir even in unpreferable coastal zones with low wave energy potential (Bevilacqua & Zanuttigh, 2011).

Overtopping type WECs optimization is appropriate for rubble mound breakwaters since an inclined surface is needed for waves to rise on it. The front surface of the rubble mound breakwater is essential for the water to accumulate in the reservoir to produce energy. The roughness and slope of the front slope of the breakwater are also significant since they affect the water volume collected in the reservoir.

The design for the optimization is also able to change some dimensional characteristics of the front slope and some other dimensional properties of the breakwater.

2.2.2 The Overtopping Breakwater for Energy Conversion (OBREC)

The Overtopping Breakwater for Energy Conversion (OBREC) is the world's first overtopping wave energy converter that is totally breakwater integrated. In Naples Harbour, a full-scale prototype was built with a reservoir capable of capturing overtopping waves and generating electricity. OBREC is put on the existing breakwater substituting section of the rubble mound front layer. The overtopping waves are channeled into a pool by a specifically built concrete structure with a steep impervious front slope. Low-head turbines are used to collect energy from the difference in water levels between the reservoir level and sea level (Contestabile, 2016).

OBREC is primarily distinguished by simpler and less expensive operation and maintenance costs. No movable components are used for the first conversion system. The only moving components in the system are the turbine shaft and the flow-controlling gates. The device is economically more feasible than offshore floating WECs because of the infrastructure sharing and the resulting decrease in building costs. Furthermore, A significant wave overtopping decrease for a rubble mound

structure with a front reservoir was verified by Burchart and Andersen (2006). The authors also showed that structures with a front reservoir are more advantageous than traditional rubble mound cross sections, such as beamed and mild slope structures, in terms of efficiency and cost (Contestabile et.al., 2019). However, offshore WECs generally produce more energy than onshore devices like OBREC type structures because of wave height decrease in shallow water region due to wave shoaling effect.

2.2.2.1 Optimization of OBREC

For the OBREC's preliminary design two test sessions were conducted in 2012 and 2014 . Tests performed in 2012 on a 2D model size were intended to determine how the OBREC differed from a standard breakwater and to comprehend the device's hydraulic and structural response to various wave situations. According to the tests Vicinanza (2014) mentions, 48 experiments were done as part of the experimental program under both extreme wave conditions with a 100-year return period and average wave conditions by taking into account the Mediterranean wave environment, the integration of the OBREC into the conventional breakwater frequently enhances the hydraulic performance, according to the results of this laboratory testing campaign. As the results of the tests, overtopping at the rear side of the breakwaters is decreased, and reflection coefficients are nearly equivalent to or lower than those measured for the conventional breakwaters because of the inclined ramp and the wave energy absorption into the reservoir.

In the laboratory tests conducted in 2014 (as mentioned in the study of Contestabile, 2019), the loadings impacted on by the wave effect on the different OBREC components were then taken into consideration in order to thoroughly analyze the difference between the flat and curved ramps. According to the tests, the device with the curved frontal ramp had an overtopping discharge that was around 20% less. As a result, the curved ramp produced less energy stored for OBREC. According to measurements made in all the experiments conducted, the lower slope on the upper

part of the curved ramp compared to the flat one signified a considerable load reduction of between 30 and 40 percent.

After the breakwater stability was assured in terms of overtopping, reflection and wave impact forces and flat and curved ramps were tested when the OBREC integrated into a conventional rubble mound breakwater in the experimental tests, the productivity and overtopping tests of OBREC was investigated.

In the study Iuppa (2018), both the experimental tests and numerical simulation study were performed and the reservoir overtopping results for OBREC optimization were compared which is one of the most important parameter for the efficiency of OBREC. The method suggested in Eurotop Manual (2007) for surging or nonbreaking waves on steep slope which are given in Eqn 2.1 and other methods were used in this study. The results of Eurotop Manual (2017) method are evaluated as coherent with the experimental results. The comparison of experimental test results and numerical test results for the methods are given in Figure 2.14.

$$\frac{q}{\sqrt{g * Hs^3}} = 0.2 * \exp\left(-2.6 \frac{Rc}{Hs * \gamma f * \gamma \beta * \gamma v}\right) \qquad Eqn\ 2.1$$

where;

g : Gravitational Acceleration

Hs : Significant Wave Height

q : Overtopping Volume Through Reservoir of Overtopping WEC

R_c : Reservoir Crest Height

γ_f : Influence Factor for Roughness Elements

γ_v : Influence Factor for Wave Wall

γ_β : Influence Factor for Oblique Wave Attack

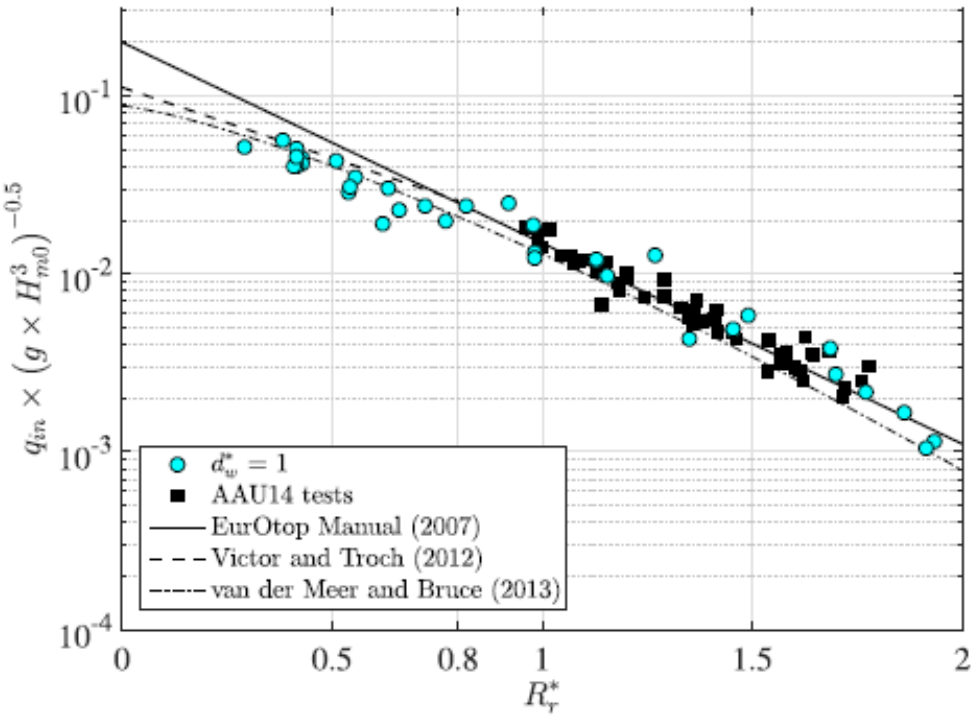

Figure 2.14 Comparison of Dimensionless Average Overtopping Discharge Results of Experimental Tests and Numerical Simulation (Iuppa et al.,2018)

Palma (2019) study also conducted the experiments and numerical study for the comparison of overtopping volumes and wave forces exerted on OBREC. The Eurotop Manual (2016) method for the slopes such as dikes are also compared with the results which is given in Eqn 2.2 and the comparison of overtopping volumes are given in Figure 2.15. The Eurotop Manual (2016) method is also evaluated as consistent with a slight underestimation in overtopping.

$$\frac{q}{\sqrt{g * Hs^3}} = 0.09 * \exp(-\left(1.5 \frac{Rc}{Hs * \gamma f * \gamma \beta * \gamma v}\right)^{1.2} \qquad \text{Eqn 2.2}$$

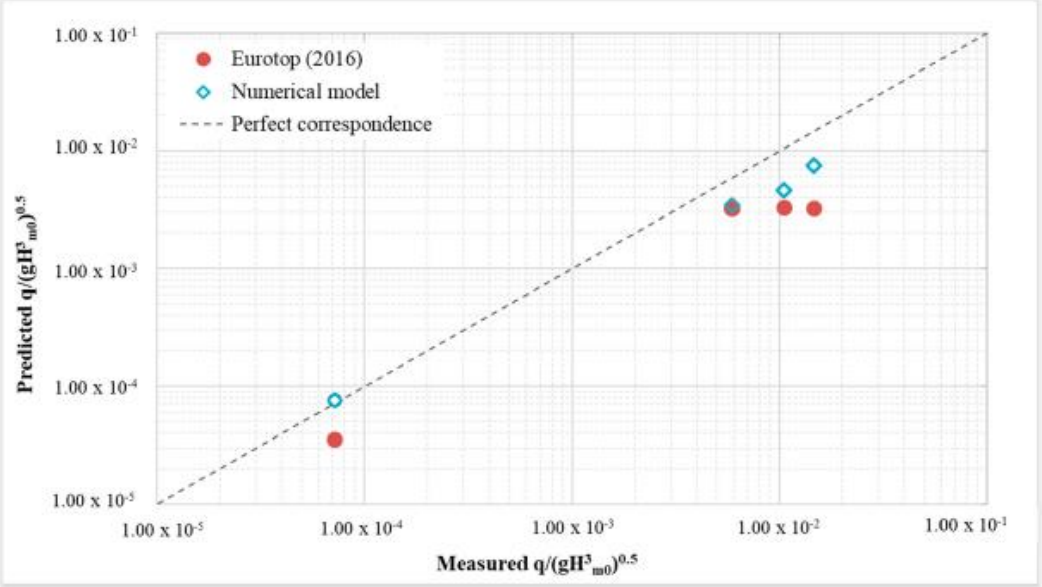

Figure 2.15 The Experimental, Numerical, and Theoretical Overtopping Results for Normal Wave Conditions (Palma, 2019)

As told in Contestabile (2016), the first optimization studies of OBREC were performed for the San Vincenzo Breakwater which is a traditional rubble mound breakwater in Naples, Italy. The breakwater was selected because of climatic, logistic and environmental reasons. The wave energy potential of this site is one of the highest in the coasts of Italy with an average wave power of 2.5 kN/m (Iuppa et al.,2015).

OBREC optimization studies were conducted for different sites. In Contestabile (2016), the target site was the southwest coast of Australia since it is one of the most energetic coastal areas in the World and many available coastal structures occur for optimization in the region. The nearshore wave transformation was performed by MIKE 21 SW Model with the bathymetry data provided by GEBCO (General Bathymetric Chart of Oceans). 150m grid resolution for shallow depths and 1000m for deeper regions than 500m. Then, the structural dimensions of OBREC were decided by a designed tool OBRECsim.

Lauro (2017), then optimizes an OBREC design for San Antonio Port, Chile coast. The CFSR and Era-Interim wind data is used by WAM Model to provide offshore wave data and SWAN Wave Model is used for the propagation of the waves through the selected breakwater. OBRECsim Model was again utilized for site specific OBREC design in this study. As the result of the study, the power rate of the optimized OBREC at the San Antonio Port was predicted as 1.62 kW/m.

Kralli (2019) utilizes Harmony Search Algorithm as an optimization technique with Eqn 2.1 as the overtopping formula to optimize OBREC to Heraklion Port Breakwater in Greece. The nearshore wave transformation was simulated by applyng a mild-slope model.

Cavallaro (2020) study presents another OBREC optimization by utilizing EMODNET and Italian Navy Hydrographic Institute bathymetry data and they also use SWAN Model for nearshore wave transformation. The optimization was performed for Harbor of Pantelleria which is a small island in Italy and the goal is to provide significant energy production for the need of the island community. They estimated that the optimized OBREC can meet more than 60% energy demand of the island in case of it is integrated into the target breakwater.

2.2.2.2 Breakwater Integration of OBREC

The sketch of OBREC cross-section and the picture of the OBREC prototype are given in Figures 2.16 and 2.17 to investigate the integration of OBREC to San Vincenzo Breakwater in Naples, Italy. The properties of the breakwater is critical for the integration of OBREC. The San Vincenzo breakwater is a traditional rubble mound breakwater that extends for approximately 1475 meters. The armor layer for the first 1150 meters is built of antifers, that are 2 meters long and weigh roughly 12 tons, whereas the remaining 325 meters of the breakwater are constructed with tetrapods. The armor layer has a slope of around 1:2 and the depth of the San

Vincenzo breakwater changes from 18 meters close to the coast to 35 meters at the end of the breakwater (Contestabile et al., 2017).

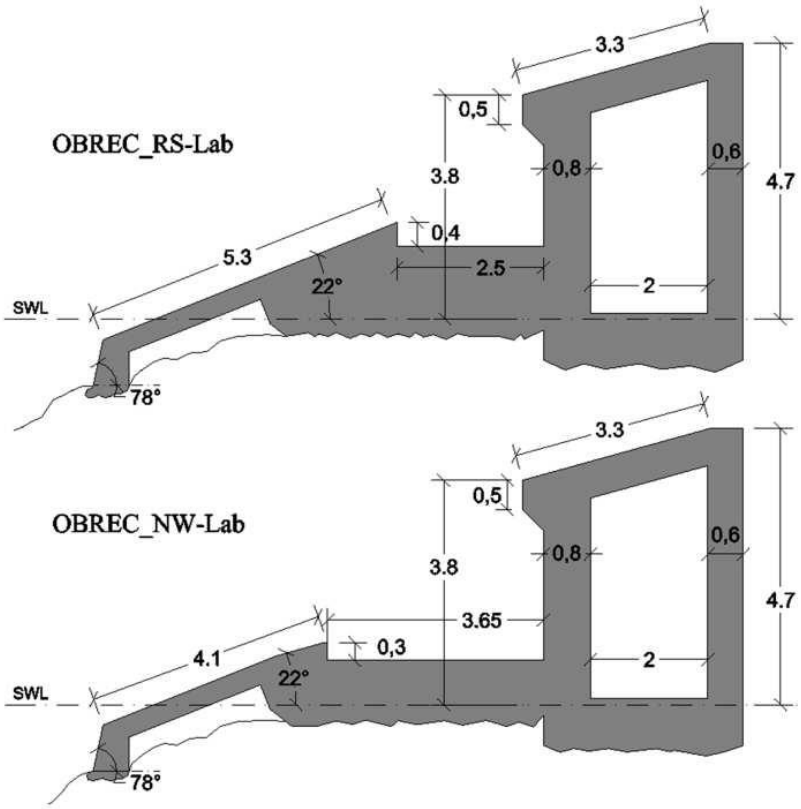

Figure 2.16 Cross Sections of Two Different Geometric Configuration in OBREC (Contestabile et al., 2017).

Figure 2.17 OBREC Prototype Integrated in San Vincenzo Breakwater in Naples (Contestabile et al., 2017).

The integrated secondary conversion system for OBREC is shown in Figure 2.18. The integration of the WEC needs the armor rocks in the upper side to be removed permanently for the front side of the breakwater. The reservoir and crest of the overtopping WEC and breakwater may be constructed as cast-in-place or precast concrete. In the back side of the breakwater, some modifications should also be done for the integration of a secondary conversion system. The upper of rocks should be also removed for the backside the low head turbine and the other parts of the mechanism is integrated to the breakwater, concrete part may be constructed on the rocks.

In addition, the findings of laboratory testing session show that the integration of the OBREC into the traditional breakwater often improves the stability of the breakwater. Because of the inclined ramp and the absorption of wave energy into the reservoir, overtopping at the back side of the breakwaters is reduced, and reflection coefficients are almost equal to or lower than those observed for the traditional breakwaters (Vicinanza, 2014).

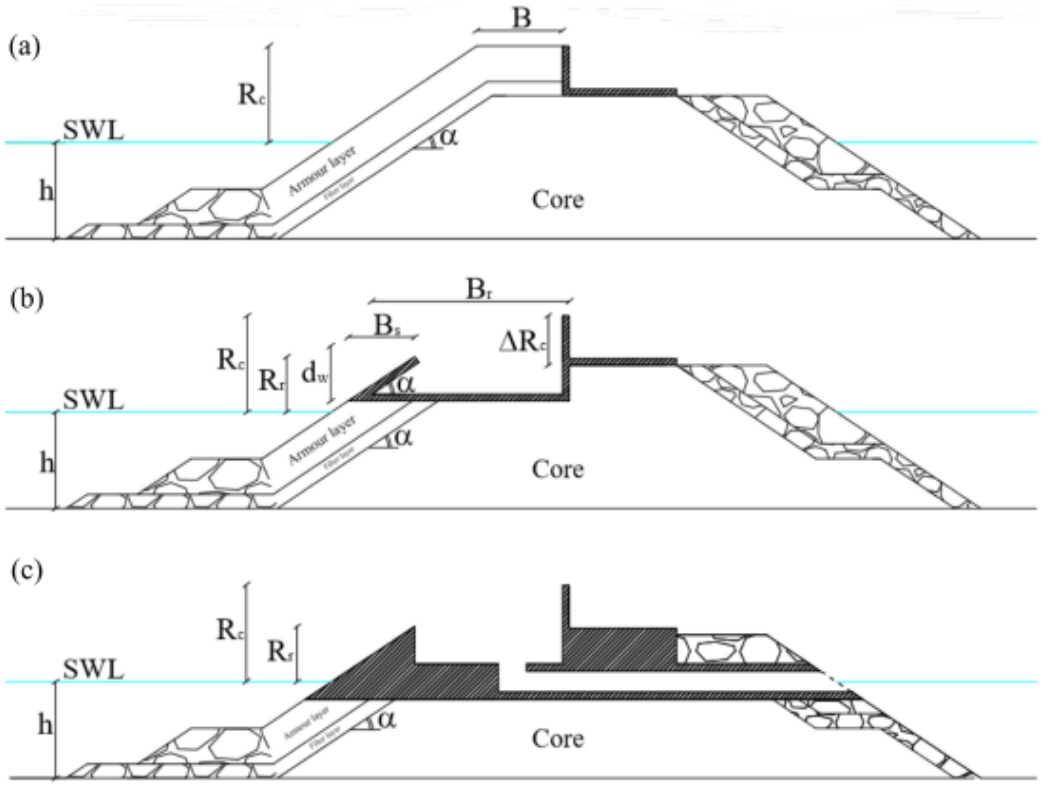

Figure 2.18 (a) The traditional rubble mound breakwater, (**b**) the OBREC physical model and (**c**) the OBREC numerical model (adapted from Vicinanza 2014) (Palma, 2019)

Where;

B : Breakwater Crest Width

B_r : Reservoir Width

B_s : Reservoir Crest Width

D_w : Reservoir Head

h : Water Depth

R_c : Breakwater Crest Height

R_r : Reservoir Crest Height

α : Slope of Front Face of the Breakwater

CHAPTER 3

METHODOLOGY

In this thesis, the optimization of OBREC type overtopping type wave energy converters into the existing breakwaters in the Black Sea coast of Turkey is studied by modeling the wave climate in front of selected breakwaters and developing an optimization tool to determine the best OBREC cross-section based on maximum energy production. First, the pilot sites were decided by considering structural and wave climate criteria. Then, the wave climate study was performed by using the deep water wave data, and bathymetry was prepared for the near-shore wave modeling. The wave transformation was modeled to obtain the wave data in front of the pilot breakwaters by using SWAN Wave Model. Finally, the optimization tool was utilized to obtain the dimensions of OBREC type overtopping WEC and energy production values. The methodology of the study is presented in the flowchart to clearly show the significant processes of this study in order in Figure 3.1.

Figure 3.1 Flowchart for The Methodology of The Study

3.1 Selection of Pilot Sites

The fisheries, marinas, and commercial ports are evaluated in the aspect of economic viability, frequency of use, and purpose of use. The fisheries are selected as the target structures since the idle fisheries are economically inefficient, numerous, and mostly unutilized on the Black Sea coasts of Turkey. The idle fisheries may be reintroduced into the economy through electricity generation if wave energy converters are integrated into their breakwaters. Another advantage of idle fisheries is that they are easy to choose concerning the structural attributes since there are numerous idle fisheries in each part of the Black Sea Coasts of Turkey. Structural criteria such as the length, depth, and orientation of main breakwater and secondary breakwater were evaluated based on the literature information in Mariani (2021) and Contestabile (2017).

Main parameters type considered for the site selection is intensity criteria which are dock capacity, number of boats using the fishery, and density in and out of fishing season. For the idle fisheries, the number of boats using the fishery and density both in and out of the fishing season are low. These statistics tell that the idle fisheries are economically ineffective. Moreover, even for fisheries that are being intensely used, the integration of WEC into the breakwaters does not have any negative effect on the usage of the fisheries.

The other parameters used in the study are related to breakwater properties. The length of the breakwater shows the extent of the wave energy converter that can be applied along the breakwater which is highly related to the total energy amount calculations which can be produced in the case the WEC is constructed throughout the main breakwater.

The depth of the breakwater affects the height of the incoming waves and the overtopping volume. For energy production, higher waves in high frequency are valuable.

The orientation of the breakwater is critical in the aspect of incoming wave directions. When the angle between wave orthogonal and breakwater length differs from 90^{o}, the wave capturing system of Overtopping WECs is starting to work in a less effective way. Since the waves are refracting while propagating through the shore, the waves tend to hit closer to perpendicular to the breakwaters which are parallel to the shoreline. Therefore, the breakwater parallel to the shoreline is preferable in terms of orientation.

In the Black Sea Coasts of Turkey, 4 pilot sites were determined by considering the structural and intensity criteria. The selected breakwaters are the breakwaters of Cayeli Fishery, Cide Fishery, Amasra Port and Kiyikoy Fishery which are shown in Figure 3.2.

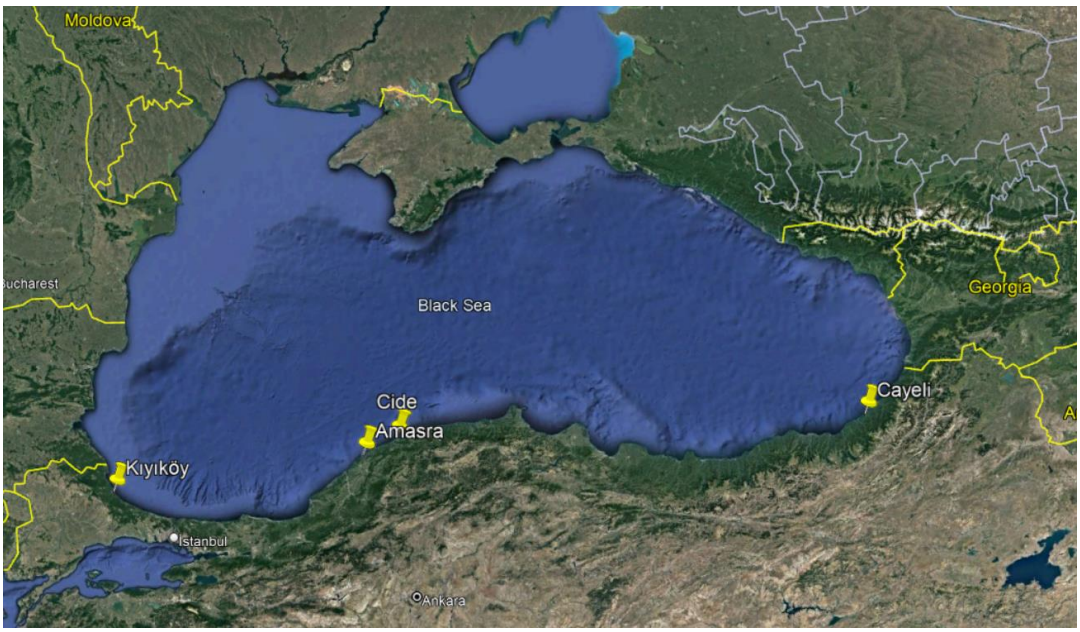

Figure 3.2 Pilot Sites in the Black Sea (Google Earth, 2022)

3.2 Wave Climate Study for SWAN Wave Model

The wave heights and wave frequency propagating through the breakwater is needed to be analyzed for the energy production and WEC optimization for a breakwater. Because the overtopping volume in long term is needed to be calculated and predicted by analyzing the wave frequency in front of the breakwater. Therefore, SWAN Model is utilized to transform the waves from deep water to the nearshore.

SWAN wave model uses wind, bottom, and current variables to calculate accurate wave characteristics in coastal regions, lakes, and rivers. The wave action balance equation is the basis for the model. SWAN, on the other hand, could be applied to any scale that is related to wind-generated surface gravity waves. (Delft University of Technology-Environmental Fluid Mechanics Section, 2021)

First, wave data was gathered for the years 1979-2021 from the ECMWF Era5 database. The data points are selected on the boundaries of large domains for each study field which are shown in the Figure 3.3, 3.4 and 3.5. ERA5 database presents numerous atmospheric, terrestrial, and marine climate variables which are estimated hourly. The data resolve the atmosphere utilizing 137 levels from the ground up to an altitude of 80 km, covering the Earth on a grid of 30 km. At lowered spatial and temporal resolutions, ERA5 has information on the uncertainty of all variables (Guillory, 2022).

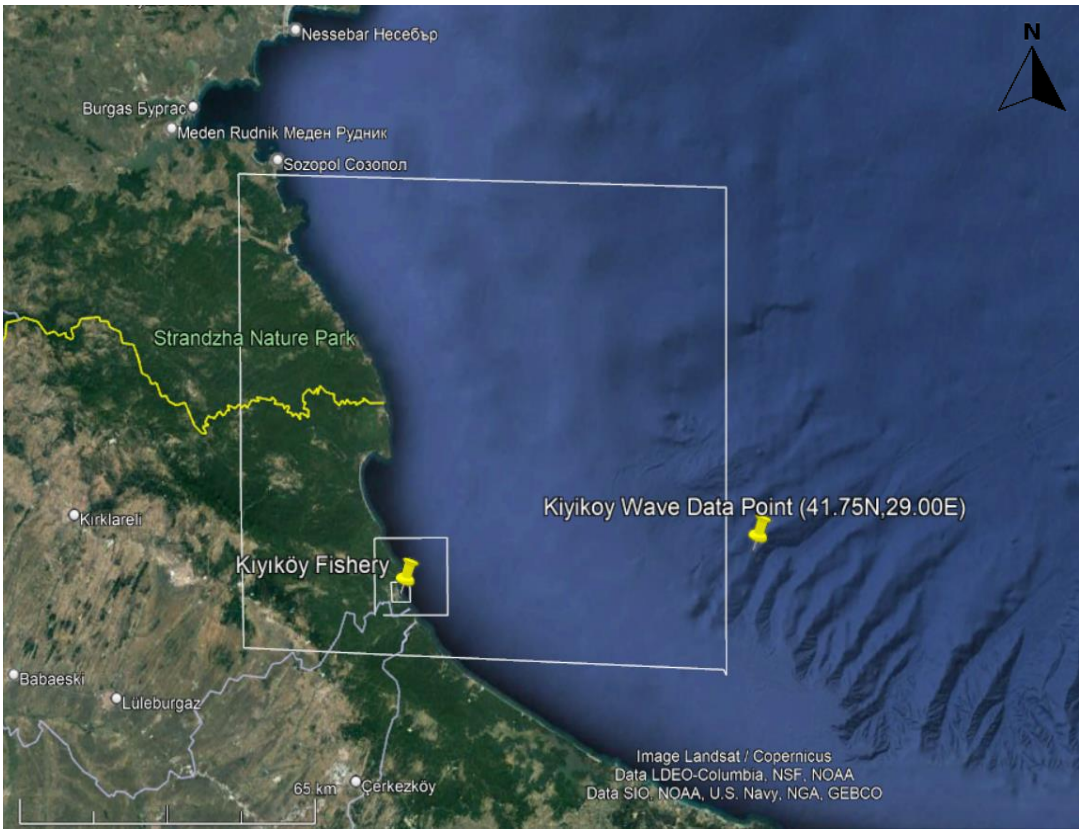

Figure 3.3 Kiyikoy Wave Data Points and Model Domains (Google Earth, 2022)

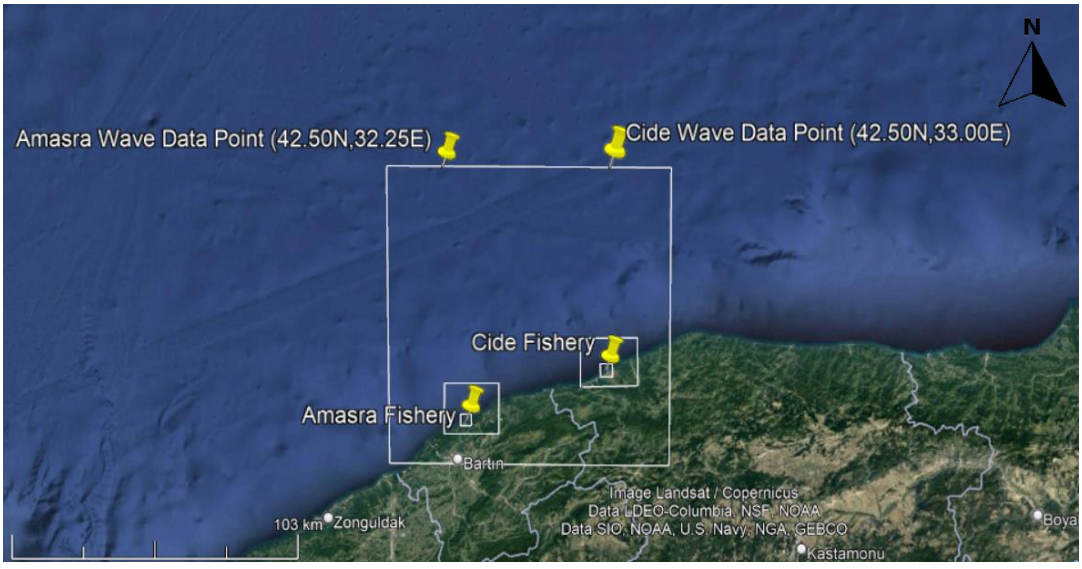

Figure 3.4 Amasra and Cide Wave Data Points and Model Domains (Google Earth, 2022)

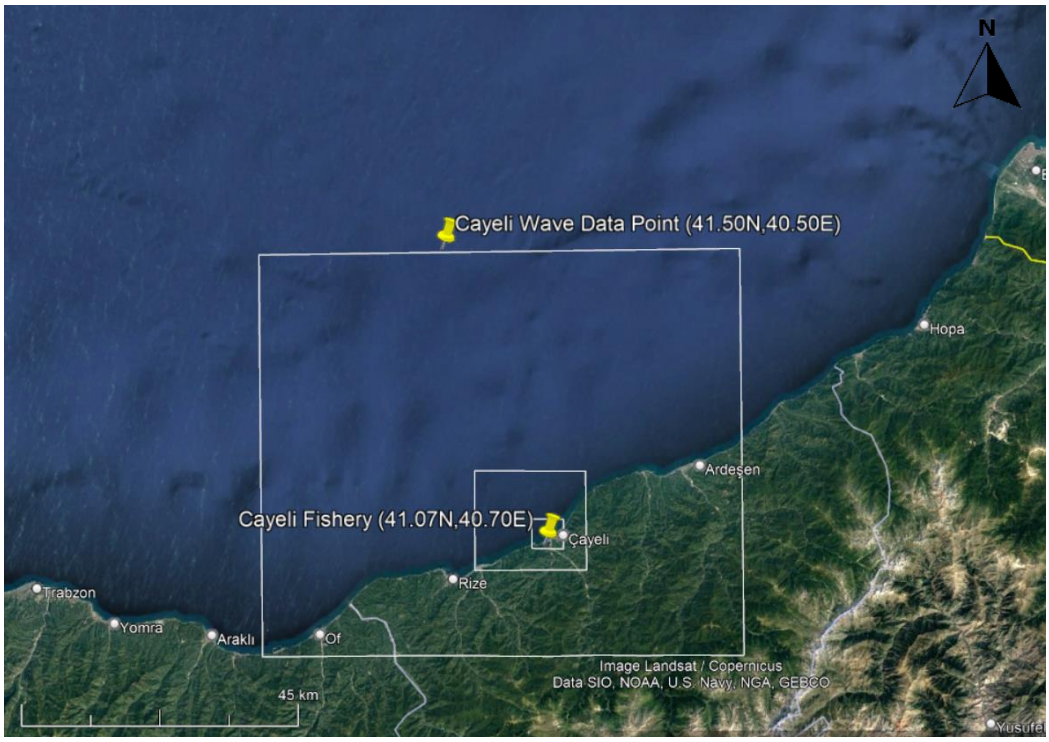

Figure 3.5 Cayeli Wave Data Points and Model Domains (Google Earth, 2022)

Wave data for the 43 years were processed by the MATLAB code which creates wave frequency tables, cumulative wave tables and exceedance probability tables for different wave height values with intervals of 0.4m. Furthermore, seasonal and monthly exceedance probability tables were also created for the evaluation of the results and discussions.

SWAN wave models were performed to obtain accurate wave transformation results. In the model, depth-induced wave shoaling effect was applied to the waves in the deep water region. Nested simulations were made to be able to reach a 10m grid size to obtain the wave height data at the toe of the breakwaters at 10m intervals. This gives the opportunity to evaluate the wave height difference on the breakwaters which is one of the main discussions of this study.

On the other hand, bathymetry data was gathered from EMODNET (European Marine Observation and Data Network) which is European cooperation that manages and develops projects. Hydrographic offices, research institutes, and industrial

enterprises conduct and maintain bathymetric investigations, which intersect and support each other geographically. For European seas, a standardized EMODnet Digital Terrain Model (DTM) was created using bathymetric surveying sets of data and Satellite Derived Bathymetry data sets. The grid resolution of the bathymetric data is 1/16 × 1/16 arc minutes (about 115 * 115 meters) (EMODnet Bathymetry, 2022).

The bathymetry data taken from EMODNET were processed by using Golden Software-Surfer. The data were gridded by using kriging to create 3 different domains for the SWAN wave model. These 3 domains were prepared for every 4 breakwaters. The grid sizes, number of grids, and size of domains of the large, intermediate, and small domains are shown in Tables 3.1, 3.2, and 3.3, respectively.

Table 3.1 Properties of the Large Domains

Properties of Large Domains	**Kiyikoy**	**Amasra**	**Cide**	**Cayeli**
Grid Size (m)	250	250	250	250
Number of Grids	400	400	400	350
Size of Domain (km^2)	100 x 100	100 x 100	100 x 100	87.5 x 87.5

Table 3.2 Properties of the Intermediate Domains

Properties of Intermediate Domain	**Kiyikoy**	**Amasra**	**Cide**	**Cayeli**
Grid Size	50	50	50	50
Number of Grids	400	400	400	400
Size of Domain (km^2)	20 x 20	20 x 20	20 x 20	20 x 20

Table 3.3 Properties of the Small Domains

Small Domain	**Kiyikoy**	**Amasra**	**Cide**	**Cayeli**
Grid Size	10	10	10	10
Number of Grids	400	400	400	400
Size of Domain (km^2)	4 x 4	4 x 4	4 x 4	4 x 4

Since it is proper to start the model from deep water with the wave data taken from a deep water region, large domains' lengths were decided to be 10 km long for Kiyikoy, Amasra and Cide sites, however 87.5 km large domain length were evaluated as adequate for Cayeli region due to the steep bottom slope. All the other intermediate and small domains are prepared with the same grid sizes and number of grids. Multiple models were performed with different grid sizes and number of grids before the selection, then the used domain properties are decided as the most convenient ones for these cases.

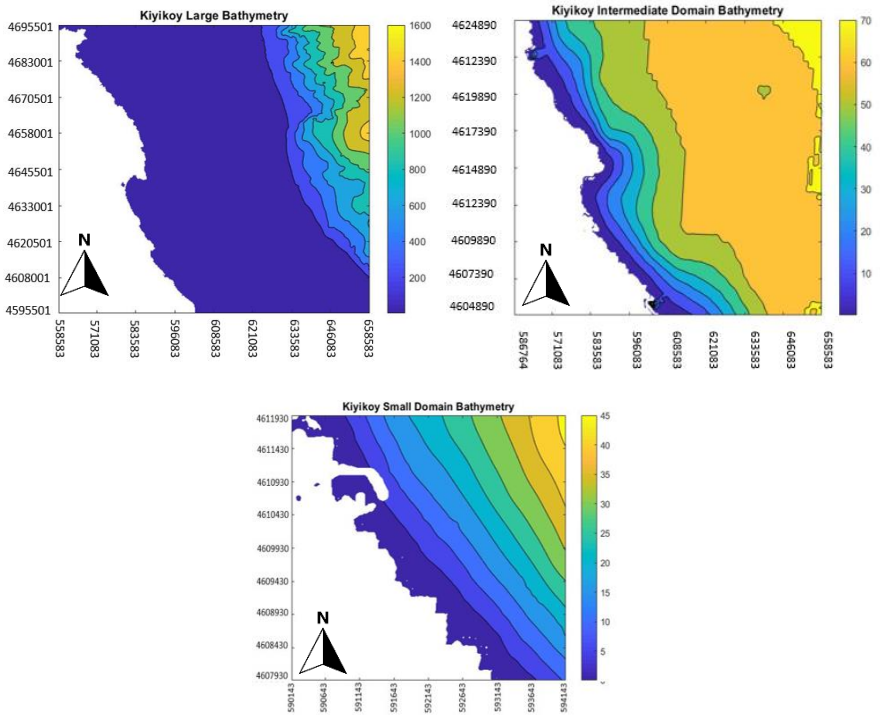

Figure 3.6 Bathymetry of Kiyikoy in 3 Domains

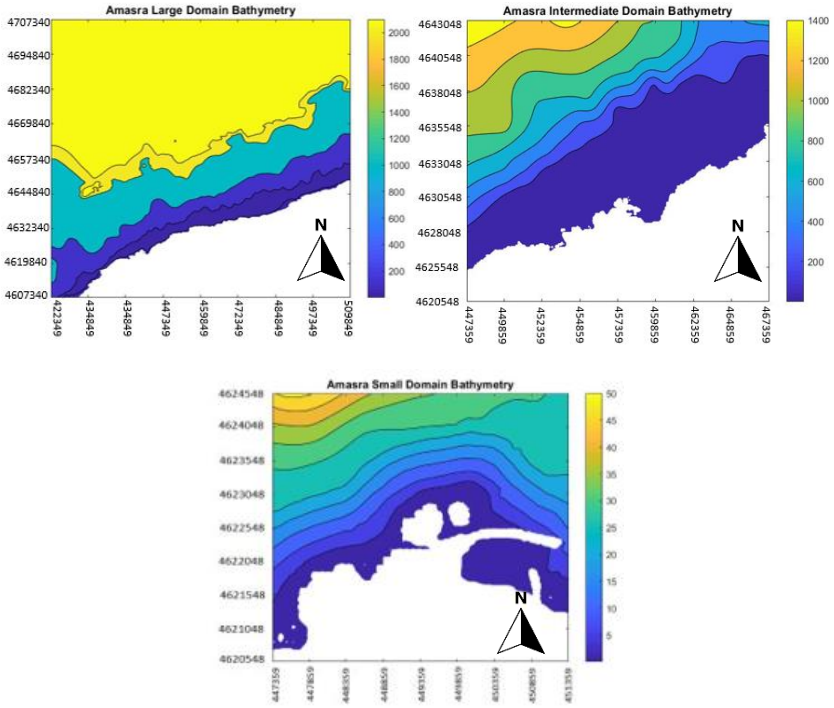

Figure 3.7 Bathymetry of Amasra in 3 Domains

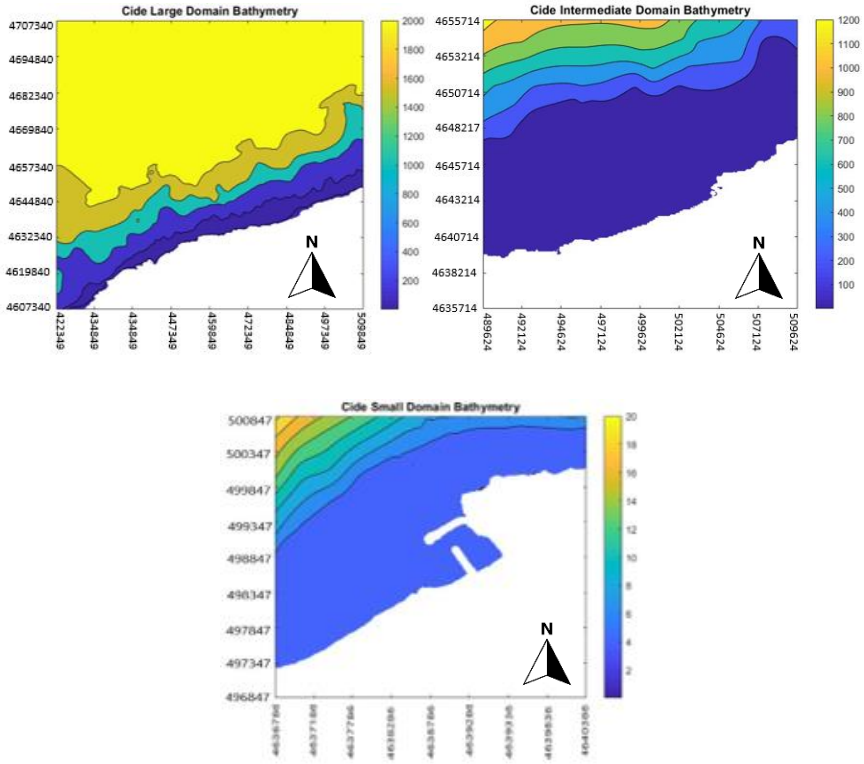

Figure 3.8 Bathymetry of Cide in 3 Domains

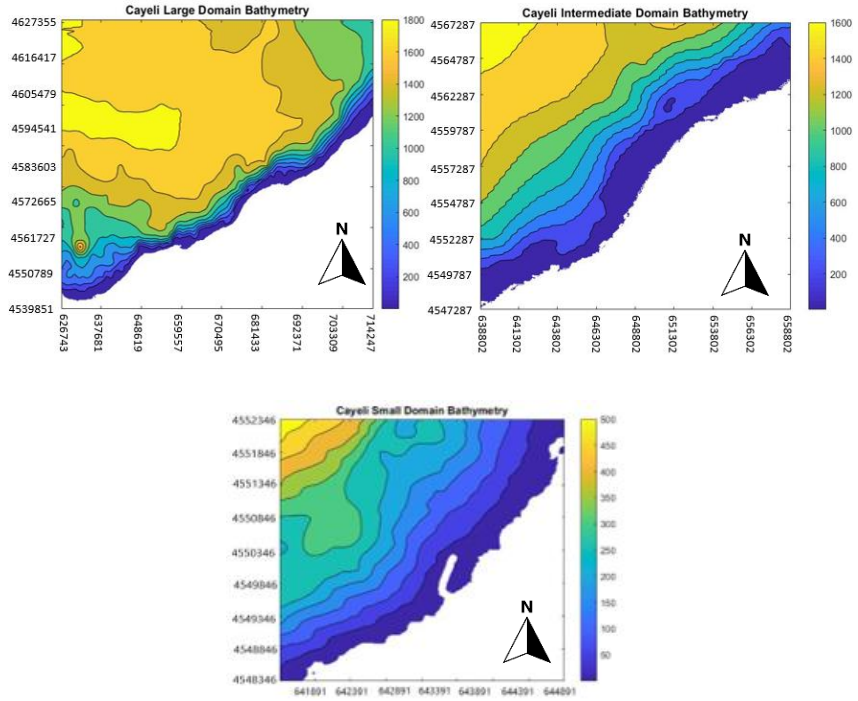

Figure 3.9 Bathymetry of Cayeli in 3 Domains

3.2.1 Nearshore Bathymetry at The Selected Sites

Bathymetry data were taken for 4 pilot sites, and each of them was used for the relevant study area. The bathymetry data were compared with the bathymetric maps prepared by the Turkish Naval Forces The Office of Navigation, Hydrography and Oceanography (Turkish Naval Forces The Office of Navigation, Hydrography and Oceanography, n.d.). The bathymetric maps are evaluated as they are compatible with each other. Although the large and intermediate bathymetric domains were prepared by using only EMODnet Bathymetry data, the data from the charts of Turkish Naval Forces the Office of Navigation, Hydrography and Oceanography and the archive of the European Marine Observation and Data Network (EMODnet) were utilized to rebuild the morphology of the nearshore sea bottom for the small domains.

3.3 Overtopping Type WEC Optimization Algorithm

The working principle of overtopping-based WECs is accumulating as much water in their reservoir by overtopping. Therefore, it is critical to decide the dimensions of the overtopping type WECs for optimizing the overtopping volume and head of the water collected in the reservoir.

The inputs are H_s and corresponding f values, h_s, n_1, n_2, γ_f, γ_β and γ_v. The main inputs of the algorithm are the wave frequency data (H_s and f) in front of the breakwater for selected sea states that is why the wave frequency tables were created and the modeling were performed. The frequency of waves in the intervals of 0.4m was used in the algorithm as coming from 16 different directions. h_s value is the height of the water column inside the pipe above turbine which was decided as 0.85m considering the efficiency of Kaplan type turbines as suggested in Kralli (2019). n_1 and n_2 are the algorithm variables. n_1 was chosen as 100 for the accuracy of calculations and n_2 was selected as 27 for 9 different wave heights from 3 directions with intervals of 45

degrees. γ_f value was taken as 1 since the optimized ramp surface is concrete although the breakwater surface is rock, γ_β was taken as 1 since there is no berm in any studied breakwaters, γ_v was also taken as 1 since the approach angle of all the waves is close or equal to zero as suggested in EurOtop Manual (2018). The flowchart of the algorithm written in MATLAB is also presented below to clarify all the inputs, equations and the outputs of the algorithm. In addition, important breakwater parameters are shown in Figure 3.10.

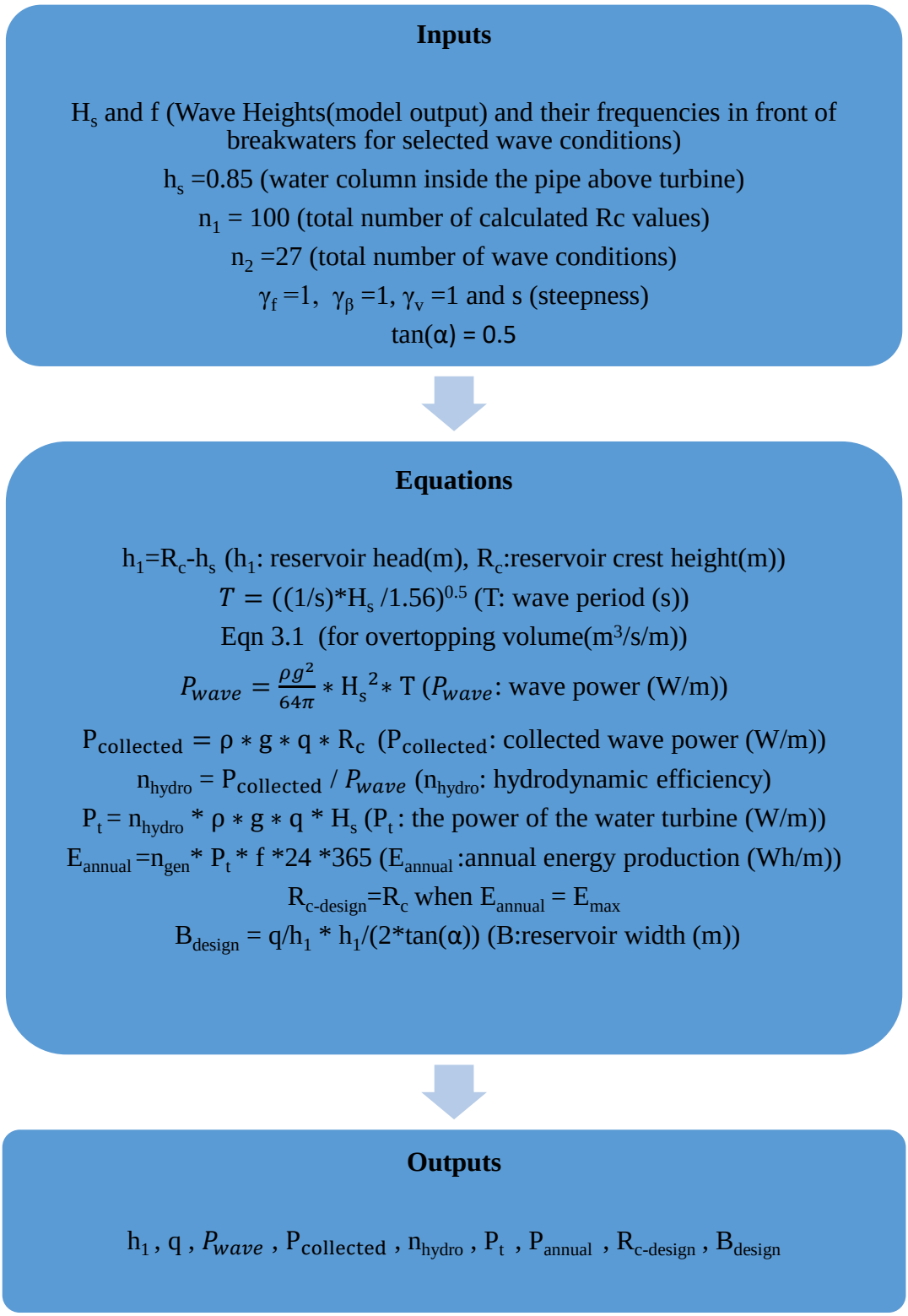

Figure 3.10 The Inputs, Equations and Outputs of Optimization Algorithm

The formulas used by the optimization tool are given in Figure 3.10. The most critical part of the optimization is the overtopping volume calculations in which Equation 3.1 was used.

$$\frac{q}{\sqrt{g * Hs^3}} = 0.2 * \exp(-2.6 \frac{Rc}{Hs * \gamma f * \gamma \beta * \gamma v}) \qquad eqn\ 3.1$$

where;

g : Gravitational Acceleration

Hs : Significant Wave Height

q : Overtopping Volume Through Reservoir of Overtopping WEC

R_c : Reservoir Crest Height

γ_f : Influence Factor for Roughness Elements

γ_v : Influence Factor for Wave Wall

γ_β : Influence Factor for Oblique Wave Attack

The idea behind the usage of this formula for overtopping in WECs is the similarity of overtopping cases between accumulation to the reservoir in an overtopping WEC system and overtopping through the back side of a rubble mound breakwater. overtopping volumes. The experimental studies conducted by Iuppa (2019) show the applicability of the overtopping formula in EurOtop 2018 for overtopping wave energy converters similar to OBREC.

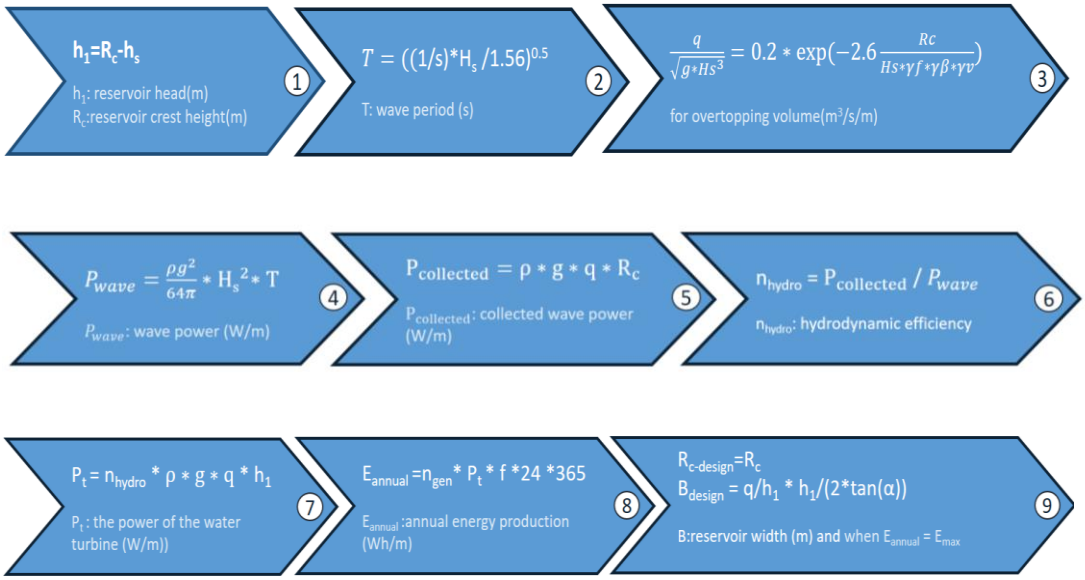

Figure 3.11 The Flowchart of Optimization Algorithm

As shown in the flowchart of optimization algorithm in Figure 3.11, first reservoir head values were calculated by using different R_c values in the range of 0-3m. Wave period values were calculated with significant wave height (Hs) values for each sea states which is the output of wave model. Then, overtopping volume were calculated for each sea states with the overtopping formula provided from Eurotop (2018) Manual. Wave power in front of the breakwater and collected wave power were calculated by reservoir overtopping volume and significant wave height and wave period values calculated in previous steps. The ratio of wave power in front of the breakwater and collected wave power was determined as hydrodynamic efficiency. After that, The power of the water turbine was calculated by the formula seven. Finally, annual energy production, design reservoir crest height and reservoir width were determined with the formulas 8 and 9 given in the flowchart.

The front slope of the WEC system behaves like a low crested rubble mound breakwater surface. Since the reservoir crest height of a rubble mound integrated overtopping WEC design is much shorter than the crest of a regular rubble mound breakwater, the mean overtopping discharge amounts through the reservoir becomes greater in overtopping WEC rather than the overtopping volume passing through the

harbor side of a rubble mound breakwater. That is why the mentioned overtopping formula is used to calculate overtop volume through the overtopping WEC to reach the optimum energy amounts in addition to the affirmative experimental results for usage of the formula in Iuppa (2019).

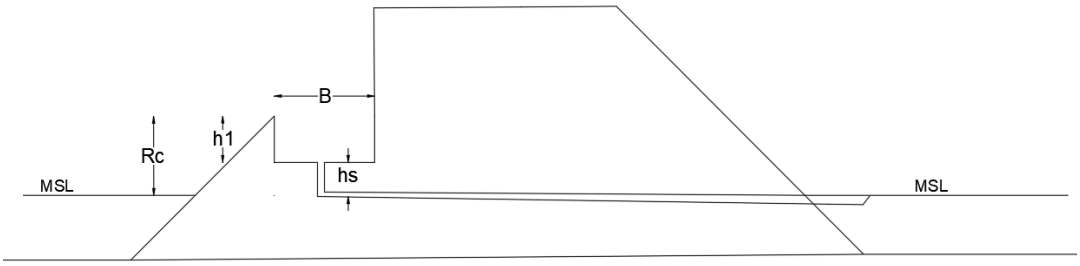

Figure 3.12 The cross-section of Optimized Overtopping WEC

The other key point for the energy production of an overtopping WEC is the head of the water accumulated in the reservoir. The head of the water is directly related with the reservoir height (shown as h1). In the all cases calculated in the algorithm, the mean reservoir overtopping volume is greater than the reservoir volume, therefore the reservoir is assumed as full in all cases considered for energy production. Even the energy production is possible for the other wave conditions, the wave conditions where the deep water wave height is 0.8m in deep water are not been taken into account for energy production in this optimization methodology due to the ineffective working performance of first and second conversion system of the WEC system for the conditions when the overtopping volume is lower than the reservoir volume.

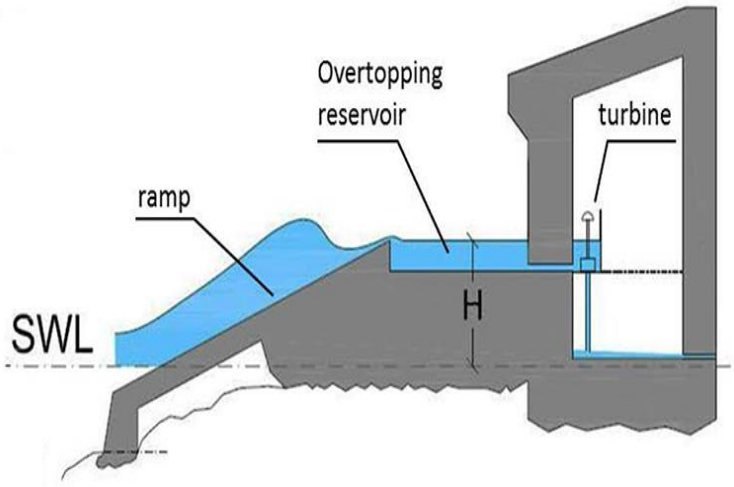

Figure 3.13 Presentation of Overtopping Type WEC Integrated into a Rubble Mound Breakwater (Iuppa et al.,2016)

The head of the water accumulated in the reservoir is represented as H in Figure 3.11. In the optimization calculations when the reservoir crest height is increased, the head of the water also increases but the overtopping volume through the reservoir decreases. However, when the reservoir crest height is decreased, the head of the water also decreases, and the overtopping volume increases. The overtopping volume and the reservoir head are both directly related to the energy production since an increase in any of them increases the efficiency of the turbines. Thus, the prepared algorithm decides the best section properties which choose the optimum overtopping crest height which also specifies the head of the reservoir. The best balance between them is decided by the algorithm to find the most efficient energy amounts for the relevant wave climate.

The wave power in front of the breakwaters are represented by P_{wave} and the wave power gathered by the WEC system is represented by $P_{collected}$ in the formulas below which is obtained from the studies of Lander (2012). $P_{collected}$ is the potential energy of the water accumulated in the reservoir. R_c is used as the head of the water in the reservoir which is equal to the summation of reservoir head (h_1) and reservoir height (h_s) as an assumption.

The efficiency of energy collection of the overtopping WEC system is also calculated as the ratio of $P_{collected}$ to P_{wave} shown in Equation 3.4. Since the overtopping volume is important for the energy production in this optimization, significant period (T_s) values for each wave state were used rather than the energy period (T_e) as the period values in Equation 3.2.

$$P_{wave} = \frac{\rho g^2}{64\pi} H^2 \mathrm{T} \qquad \text{Eqn 3.2}$$

$$\mathrm{P_{collected}} = \rho g q \mathrm{R_c} \qquad \text{Eqn 3.3}$$

$$\mathrm{n, hydro} = \frac{\mathrm{P_{collected}}}{P_{wave}} \qquad \text{Eqn 3.4}$$

Then, the power of the water turbine, P_t and annual energy production, E_{annual} are calculated by the Equations 3.5 and 3.6. The hydrodynamic efficiency, gravitational acceleration, overtopping volume and reservoir head are all directly proportional with the power of the water turbine. Annual energy production is also calculated as shown Equation 3.6 where the efficiency value for secondary and tertiary conversion, n_{gen} is also used as 0.45 as an average value for the electrical generation from the Kaplan turbine as suggested in Kralli (2019).

$$P_t = n_{hydro} * \rho * g * q * H \qquad \text{Eqn 3.5}$$

$$E_{annual} = n_{gen} * P_t * f * 24 * 365 \qquad \text{Eqn 3.6}$$

In the study of Kralli (2019), Harmony Search Algorithm was used to perform all the calculations and optimization which based on stochastic random search technique and produces one solution for each iteration. However, Kralli (2019) was based on this study, the algorithm used in this thesis calculates the overtopping water amounts through the reservoir for all the wave heights and related frequency for each

reservoir crest height value as the different approach than Kralli (2019) study. The optimization calculations are done for all the reservoir crest heights in the interval of 0-3m. Then, the produced energy amounts are calculated for all the reservoir crest height values and best reservoir crest height value is selected which provides the greatest energy value. After the optimum reservoir crest height is chosen by the algorithm, the reservoir width value is calculated by using the overtopping volume and optimum reservoir crest height which is the optimization approach making the difference for this study. The reservoir head is also maximized for all the wave frequencies by the reservoir width value calculated by the algorithm.

When the optimization is performed by the algorithm, two significant assumptions are made. First, the head of the water in the reservoir is assumed as equal to the reservoir crest height which means the reservoir is full when the studied waves hit the breakwater. Even the reservoir crest height and reservoir width are designed to theoretically provide the reservoir full in the working hours, the head is not supposed to be equal to the reservoir crest height all the time for specified waves in possible site applications of the WEC.

The other assumption is ignoring the deep water waves for the energy production which have wave heights below 0.8m. It is observed after the wave model that the wave heights of the majority of the ignored waves are below 0.5m in front of the breakwater. The wave heights below the reservoir crest heights cause little overtopping volumes. But, it can still contribute to the amount of produced energy in the site applications which could cause higher practical energy amounts than the calculated energy amounts.

The algorithm benefits from the mentioned methodology to optimize the best cross-sections for the overtopping WEC to the breakwaters and it calculates the energy amounts that could be provided by this optimized system under given wave conditions. The pilot sites, the designed cross-sections and annual energy amounts for the four optimized systems are given in Chapter 4.

CHAPTER 4

RESULTS AND DISCUSSION

The candidate breakwaters were evaluated considering structural and climatic criteria. Structural factors are main breakwater and secondary breakwater length, depth, orientation, dock length, and depth. The intensity factors are dock capacity, number of fishing boats, number of other boats using, and density in and out of fishing season.

As the result of the evaluations, 3 fisheries and 1 port in Black Sea coast were selected for WEC optimization studies. The selected pilot sites are Cayeli Fishery, Cide Fishery, Amasra Port, and Kiyikoy Fishery. The pilot sites were evaluated and discussed case by case in this chapter.

First, the sites are described by the images, structural and intensity criteria tables which are given for each pilot site in the relevant part. The plans and the information in the tables were retrieved from "Fishery and Coastal Structures Situation and Needs Analysis Report (FCSSNAR)" published by the General Directorate of Railways, Ports and Airports Construction (General Directorate of Railways, Ports and Airports Construction, 2011).

Second, the sea state characteristics are presented by the wave climate results in deep water which are shown as the frequency tables for the study areas. The deep water wave conditions results were prepared by processing wave data provided by ERA-5 database for the duration 1979-2021 for the specified wave data points. Since the wave frequency table is required for the algorithm, the wave frequency tables were created with 16 directions to better evaluate the data and used the necessary ones in

the optimization phase. The geography of the regions was investigated and the waves coming from some directions were neglected because the transformed waves represent the waves in front of the breakwaters and some directions are closed by land or some islands. Therefore, all the studied breakwaters were evaluated considering the specific climatic and geographic conditions of their regions. Selected directions are written bold in the frequency tables.

SWAN wave models were conducted for all the study areas by wave frequency tables. 0.4m interval was decided to be used to obtain accurate results. Therefore, various models were made for the specified directions for all the wave heights with a 0.4m wave height interval. The wave transformation model results are presented as the deep water wave heights and wave heights at the toe of the breakwaters which are inputs and outputs of the wave models, respectively. After that, results from the optimization algorithm are given which are structural dimensions, and energy outputs of the optimized WECs. All four regions were also modelled with nested runs. The resultant wave heights are given in the tables below for each breakwater.

Overtopping WEC optimization results and energy outputs were gathered by using the optimization algorithm in the last part of the results. Since the algorithm calculates the best section properties for WEC design, it adjusts the reservoir crest heights, reservoir depths, and reservoir widths with respect to the most efficient energy-producing structural section. Thus, the frequency of the waves which have wave heights greater than 0.8m is the most significant factor for the optimization and energy production.

Finally, besides the optimization results , research goal is to evaluate the effect of marine and structural conditions of the breakwater to the efficiency and optimization of wave energy converters to the existing breakwaters in Black Sea coast of Turkey. Therefore, outputs of the research were investigated to obtain and show the effect of important parameters to the energy production process both for the wave model and optimization algorithm phases. The effect of significant parameters to energy output are evaluated with the obtained results for each case.

4.1 Cayeli Fishery

Cayeli Fishery has a 670m long main breakwater where the head of the breakwater is in deeper region than the other parts of the breakwater. When the Figure 4.1 is investigated, the depth difference may be observed as the depth decreases from 10m in the head to lower than 7m along the main breakwater.

Although the dock capacity of the Cayeli Fishery is 145 boats, the intensity is only 27.6% in fishing season and 21.3% out of fishing season. Therefore, Cayeli Fishery may be considered as an idle fishery which is not effectively used by boats in and out of the fishing seasons.

Figure 4.1 The Breakwater of Cayeli Fishery (Google Earth, 2022)

Table 4.1 Structural and Intensity Criteria for Cayeli Fishery (FCSSNAR,2011)

Structural Criteria	
Main Breakwater Length (m)	670
Secondary Breakwater Length (m)	160
Dock Length and Depth (m)	30m (-2m) , 100m (-4m)
Intensity Criteria	
Dock Capacity (boat)	145
The intensity in Fishing Season (%)	27.6
The intensity out of Fishing Season (%)	21.3

When Table 4.2 and Table 4.3 are investigated, the waves from WNW and NW directions are 64.36% of the total number of waves in Cayeli Region. Moreover, highest waves propagate from the WNW and NW directions which are main wave directions. The highest waves which have greater frequency than 0.01% come from ENE direction as 4.8m. The waves above 4m wave height in all directions is almost 7 hours in a year.

Table 4.2 Cayeli Wave Frequency Table (%) (East Directions)

H / Dir	NNE	NE	ENE	E	ESE	SE	SSE	S
0	4.21	4.02	2.28	1.31	0.91	0.61	0.30	0.15
0.4	0.95	1.63	0.56	0.16	0.13	0.14	0.11	0.05
0.8	0.06	0.17	0.01	0.00	0.00	0.00	0.00	0.00
1.2	0.00	0.01	0.00	0.00	0.00	0.00	0.00	0.00
1.6	0.00	0.00	0.00	0.00	0.00	0.00	0.00	0.00
2	0.00	0.00	0.00	0.00	0.00	0.00	0.00	0.00
2.4	0.00	0.00	0.00	0.00	0.00	0.00	0.00	0.00
2.8	0.00	0.00	0.00	0.00	0.00	0.00	0.00	0.00
3.2	0.00	0.00	0.00	0.00	0.00	0.00	0.00	0.00
3.6	0.00	0.00	0.00	0.00	0.00	0.00	0.00	0.00
4	0.00	0.00	0.00	0.00	0.00	0.00	0.00	0.00
4.4	0.00	0.00	0.00	0.00	0.00	0.00	0.00	0.00
4.8	0.00	0.00	0.00	0.00	0.00	0.00	0.00	0.00
5.2	0.00	0.00	0.00	0.00	0.00	0.00	0.00	0.00
5.6	0.00	0.00	0.00	0.00	0.00	0.00	0.00	0.00
SUM	5.22	5.84	2.85	1.48	1.04	0.75	0.41	0.21

Table 4.3 Cayeli Wave Frequency Table (%) (West Directions)

H / Dir	SSW	SW	WSW	W	WNW	NW	NNW	N
0	0.15	0.17	0.16	0.65	11.30	16.67	9.38	5.33
0.4	0.03	0.03	0.04	0.62	12.74	9.58	1.87	1.05
0.8	0.00	0.00	0.00	0.25	5.02	3.65	0.24	0.08
1.2	0.00	0.00	0.00	0.10	1.95	1.33	0.02	0.00
1.6	0.00	0.00	0.00	0.03	0.88	0.44	0.00	0.00
2	0.00	0.00	0.00	0.01	0.34	0.16	0.00	0.00
2.4	0.00	0.00	0.00	0.00	0.13	0.06	0.00	0.00
2.8	0.00	0.00	0.00	0.00	0.06	0.03	0.00	0.00
3.2	0.00	0.00	0.00	0.00	0.01	0.00	0.00	0.00
3.6	0.00	0.00	0.00	0.00	0.00	0.00	0.00	0.00
4	0.00	0.00	0.00	0.00	0.00	0.00	0.00	0.00
4.4	0.00	0.00	0.00	0.00	0.00	0.00	0.00	0.00
4.8	0.00	0.00	0.00	0.00	0.00	0.00	0.00	0.00
5.2	0.00	0.00	0.00	0.00	0.00	0.00	0.00	0.00
5.6	0.00	0.00	0.00	0.00	0.00	0.00	0.00	0.00
SUM	0.18	0.21	0.20	1.68	32.44	31.92	11.51	6.47

Several study about extreme wave conditions in Black Sea are discussed in Akpinar (2016). When the extreme wave heights in ECMWF wave data are compared with the other studies mentioned in the study, it is deduced that ECMWF extreme wave heights are smaller than the values obtained from the mentioned studies for Turkish coasts of Black Sea. Moreover, the extreme wave analysis results were provided from Cayeli Wave Climate Analysis Report prepared by METU Coastal and Ocean Engineering Laboratory (METU Coastal and Ocean Engineering Laboratory, 2022). In the report, 100 year return period significant wave height and wave period are 6.34m and 10.14s, 50 year return period significant wave height and wave period are 6.00m and 9.87s, the steepness value is also 0.0395.

Especially, for Cayeli Region, it may be considered as the extreme wave heights are lower in ECMWF data rather than the expected extreme wave height values.

Waves coming from NNE, N, NNW, NW, and WNW directions were used in the model due to the geography of the region and orientation of the breakwater, as seen in Table 4.4. Since no wave data occur greater than 0.8m in NNE and 1.2m in N directions, the results for the greater wave heights were not obtained in these directions. Also, in other studied directions greatest waves with higher frequency than 0.01% is the upper limit for wave height studied in the model.

Table 4.4 Cayeli Wave Height at Deep Water and Toe of the Breakwater

Direction	Hs deep (m)	Hs breakwater (m)
NNE	0.8	0.68
N	0.8	0.72
N	1.2	1.07
NNW	0.8	0.70
NNW	1.2	1.04
NNW	1.6	1.37
NNW	2	1.74
NNW	2.4	2.07
NNW	2.8	2.41
NNW	3.2	2.73
NW	0.8	0.68
NW	1.2	1.06
NW	1.6	1.37
NW	2	1.65
NW	2.4	1.95
NW	2.8	2.28
NW	3.2	2.62
WNW	0.8	0.56
WNW	1.2	0.84
WNW	1.6	1.01
WNW	2	1.36
WNW	2.4	1.57
WNW	2.8	1.83
WNW	3.2	2.19

After the SWAN wave model results, the optimized OBREC type overtopping WEC dimensions are given in the Table 4.5. Reservoir crest height (R_c) is 1.21m and reservoir width (B) is 0.36m which can be considered as lower reservoir crest and narrower basin than the other OBREC optimization studies such as Kralli (2019), Mariani (2021), Contestabile (2017), Lauro (2017). However, wave climates are different than the Black Sea Region in the regions of the optimized OBREC type

overtopping WEC in these studies. Since the wave heights in both deep water regions and nearshore regions are lower in this thesis study sites, the reservoir crest height and reservoir width values are already supposed to be lower than the cases in mentioned studies.

Table 4.5 Cayeli Overtopping WEC Optimization and Energy Results

Reservoir Depth (h1) (m)	0.36
Crest Height (Rc) (m)	1.21
Reservoir Width (B) (m)	0.46
Annual Energy Production (kWh/m)	110.37
Annual Energy Production for 100m (kWh)	11037

Finally, the efficiency curve for Cayeli breakwater overtopping WEC optimization is presented in Figure 4.2 to show the energy production difference with respect to reservoir crest height. The algorithm calculates overtopping volume and energy amounts for each reservoir crest height value. Then, the most efficient reservoir crest height value is selected as the design reservoir crest height. The optimum point represents the design reservoir height and the corresponding annual energy production level. In addition, according to the Turkey Electricity Statistics Report by Turkish Electricity Transmission Corporation, the annual electricity consumption in a typical household (family of 4 people) is 3036 kWh (Turkish Electricity Transmission Corporation, 2021). The Annual Energy Production for 100m optimized WEC is almost satisfy the electricity need of 4 families.

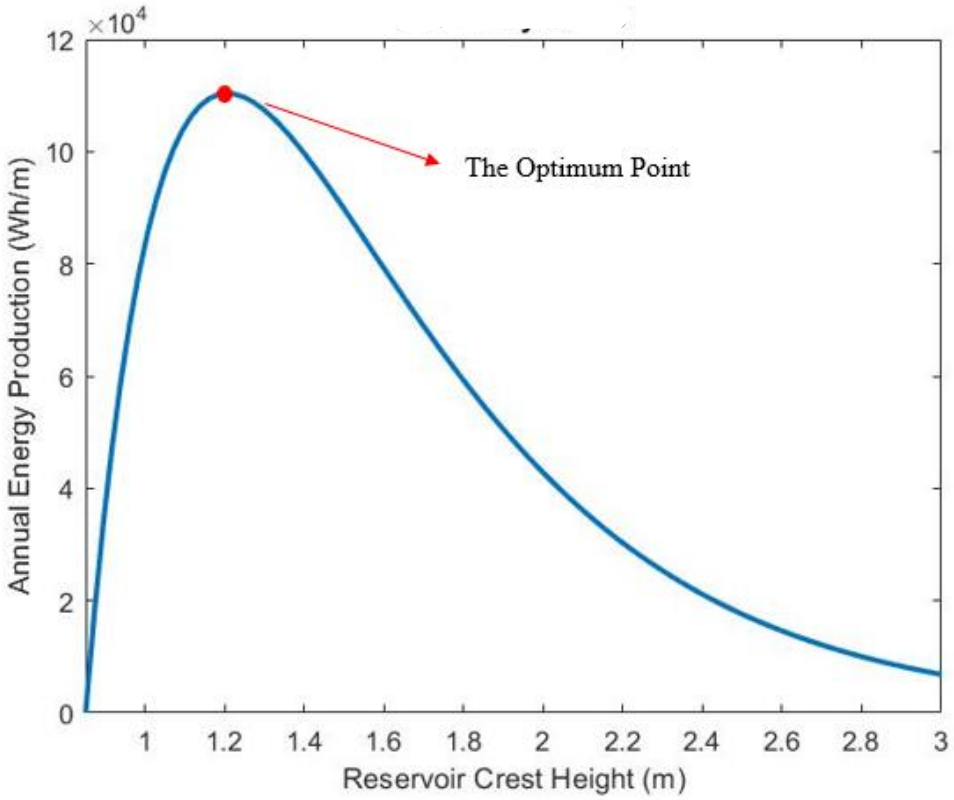

Figure 4.2 Efficiency Curve for Cayeli Breakwater Overtopping WEC Optimization

The optimum point is selected as the point in which the energy production is maximum as shown in the Figure 4.2. Due to the balance for the optimization between the reservoir head and overtopping volume, when the energy production output is low in the intervals 0-1m and 1.5-3m, it peaks close to 1.20m. Optimum crest height value is decided as 1.21m for the greatest annual energy production value 110.37 kWh/m in the attempted cases.

4.2 Cide Fishery

The main breakwater of Cide Fishery has a length 555m. The breakwater orientation is almost parallel to the shoreline as seen in Figure 4.3. Therefore, the water depth at the head of the breakwater is almost close to the water depth in the other parts of the breakwater.

Although the dock capacity of the Cide Fishery is 265 boats, the intensity is 49.4% in fishing season and only 7.9% out of fishing season as seen in Table 4.6. There is a huge usage difference between the fishing seasons and other times for Cide Fishery. It can be deduced that most of the users of the Cide Fishery are fishers and it is quite unused out of fishing season. Thus, Cide Fishery may also be classified as an idle fishery which is not availably used by boats especially out of the fishing seasons.

Figure 4.3 The Breakwater of Cide Fishery (Google Earth, 2022)

Table 4.6 Structural and Intensity Criteria for Cide Fishery (FCSSNAR,2011)

Structural Criteria	
Main Breakwater Length (m)	555
Secondary Breakwater Length (m)	512
Dock Length and Depth (m)	126,10 m (-6 m), 270 m (-3 m), 120 m (-4 m), 34 m (-5 m)
Intensity Criteria	
Dock Capacity (boat)	265
The intensity in Fishing Season (%)	49.4
The intensity out of Fishing Season (%)	7.9

Main wave directions are ENE, NE, and E, in Cide Region as seen in Table 4.7 and Table 4.8. The waves from these directions are 43.14% of the total number of waves. The highest waves which have greater frequency than 0.01% (slightly higher than 1 hour/year) come from ENE, W and WSW directions as 4.4m. The waves above 4m wave height are almost 8 hours in dominant directions and 14 hours in all directions in a year. W and WSW directions may also be considered as dominant direction however, even the waves are high in data point in deep water region, WSW waves are impossible to propagate through the Cide breakwater due to the orientation and placement of the breakwater. However, waves coming from W direction are used in the models in addition to the direction WNW, NW, NNW, N and NNE as seen in the Table 4.9. In addition to this wave analysis, the extreme wave analysis was provided from Zonguldak Eren Port Breakwater Damage and Repair Consultancy Report prepared by METU Coastal and Ocean Engineering Laboratory (METU Coastal and Ocean Engineering Laboratory, 2018). In the report, 100 year return period significant wave height and wave period are 9.11m and 11.85s, 50 year return period significant wave height and wave period are 8.76m and 11.62s, the steepness value is also 0.039.

Table 4.7 Cide Wave Frequency Table (%) (East Directions)

H / Dir	NNE	NE	ENE	E	ESE	SE	SSE	S
0	1.66	2.04	2.22	2.42	0.68	0.25	0.15	0.15
0.4	2.99	4.52	5.06	5.70	0.86	0.39	0.33	0.28
0.8	1.45	3.10	3.49	3.40	0.16	0.10	0.10	0.11
1.2	0.65	1.78	2.02	1.57	0.02	0.01	0.02	0.03
1.6	0.36	1.01	1.04	0.66	0.00	0.00	0.00	0.01
2	0.20	0.53	0.59	0.29	0.00	0.00	0.00	0.00
2.4	0.13	0.38	0.32	0.12	0.00	0.00	0.00	0.00
2.8	0.06	0.20	0.20	0.05	0.00	0.00	0.00	0.00
3.2	0.03	0.11	0.09	0.02	0.00	0.00	0.00	0.00
3.6	0.01	0.05	0.05	0.02	0.00	0.00	0.00	0.00
4	0.00	0.03	0.02	0.01	0.00	0.00	0.00	0.00
4.4	0.00	0.01	0.01	0.00	0.00	0.00	0.00	0.00
4.8	0.00	0.00	0.00	0.00	0.00	0.00	0.00	0.00
5.2	0.00	0.00	0.00	0.00	0.00	0.00	0.00	0.00
5.6	0.00	0.00	0.00	0.00	0.00	0.00	0.00	0.00
SUM	7.53	13.77	15.10	14.27	1.72	0.75	0.59	0.58

Table 4.8 Cide Wave Frequency Table (%) (West Directions)

H / Dir	SSW	SW	WSW	W	WNW	NW	NNW	N
0	0.17	0.31	0.73	0.94	1.00	1.23	1.77	1.66
0.4	0.31	0.61	2.44	2.49	1.97	2.36	3.49	3.08
0.8	0.14	0.32	1.88	1.84	1.24	1.53	2.23	1.76
1.2	0.05	0.15	1.16	1.08	0.70	0.92	1.32	0.85
1.6	0.01	0.05	0.63	0.55	0.35	0.49	0.63	0.37
2	0.00	0.01	0.32	0.31	0.20	0.28	0.29	0.17
2.4	0.00	0.01	0.17	0.17	0.12	0.13	0.16	0.09
2.8	0.00	0.01	0.08	0.10	0.05	0.09	0.07	0.05
3.2	0.00	0.01	0.04	0.05	0.03	0.04	0.03	0.02
3.6	0.00	0.00	0.02	0.02	0.02	0.02	0.01	0.01
4	0.00	0.00	0.01	0.01	0.01	0.01	0.00	0.00
4.4	0.00	0.00	0.01	0.01	0.00	0.00	0.00	0.00
4.8	0.00	0.00	0.00	0.00	0.00	0.00	0.00	0.00
5.2	0.00	0.00	0.00	0.00	0.00	0.00	0.00	0.00
5.6	0.00	0.00	0.00	0.00	0.00	0.00	0.00	0.00
SUM	0.69	1.47	7.49	7.56	5.69	7.09	10.02	8.06

Table 4.9 Cide Wave Height at Deep Water and Toe of the Breakwater

Direction	Hs deep (m)	Hs breakwater (m)
W	0.8	0.59
W	1.2	0.89
W	1.6	1.20
W	2	1.46
W	2.4	1.55
W	2.8	1.61
WNW	0.8	0.61
WNW	1.2	0.92
WNW	1.6	1.26
WNW	2	1.47
WNW	2.4	1.55
WNW	2.8	1.60
NW	0.8	0.62
NW	1.2	0.93
NW	1.6	1.21
NW	2	1.43
NW	2.4	1.54
NW	2.8	1.59
NNW	0.8	0.70
NNW	1.2	1.07
NNW	1.6	1.41
NNW	2	1.55
NNW	2.4	1.60
NNW	2.8	1.61
N	0.8	0.66
N	1.2	1.00
N	1.6	1.41
N	2	1.47
N	2.4	1.55
N	2.8	1.60
NNE	0.8	0.49
NNE	1.2	0.73
NNE	1.6	0.98
NNE	2	1.25
NNE	2.4	1.48
NNE	2.8	1.51

The SWAN wave model results were used to obtain the optimized OBREC type overtopping WEC dimensions which are given in the Table 4.10. Crest height (R_c) is 1.20m and reservoir width (B) is 0.44m.

Table 4.10 Cide Overtopping WEC Optimization and Energy Results

Reservoir Depth (h1) (m)	0.35
Crest Height (Rc) (m)	1.20
Reservoir Width (B) (m)	0.44
Annual Energy Production (kWh/m)	336.59
Annual Energy Production for 100m (kWh)	33659

Then, efficiency curve for Cide breakwater overtopping WEC optimization is given in the Figure 4.4. The optimum point is shown as the red point where the energy production is maximum. The greatest annual energy production value 336.59 kWh/m for the optimum crest height value. The Annual Energy Production for 100m optimized WEC satisfies the electricity need of 11 families.

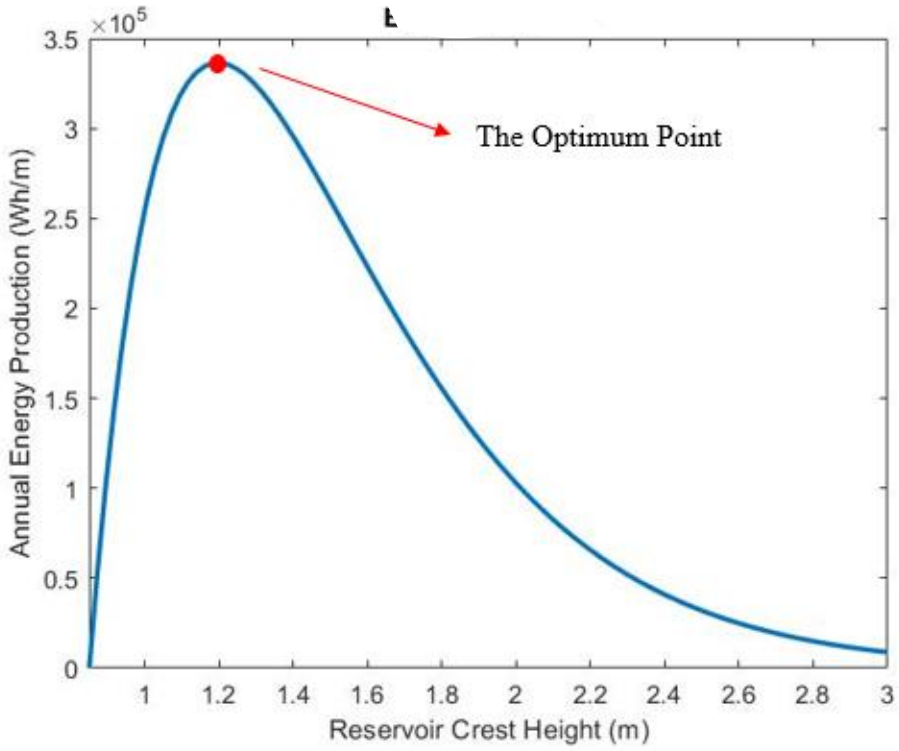

Figure 4.4 Efficiency Curve for Cide Breakwater Overtopping WEC Optimization

For the first main discussion, the seasonal distribution of waves in Cide case is analyzed by using the cumulative wave tables. Figure 4.5 shows the seasonal exceedance probabilities for Cide region to observe the difference between the seasons. When the total number of waves are compared between the seasons, there is not any significant differences for the main wave directions WNW and NW between the seasons for Cide wave data.

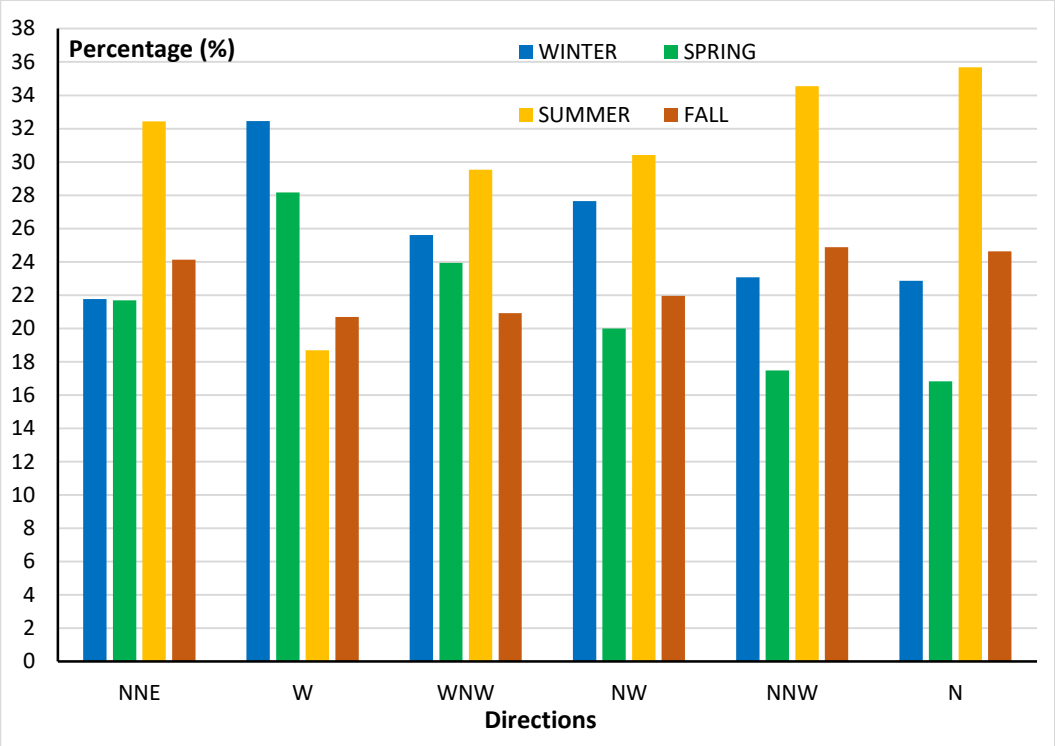

Figure 4.5 Seasonal Exceedance Probability for Cide Region

A balanced wave distribution is observed for the main wave directions WNW and NW between the seasons for Cide wave data of 43 years in the figure above. However, in the winter and fall seasons, number of waves in the interval of 2.00-3.60m are more than the number of waves in the interval of 2.00-3.60m in spring and summer seasons. This difference is critical for the overtopping WEC in terms of energy production.

When the seasonal energy production of WEC optimization for Cide Breakwater is evaluated, it can be explicitly seen in Table 4.11 that the energy production in winter and fall is higher in number than in spring and summer. Therefore, it is better to consider the number of high waves rather than the total number of waves due to the significant overtopping capacity of the high waves (2.00-3.60m in this case) for the optimization of overtopping wave energy converter into a breakwater.

Table 4.11 Seasonal Energy Production of WEC Optimization for Cide Breakwater

	ENERGY PRODUCTION (kWh/m)
WINTER	187.7
SPRING	33.3
SUMMER	27.3
FALL	106.8

4.3 Amasra Port

Amasra Port has a 655m long main breakwater. The head of the breakwater is in a deeper region than the other parts of the breakwater. The breakwater orientation is almost parallel to the shoreline as seen in Figure 4.6. In addition, there are two islands on the NW side of the breakwater which affects the incoming wave heights at the toe of the breakwater, especially for the part of the main breakwater which is close to the land.

When Table 4.12 is investigated, it is seen that the dock capacity of the Amasra Port is 160 boats, and the intensity is 62.5% in fishing season and 75% out of fishing season. The Amasra Port has higher intensity rates both in and out of the fishing season. The port is actively used for touristic activity in addition to the usage of the fishers.

Figure 4.6 The Breakwater of Amasra Port (Google Earth, 2022)

Table 4.12 Structural and Intensity Criteria for Amasra Port (FCSSNAR,2011)

Structural Criteria	
Main Breakwater Length (m)	655
Secondary Breakwater Length (m)	335
Dock Length and Depth (m)	150 m (-3 m), 60 m (-2 m), 200 m
Intensity Criteria	
Dock Capacity (boat)	160
The intensity in Fishing Season (%)	62.5
The intensity out of Fishing Season (%)	75.0

The waves from NE and ENE directions are 38.31% of the total number of waves in Amasra Region, as seen in Table 4.13 and Table 4.14. Moreover, highest waves propagate from the same direction. Thus, the main wave directions are NE and ENE. The highest waves which have greater frequency than 0.01% come from ENE direction as 4.8m. The waves above 4m wave height in all directions is almost 7 hours in a year.

Table 4.13 Amasra Wave Frequency Table (%) (East Directions)

H / Dir	**NNE**	**NE**	**ENE**	**E**	**ESE**	**SE**	**SSE**	**S**
0	2.08	2.79	3.85	1.34	0.29	0.17	0.13	0.15
0.4	3.77	5.87	8.26	1.41	0.26	0.20	0.25	0.26
0.8	1.79	3.46	5.30	0.21	0.03	0.02	0.05	0.05
1.2	0.77	1.91	2.45	0.03	0.00	0.00	0.00	0.01
1.6	0.41	1.02	1.15	0.01	0.00	0.00	0.00	0.00
2	0.21	0.51	0.60	0.00	0.00	0.00	0.00	0.00
2.4	0.10	0.34	0.24	0.00	0.00	0.00	0.00	0.00
2.8	0.08	0.13	0.15	0.00	0.00	0.00	0.00	0.00
3.2	0.04	0.08	0.08	0.00	0.00	0.00	0.00	0.00
3.6	0.02	0.03	0.03	0.00	0.00	0.00	0.00	0.00
4	0.00	0.02	0.02	0.00	0.00	0.00	0.00	0.00
4.4	0.00	0.00	0.01	0.00	0.00	0.00	0.00	0.00
4.8	0.00	0.00	0.01	0.00	0.00	0.00	0.00	0.00
5.2	0.00	0.00	0.00	0.00	0.00	0.00	0.00	0.00
5.6	0.00	0.00	0.00	0.00	0.00	0.00	0.00	0.00
SUM	9.27	16.16	22.15	3.01	0.58	0.40	0.44	0.47

Table 4.14 Amasra Wave Frequency Table (%) (West Directions)

H / Dir	SSW	SW	WSW	W	WNW	NW	NNW	N
0	0.21	0.43	0.85	1.04	1.21	1.23	1.70	2.09
0.4	0.35	0.68	2.34	2.81	1.93	2.25	3.51	3.69
0.8	0.11	0.29	1.51	1.91	1.16	1.39	2.32	2.05
1.2	0.03	0.10	0.77	0.93	0.57	0.80	1.32	0.93
1.6	0.00	0.02	0.34	0.46	0.27	0.39	0.65	0.40
2	0.00	0.00	0.17	0.22	0.16	0.21	0.31	0.16
2.4	0.00	0.00	0.07	0.11	0.08	0.10	0.19	0.09
2.8	0.00	0.01	0.04	0.06	0.03	0.05	0.07	0.05
3.2	0.00	0.00	0.02	0.03	0.02	0.02	0.03	0.03
3.6	0.00	0.00	0.00	0.01	0.02	0.01	0.02	0.01
4	0.00	0.00	0.01	0.01	0.00	0.00	0.00	0.01
4.4	0.00	0.00	0.00	0.00	0.00	0.00	0.01	0.00
4.8	0.00	0.00	0.00	0.00	0.00	0.00	0.00	0.00
5.2	0.00	0.00	0.00	0.00	0.00	0.00	0.00	0.00
5.6	0.00	0.00	0.00	0.00	0.00	0.00	0.00	0.00
SUM	0.71	1.54	6.13	7.57	5.47	6.46	10.12	9.52

NW, NNW, N, NNE and NE directions were used in the model owing to the orientation of the breakwater. There is not any wave data higher than 2.8m with higher frequency than 0.01% which is the upper limit for wave height studied in the model for Amasra site as seen in Table 4.15. However, the extreme wave analysis was provided from Zonguldak Eren Port Breakwater Damage and Repair Consultancy Report (METU Coastal and Ocean Engineering Laboratory, 2018). In the report, 100 year return period significant wave height and wave period are 9.11m and 11.85s, 50 year return period significant wave height and wave period are 8.76m and 11.62s, the steepness value is also 0.039.

Table 4.15 Amasra Wave Height at Deep Water and Toe of the Breakwater

Direction	Hs deep(m)	Hs breakwater(m)
NW	0.80	0.64
NW	1.20	0.93
NW	1.60	1.2
NW	2.00	1.49
NW	2.40	1.76
NW	2.80	2.03
NNW	0.80	0.66
NNW	1.20	0.98
NNW	1.60	1.29
NNW	2.00	1.58
NNW	2.40	1.88
NNW	2.80	2.16
N	0.80	0.66
N	1.20	1.01
N	1.60	1.29
N	2.00	1.61
N	2.40	1.92
N	2.80	2.22
NNE	0.80	0.5
NNE	1.20	0.74
NNE	1.60	1.01
NNE	2.00	1.44
NNE	2.40	1.51
NNE	2.80	1.7
NE	0.80	0.62
NE	1.20	0.91
NE	1.60	1.17
NE	2.00	1.44
NE	2.40	1.69
NE	2.80	1.98

The results of OBREC type overtopping WEC optimization dimensions for Amasra breakwater are given in the Table 4.16. Crest height (R_c) is 1.29m and reservoir width (B) is 0.55m which are slightly higher than the dimensions of the WECs in Cayeli and Cide cases.

Table 4.16 Amasra Overtopping WEC Optimization and Energy Results

Reservoir Depth (h1) (m)	0.44
Crest Height (Rc) (m)	1.29
Reservoir Width (B) (m)	0.55
Annual Energy Production (kWh/m)	478.54
Annual Energy Production for 100m (kWh)	47854

Efficiency curve for Amasra breakwater overtopping WEC optimization is given in the Figure 4.7. The optimum point represents the maximum energy production value as 478.54 kWh/m and the optimum crest height value as 1.29m. The annual energy production for 100m optimized WEC satisfies the electricity need of 16 families approximately.

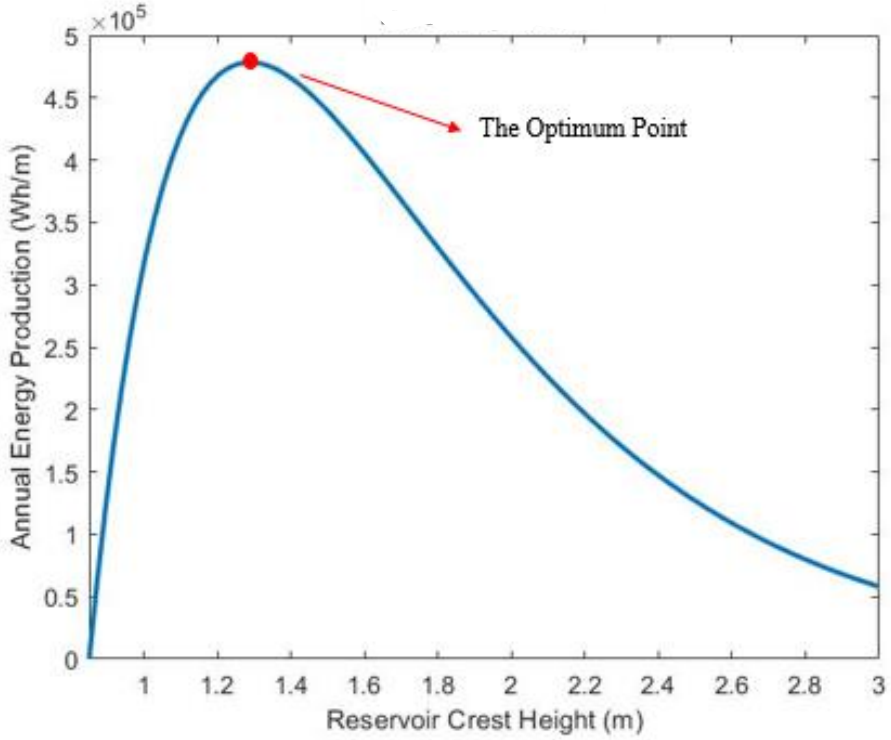

Figure 4.7 Efficiency Curve for Amasra Breakwater Overtopping WEC Optimization

The depth effect on wave height and energy output was investigated in the case of Amasra Breakwater overtopping WEC optimization. The wave heights were taken from the model results of the Amasra Region at the depths of 7m, 9m, and 12m in front of the breakwater and given in Table 4.17. When the wave height results are compared, it can be noticed that the wave heights are greater when the depth is higher in front of the breakwater. This causes a significant energy difference between the sections of the optimized WEC. Therefore, two approaches could be taken in this situation, one of them is designing the WEC cross-section with respect to the midpoint of the breakwater. The other approach could be designing every section of the WEC according to the wave heights acquired from the models for selected points on the breakwater. However, optimizing the WEC with different cross-sections may become inefficient due to the possible little differences between the sections. The

cross-section differences like the 5 cm difference between the reservoir crest heights of the two sections may become impracticable when the WEC will be built.

Table 4.17 Wave Height Values at the depths 7m, 9m and 12m at the Toe of Amasra Breakwater

Depth at Toe / Directions	Hs Deep Water (m)	7m	9m	12m
NW	0.80	0.45	0.65	0.68
NW	1.20	0.69	0.93	0.98
NW	1.60	0.97	1.21	1.25
NW	2.00	1.21	1.49	1.55
NW	2.40	1.35	1.77	1.83
NW	2.80	1.53	2.05	2.15
NNW	0.80	0.63	0.67	0.68
NNW	1.20	0.92	0.98	1.00
NNW	1.60	1.20	1.29	1.31
NNW	2.00	1.48	1.58	1.60
NNW	2.40	1.8	1.9	1.94
NNW	2.80	2.01	2.15	2.22
N	0.80	0.62	0.66	0.68
N	1.20	0.91	0.99	1.02
N	1.60	1.19	1.26	1.30
N	2.00	1.5	1.57	1.61
N	2.40	1.79	1.9	1.94
N	2.80	2.1	2.18	2.25
NNE	0.80	0.62	0.65	0.67
NNE	1.20	0.9	0.95	0.98
NNE	1.60	1.19	1.26	1.28
NNE	2.00	1.48	1.53	1.58
NNE	2.40	1.68	1.76	1.81
NNE	2.80	1.95	2.05	2.14
NE	0.80	0.52	0.62	0.60
NE	1.20	0.84	0.92	0.90
NE	1.60	1.04	1.16	1.12
NE	2.00	1.28	1.44	1.40
NE	2.40	1.54	1.7	1.64
NE	2.80	1.79	1.96	1.89

Table 4.18 Energy Output at the Depths 7m, 9m, and 12m at the Toe of Amasra Breakwater

Section	Depth (m)	Energy Output Annual per meter (Wh)
1	7	332623
2	9	448511
3	12	482031

Energy output calculated by using the wave heights at the depths of 7m, 9m, and 12m are given in Table 4.18. The input wave heights of this calculation are the wave heights given in Table 4.17. The cross-section of the WEC was optimized with respect to the wave heights for the depth of 9m since it is the average depth of the Amasra Breakwater. The energy difference between the sections of the breakwater is at a significant level. The energy produced in section 1 is 26% lower than the energy produced in section 2 and the energy produced in section 3 is %9 higher than the energy produced in section 2.

In the literature, since the focus is on the single point WEC optimization into breakwaters, the wave difference may occur along the breakwaters was not studied in detail. However, as a result of this study, it is noticed that wave height differences due to refraction, diffraction and shoaling along the breakwaters may cause substantial effects for the optimization process and it is critical for wave energy production. Therefore, for the energy calculations, assuming the energy production the same along a long part of any breakwater may be deceptive and it may create a significant level of uncertainty in the optimization. Thus, it can be deduced from the results that calculating the energy amount produced by a breakwater integrated WEC and using it for energy production of a 100m section of the breakwaters may be risky in the aspect of calculations for the physical applications of breakwater integrated WECs.

4.4 Kiyikoy Fishery

The main breakwater of Kiyikoy Fishery has a length of 290m which is shorter than the other pilot breakwaters. The main breakwater orientation is close to parallel to the shoreline as seen in Figure 4.8.

When Table 4.19 is investigated, it is seen that even though the dock capacity of the Kiyikoy Fishery is 300 boats, the intensity is 136.4% in fishing season and 89.1% out of fishing season. The intensity of the fishing season shows the overuse of the fishery and the need for bigger fisheries in the same region. There is a significant usage difference between the fishing seasons and other seasons for Kiyikoy Fishery. An important amount of the users of Kiyikoy Fishery are fishers but, it is also intensively used out of fishing season. Thus, Cayeli Fishery may also be classified as an active fishery.

Figure 4.8 The Breakwater of Kiyikoy Fishery (Google Earth, 2022)

Table 4.19 Structural and Intensity Criteria for Kiyikoy Fishery (FCSSNAR,2011)

Structural Criteria	
Main Breakwater Length (m)	290
Secondary Breakwater Length (m)	140
Dock Length and Depth (m)	251.5 m (-2 m)
Intensity Criteria	
Dock Capacity (boat)	300
The intensity in Fishing Season (%)	136.4
The intensity out of Fishing Season (%)	89.1

In Kiyikoy Region, main wave directions are NE, ENE and NNE directions from Table 4.20 and 4.21. The waves from these directions are 60.77% of the total number of waves. The highest waves which have greater frequency than 0.01% (slightly higher than 1 hour/year) come from NNE direction as 5.6m. The frequency 0.11% corresponds to 10 hours in a year in the data. The waves above 4m wave height in NNE direction is close to 10 hours in a year. In addition, the waves higher than 4.4m is almost 18 hours in a year in all directions. N direction is also considered as the fourth dominant direction but, after the model results are evaluated, it is noticed that the waves coming from north have significant decrease in wave height due to the topography of the Kiyikoy and location of the Kiyikoy Fishery which is protected by a bay which is in the large boundary of model. In addition, the extreme wave analysis was provided from IGA Wave Climate Analysis Report prepared by METU Coastal and Ocean Engineering Laboratory (METU Coastal and Ocean Engineering Laboratory,2020). In the report, 100 year return period significant wave height and wave period are 8.58m and 11.78s, 50 year return period significant wave height and wave period are 8.03m and 11.33s, the steepness value is also 0.039.

Table 4.20 Kiyikoy Wave Frequency Table (%) (East Directions)

H / Dir	NNE	NE	ENE	E	ESE	SE	SSE	S
0	2.36	3.49	4.68	2.95	1.61	0.94	0.69	0.67
0.4	5.94	7.40	9.02	2.17	0.84	0.51	0.47	0.64
0.8	3.88	4.46	4.56	0.33	0.11	0.08	0.09	0.22
1.2	2.39	2.21	1.90	0.07	0.02	0.01	0.02	0.06
1.6	1.51	1.26	0.89	0.01	0.00	0.00	0.00	0.01
2	0.92	0.72	0.44	0.00	0.00	0.00	0.00	0.00
2.4	0.55	0.40	0.22	0.00	0.00	0.00	0.00	0.00
2.8	0.32	0.20	0.11	0.00	0.00	0.00	0.00	0.00
3.2	0.20	0.12	0.06	0.00	0.00	0.00	0.00	0.00
3.6	0.14	0.10	0.03	0.00	0.00	0.00	0.00	0.00
4	0.07	0.05	0.02	0.00	0.00	0.00	0.00	0.00
4.4	0.04	0.04	0.01	0.00	0.00	0.00	0.00	0.00
4.8	0.02	0.02	0.00	0.00	0.00	0.00	0.00	0.00
5.2	0.01	0.00	0.00	0.00	0.00	0.00	0.00	0.00
5.6	0.01	0.00	0.00	0.00	0.00	0.00	0.00	0.00
SUM	18.36	20.47	21.94	5.53	2.58	1.54	1.27	1.60

Table 4.21 Kiyikoy Wave Frequency Table (%) (West Directions)

H / Dir	SSW	SW	WSW	W	WNW	NW	NNW	N
0	1.04	0.93	0.43	0.31	0.37	0.45	0.81	1.45
0.4	1.83	1.94	0.60	0.39	0.45	0.73	1.44	3.24
0.8	0.99	1.15	0.24	0.14	0.17	0.40	0.86	2.15
1.2	0.52	0.41	0.07	0.04	0.06	0.19	0.53	1.35
1.6	0.20	0.15	0.02	0.01	0.02	0.07	0.24	0.89
2	0.06	0.04	0.00	0.00	0.01	0.03	0.11	0.50
2.4	0.02	0.01	0.00	0.00	0.00	0.02	0.05	0.35
2.8	0.00	0.00	0.00	0.00	0.00	0.00	0.03	0.24
3.2	0.00	0.00	0.00	0.00	0.00	0.00	0.01	0.14
3.6	0.00	0.00	0.00	0.00	0.00	0.00	0.01	0.08
4	0.00	0.00	0.00	0.00	0.00	0.00	0.00	0.04
4.4	0.00	0.00	0.00	0.00	0.00	0.00	0.00	0.03
4.8	0.00	0.00	0.00	0.00	0.00	0.00	0.00	0.01
5.2	0.00	0.00	0.00	0.00	0.00	0.00	0.00	0.00
5.6	0.00	0.00	0.00	0.00	0.00	0.00	0.00	0.00
SUM	4.66	4.64	1.35	0.90	1.08	1.89	4.10	10.46

Table 4.22 Kiyikoy Wave Height at Deep Water and Toe of the Breakwater

Direction	Hs deep (m)	Hs breakwater (m)
NNE	0.80	0.52
NNE	1.20	0.75
NNE	1.60	0.98
NNE	2.00	1.21
NNE	2.40	1.49
NNE	2.80	1.54
NE	0.80	0.63
NE	1.20	0.93
NE	1.60	1.21
NE	2.00	1.50
NE	2.40	1.79
NE	2.80	2.16
ENE	0.80	0.70
ENE	1.20	1.04
ENE	1.60	1.37
ENE	2.00	1.68
ENE	2.40	2.02
ENE	2.80	2.33
ENE	3.20	2.59
E	0.80	0.73
E	1.20	1.08

The SWAN wave model results were utilized to gather the optimized OBREC type overtopping WEC dimensions which are given in the Table 4.23. Crest height (R_c) is 1.32 m and reservoir width (B) is 0.59m which are the highest values between the optimizations in this study. But the greatest dimensional differences between the designed sections are almost 12 cm in reservoir crest heights and 13 cm in reservoir widths.

Table 4.23 Kiyikoy Overtopping WEC Optimization and Energy Results

Reservoir Depth (h1) (m)	0.47
Reservoir Crest Height (Rc) (m)	1.32
Reservoir Width (B) (m)	0.59
Annual Energy Production (kWh/m)	885.47
Annual Energy Production for 100m (kWh)	88547

Efficiency curve for Kiyikoy breakwater overtopping WEC optimization is given in the Figure 4.9 where the maximum energy production value as 885.47 kWh/m and the optimum crest height value as 1.32 m in the optimum point. The annual energy production for 100m optimized WEC satisfies the electricity need of 30 families approximately.

WEC optimization for Kiyikoy Breakwater has the highest energy output. It also has the highest reservoir crest height since the algorithm decides the most efficient crest height value with the optimum balance of overtopping volume and reservoir head. Therefore, higher energy production values are expected for the overtopping WEC designs with higher reservoir crest heights. Overall, when the optimized Kiyikoy overtopping WEC theoretically produces the most energy among the 4 optimized overtopping WECs in this study, Cayeli overtopping WEC produces the least energy.

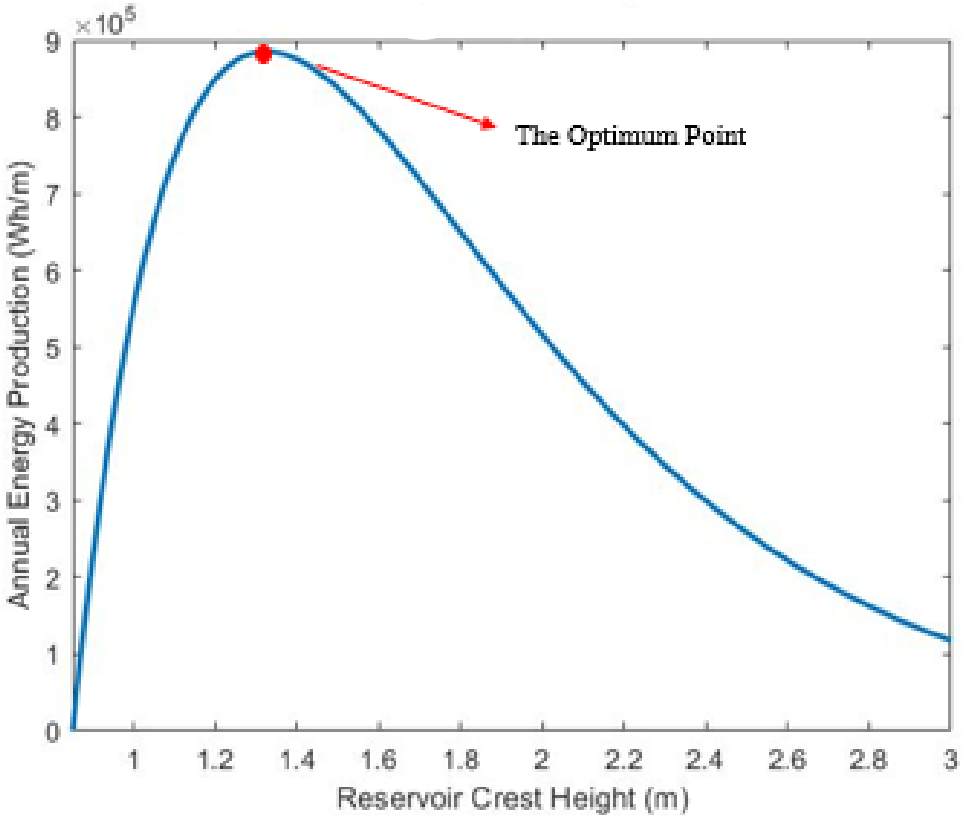

Figure 4.9 Efficiency Curve for Kiyikoy Breakwater Overtopping WEC Optimization

By considering all cases, the working hour and energy production relationship is investigated since the working hour of a WEC is an important factor for site selection and other technical decisions for WEC optimization. The total working hours for all pilot breakwaters in this case, calculated as the total time when the deep water waves are greater than 0.8m and at the same time the waves in front of the breakwater are greater than 0.5m in a year.

Table 4.24 Working Hours Percent and Annual Energy Production for Kiyikoy Breakwater WEC Optimization

	Reservoir Crest Height (Rc)	Reservoir Width (B)	Working Hours/Total Hours (%)	Annual Energy Production (kWh/m)	The Number of Households which the production meet electricity demand
Kiyikoy	1.32	0.59	17.6	885.5	30
Cide	1.21	0.44	20.4	336.6	11
Amasra	1.29	0.55	20.3	478.5	16
Cayeli	1.21	0.46	14.5	110.4	4

In the Table 4.24, when the working hour/total hour percent of optimized Amasra Breakwater WEC is greater than the optimized Kiyikoy Breakwater WEC, annual energy production in Amasra Breakwater WEC is lower than Kiyikoy Breakwater WEC. Also, optimized Cayeli Breakwater WEC has the lowest working hours' rate and annual energy production amount among these 4 cases.

The results show that there is not a direct relationship between working hours and energy production because the wave heights coming through the WEC are also a critical factor for energy production. Even though, the total number of the counted waves is higher for Amasra WEC, the fewer and higher waves in the case of Kiyikoy provide the optimized Kiyikoy WEC to produce more energy than in the Amasra Case. Thus, although the working hour of a WEC is important criteria for decisions about WEC optimization, it should not be considered regardless of incoming wave heights through the WECs in further studies. In addition, the highest dimensional differences between the designed sections are 11 cm in reservoir crest heights and 15 cm in reservoir widths among the optimized cases. WEC optimization for Kiyikoy Breakwater has the highest energy output. It also has the highest reservoir crest height since the algorithm decides the most efficient crest height value with the optimum balance of overtopping volume and reservoir head.

CHAPTER 5

CONCLUSION

The main goal of this thesis study is to investigate the effects of marine and structural conditions of the breakwater on the efficiency and optimization of wave energy converters in the existing breakwaters on the Black Sea coast of Turkey. This study also aims to contribute to reintroducing idle fisheries into the economy by integrating wave energy converters into their breakwaters.

In Turkey's Black Sea shores, idle fisheries are economically inefficient, and mainly unutilized. Idle fisheries may become profitable through electricity generation, and they may be returned to the market considering that wave energy converters are integrated into breakwaters. All fisheries along the Black Sea shores were evaluated for the selection of idle fisheries. Several structural parameters are assessed, including the length, depth, and direction of the main and secondary breakwaters. The selected breakwaters are considered as appropriate for both marine and structural conditions.

For the overtopping WEC optimization of a breakwater, the wave heights and wave frequency propagating through the breakwater were studied. So because the overtopping volume in short and long time intervals may be computed and estimated by examining the wave frequency data in front of the breakwater. Thus, wave model by SWAN Software is used to transform waves from deep sea to nearshore. The required bathymetry data were obtained from EMODNET Bathymetry Portal and the wave data were obtained for the years 1979-2021 from the ECMWF Era5 database. The results of the wave transformation are evaluated as proper by taking the effect of physical processes and site-specific bathymetric and climatic conditions. In addition, it is observed that SWAN Wave Model works

satisfactorily on wave transformation for the conditions of the Black Sea Coast of Turkey.

At last, by developing an optimization algorithm, the integration of overtopping type wave energy converters into existing breakwaters was examined. The designed sections of overtopping WEC and energy outputs were produced by the optimization algorithm. The energy outputs and wave model results were beneficial for the investigation of the effects of marine and structural conditions of the breakwater on the efficiency and optimization of overtopping WECs into the existing breakwaters in the Black Sea coast of Turkey.

The significant findings of this research were discussed in detail in the discussion part. Firstly, the depth effect on wave height and energy output was investigated in the case of Amasra Breakwater overtopping WEC optimization. When the depth in front of the breakwater is higher, the wave heights are also higher. This results in a large energy difference between the segments of optimized WECs. Therefore, it can be deduced that incoming wave height variations along the breakwaters can have a significant impact on the optimization process. As a result, assuming the energy production is the same along a large section of any breakwater for energy estimates can be misleading and lead to a high amount of uncertainty for the optimization process.

Secondly, the effect of the seasonal distribution of waves on energy production for Cide Breakwater was evaluated. Due to the substantial overtopping potential of the high waves for the crest height of the designed WEC, it is best to consider the frequency of high waves rather than the overall frequency and the total number of waves when optimizing an overtopping wave energy converter into a breakwater.

Lastly, the effect of working hours of a breakwater integrated overtopping WEC on energy production was evaluated and it is deduced that there is no direct relationship between working hours and energy output. As a consequence, even though the working hour of a WEC is an essential parameter for WEC optimization, it should not be taken into account independent of incoming wave heights.

Ultimately, this study includes the wave transformation process and overtopping WEC into 4 selected breakwaters. Since wave energy converter optimization into breakwaters is a newly-emerging research area, numerous further studies may be conducted. The experimental studies may investigate the overtopping volume and energy output for overtopping type WEC. Also, physical experiments for overtopping volume through the rear side of the breakwater for the optimized system can be performed to test the stability of overtopping type WEC integrated breakwaters. Furthermore, cost may be analysed for the overtopping WEC integration into the breakwaters and the produced energy in the WEC optimization. Moreover, the algorithm may be improved by time dependent water accumulation into the reservoir approach and hourly based wave approach. Lastly, overtopping type WECs can be optimized for different types of turbines.

REFERENCES

Aderinto, T., & Li, H. (2018). Ocean Wave Energy Converters: Status and challenges. *Energies*, *11*(5), 1250. https://doi.org/10.3390/en11051250

Akpınar, A., & Kömürcü, M. İ. (2012). Wave energy potential along the south-east coasts of the Black Sea. *Energy*, *42*(1), 289–302. https://doi.org/10.1016/j.energy.2012.03.057

Akpınar, A., & Kömürcü, M. İ. (2013). Assessment of wave energy resource of the Black Sea based on 15-year numerical hindcast Data. *Applied Energy*, *101*, 502–512. https://doi.org/10.1016/j.apenergy.2012.06.005

Akpınar, A., Bingölbali, B., & Van Vledder, G. P. (2016). Wind and wave characteristics in the Black Sea based on the swan wave model forced with the CFSR winds. *Ocean Engineering*, *126*, 276–298. https://doi.org/10.1016/j.oceaneng.2016.09.026

Altas, İ. H., & Sahin, E. (2019). Dünyada ve Türkiye'de Dalga Enerjisi. *Karadeniz Teknik Üniversitesi Elektrik Mühendisliği*, 43–53.

Aydoğan, B., Ayat, B., & Yüksel, Y. (2013). Black Sea Wave Energy Atlas from 13 years Hindcasted Wave Data. *Renewable Energy*, *57*, 436–447. https://doi.org/10.1016/j.renene.2013.01.047

Bevilacqua, G., & Zanuttigh, B. (2011). Overtopping Wave Energy Converters: general aspects and stage of development. Università di Bologna.

Blackledge, J., Coyle, E., Kearney, D., McGuirk, R., & Norton, B. (2013). Estimation of wave energy from wind velocity. *Engineering Letters*, *21*, 158–170.

Cabral, T., Clemente, D., Rosa-Santos, P., Taveira-Pinto, F., Morais, T., Belga, F., & Cestaro, H. (2020). Performance assessment of a hybrid wave energy converter integrated into a harbor breakwater. *Energies*, *13*(1). https://doi.org/10.3390/en13010236

Contestabile, P., Di Lauro, E., Buccino, M., & Vicinanza, D. (2016). Economic assessment of overtopping breakwater for energy conversion (OBREC): A case study in western australia. Sustainability, 9(1), 51. https://doi.org/10.3390/su9010051

Contestabile, P., Vincenzo, F., Di Lauro, E., & Vicinanza, D. (2017). Full-scale prototype of an overtopping breakwater for Wave Energy Conversion. *Coastal Engineering Proceedings*, (35), 12. https://doi.org/10.9753/icce.v35.structures.12

Czech, B., & Bauer, P. (2012). Wave Energy Converter Concepts : Design challenges and classification. *IEEE Industrial Electronics Magazine*, *6*(2), 4–16. https://doi.org/10.1109/mie.2012.2193290

Drew, B., Plummer, A. R., & Sahinkaya, M. N. (2009). A review of Wave Energy Converter Technology. *Proceedings of the Institution of Mechanical Engineers, Part A: Journal of Power and Energy*, *223*(8), 887–902. https://doi.org/10.1243/09576509jpe782

Bathymetry. European Marine Observation and Data Network (EMODnet). (2022, May 18). Retrieved June 27, 2022, from https://emodnet.ec.europa.eu/en/bathymetry

ExxonMobil. (2012). *The outlook for energy: a view to 2040*. Texas.

Falcão, A. F. (2010). Wave Energy Utilization: A review of the technologies. *Renewable and Sustainable Energy Reviews*, *14*(3), 899–918. https://doi.org/10.1016/j.rser.2009.11.003

Guillory, A. (2022, June 17). *ERA5*. ECMWF. Retrieved June 27, 2022, from https://www.ecmwf.int/en/forecasts/datasets/reanalysis-datasets/era5

Hakulinen, J. (2020, March 30). *Energy oy*. AW. Retrieved June 29, 2022, from https://aw-energy.com/blogs/why-wave-energy-is-here-to-stay/

Harada, C. (2009). *Wave power station*. Energy and the environment a coastal perspective. Retrieved May 31, 2022, from https://coastalenergyandenvironment.web.unc.edu/ocean-energy-generating-technologies/wave-energy/oscillating-water-column/

International Renewable Energy Agency. (2014). Wave Energy: Technology Brief. IRENA Ocean Energy Technology Brief 4.

Isaacs, J. D., & Seymour, R. J. (1973). The ocean as a power resource. *International Journal of Environmental Studies*, *4*(1), 201–205. https://doi.org/https://doi.org/10.1080/00207237308709563

Iuppa, C., Contestabile, P., Cavallaro, L., Foti, E., and Vicinanza, D. (2016). Hydraulic performance of an innovative breakwater for overtopping wave energy conversion. Sustainability 8:1226. doi: 10.3390/su8121226

Iuppa, C., Cavallaro, L., Musumeci, R. E., Vicinanza, D., & Foti, E. (2019). Empirical overtopping volume statistics at an Obrec. *Coastal Engineering*, *152*, 103524. https://doi.org/10.1016/j.coastaleng.2019.103524

Keskin Citiroglu, H., & Okur, A. (2014). An approach to wave energy converter applications in Eregli on the western Black Sea coast of Turkey. *Applied Energy*, *135*, 738–747. https://doi.org/10.1016/j.apenergy.2014.05.053

Kralli, V.-E., Theodossiou, N., & Karambas, T. (2019). Optimal design of overtopping breakwater for energy conversion (OBREC) systems using the harmony search algorithm. *Frontiers in Energy Research, 7*. https://doi.org/10.3389/fenrg.2019.00080

Kofoed, J. P. (2000). Wave overtopping of marine structures—utilization of wave energy (Ph.D. thesis). Aalborg University. Hydraulics & Coastal Engineering Laboratory, Department of Civil Engineering, Aalborg University, Aalborg, Denmark.

Korde, U. A. (2000). Control system applications in wave energy conversion. *OCEANS 2000 MTS/IEEE Conference and Exhibition. Conference Proceedings*, *3*, 1817–1824. https://doi.org/10.1109/oceans.2000.882202

Lander, V. (2012). Optimization of the hydrodynamic performance of overtopping wave energy converters: experimental study of optimal geometry and probability distribution of overtopping volumes (Ph.D. thesis). Department of Civil Engineering, Ghent University, Ghent, Belgium.

López, I., Andreu, J., Ceballos, S., Martínez de Alegría, I., & Kortabarria, I. (2013). Review of wave energy technologies and the necessary power-equipment. *Renewable and Sustainable Energy Reviews*, *27*, 413–434. https://doi.org/10.1016/j.rser.2013.07.009

Mariani, A., Crispino, G., Contestabile, P., Cascetta, F., Gisonni, C., Vicinanza, D., & Unich, A. (2021). Optimization of low head axial-flow turbines for an overtopping breakwater for energy conversion: A case study. *Energies*, *14*(15), 4618. https://doi.org/10.3390/en14154618

METU Coastal and Ocean Engineering Laboratory. (2018). *Zonguldak Eren Limanı Dalgakıran Yapıları Hasar ve Onarımı Danışmanlık Hizmetleri Projesi Sonuç Raporu*

METU Coastal and Ocean Engineering Laboratory. (2020). *IGA Dalga İklimi Analizi Raporu*

METU Coastal and Ocean Engineering Laboratory. (2022). *Rize Çayeli Rüzgar ve Dalga İklimi Analizi*

Mohd Yusop, Z., Ibrahim, M. Z., Jusoh, M. A., Albani, A., & A. Rahman, S. J. (2020). Wave-activated-body energy converters technologies: A Review. *Journal of Advanced Research in Fluid Mechanics and Thermal Sciences*, *76*(1), 76–104. https://doi.org/10.37934/arfmts.76.1.76104

Mørk Gunnar, Barstow, S., Kabuth, A., & Pontes, M. T. (2010). Assessing the global wave energy potential. *29th International Conference on Ocean, Offshore and Arctic Engineering*, *3*. https://doi.org/10.1115/omae2010-20473

Mustapa, M. A., Yaakob, O. B., Ahmed, Y. M., Rheem, C.-K., Koh, K. K., & Adnan, F. A. (2017). Wave Energy Device and Breakwater Integration: A Review. *Renewable and Sustainable Energy Reviews*, *77*, 43–58. https://doi.org/10.1016/j.rser.2017.03.110

Polinder, H., & Scuotto, M. (2005). Wave Energy Converters and their impact on Power Systems. *2005 International Conference on Future Power Systems*. https://doi.org/10.1109/fps.2005.204210

Prasad, K. A., Chand, A. A., Kumar, N. M., Narayan, S., & Mamun, K. A. (2022). A critical review of power take-off wave energy technology leading to the conceptual design of a novel wave-plus-photon energy harvester for island/coastal communities' energy needs. *Sustainability*, *14*(4), 2354. https://doi.org/10.3390/su14042354

Radhakrishnan, P. V., & Senthil Prakash, M. N. (2020). A Review of Breakwater Integrated Wave Energy Converter . *International Journal of New Innovations in Engineering and Technology*, *14*(3), 18–31.

Sarmento, A. J., & Falcão, A. F. (1985). Wave generation by an oscillating surface-pressure and its application in wave-energy extraction. *Journal of Fluid Mechanics*, *150*, 467–485. https://doi.org/10.1017/s0022112085000234

Seyboth, K., Matschoss, P., Kadner, S., Zwickel, T., Eickemeier, P., Hansen, G., Schloemer, S., & Stechow, C. von. (2011). (tech.). (O. Edenhofer, R. Pichs-Madruga, & Y. Sokona, Eds.) *Special Report on Renewable Energy Sources and Climate Change Mitigation*. Cambridge University Press.

Soares, C. G., Bhattacharjee, J., Tello, M., & Pietra, L. (2012). Review and classification of Wave Energy Converters. *Maritime Engineering and Technology*, 599–608. https://doi.org/10.1201/b12726-84

Sorensen, B. (2011). Wave Energy Utilization in Europe: Current status and Perspectives. *Renewable Energy*, 487–500. https://doi.org/10.4324/9781315793245-115

The Ocean Economy in 2030. (2017). The Ocean Economy in 2030. https://doi.org/10.1787/16e4aefb-en

The Queen's University of Belfast. (2002). (rep.). Islay LIMPET wave power plant.

Turkiye Elektrik Istatistikleri Subat 2021 - EMO. (n.d.). Retrieved July 20, 2022

Uygur, R. Demirci, H. Saruhan et al. (2006). Batı Karadeniz Bölgesindeki Dalga Enerjisi Potansiyelinin Araştırılması. PAJES - Pamukkale University Journal of Engineering Sciences. 12 (1), 7–13.

Van der Meer, J. W., Allsop, N., Bruce, T., De Rouck, J., Kortenhaus, A., Pullen, T., … Zanuttigh, B. (2016). *EurOtop: Manual on wave overtopping of sea defences and related structures : an overtopping manual largely based on European research, but for worlwide application* (2nd ed.).

Vicinanza, D., Contestabile, P., Quvang Harck Nørgaard, J., & Lykke Andersen, T. (2014). Innovative rubble mound breakwaters for overtopping wave energy conversion. *Coastal Engineering*, *88*, 154–170. https://doi.org/10.1016/j.coastaleng.2014.02.004

Villate, J. L. (2016). *OES annual report 2016: Spain: Technology demonstration*. Ocean Energy Systems. Retrieved June 1, 2022, from https://report2016.ocean-energy-systems.org/country-reports/spain/technology-demonstration/

Wang, L., Isberg, J., & Tedeschi, E. (2018). Review of Control Strategies for Wave Energy Conversion Systems and their validation: The wave-to-wire approach. *Renewable and Sustainable Energy Reviews*, *81*, 366–379. https://doi.org/10.1016/j.rser.2017.06.074

Palma, G., Mizar Formentin, S., Zanuttigh, B., Contestabile, P., & Vicinanza, D. (2019). Numerical simulations of the hydraulic performance of a breakwater-integrated overtopping wave energy converter. *Journal of Marine Science and Engineering*, *7*(2), 38. https://doi.org/10.3390/jmse7020038

APPENDICES

A. Cayeli Small Domain, Wave Heights in SWAN Model Results

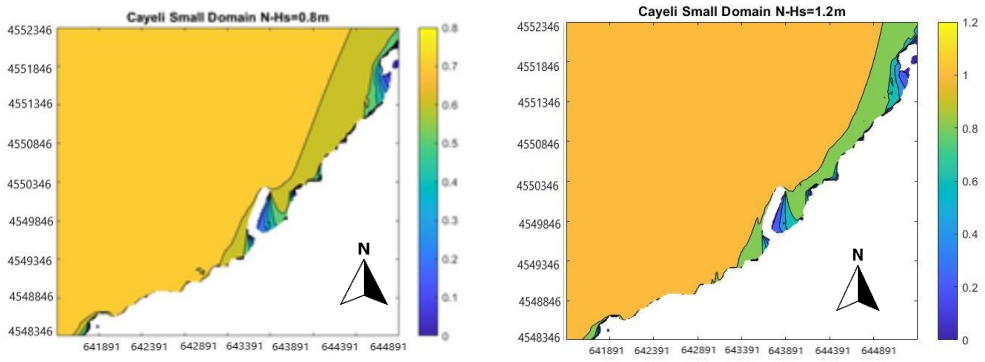

Figure A. 1 Cayeli Small Domain Model N direction

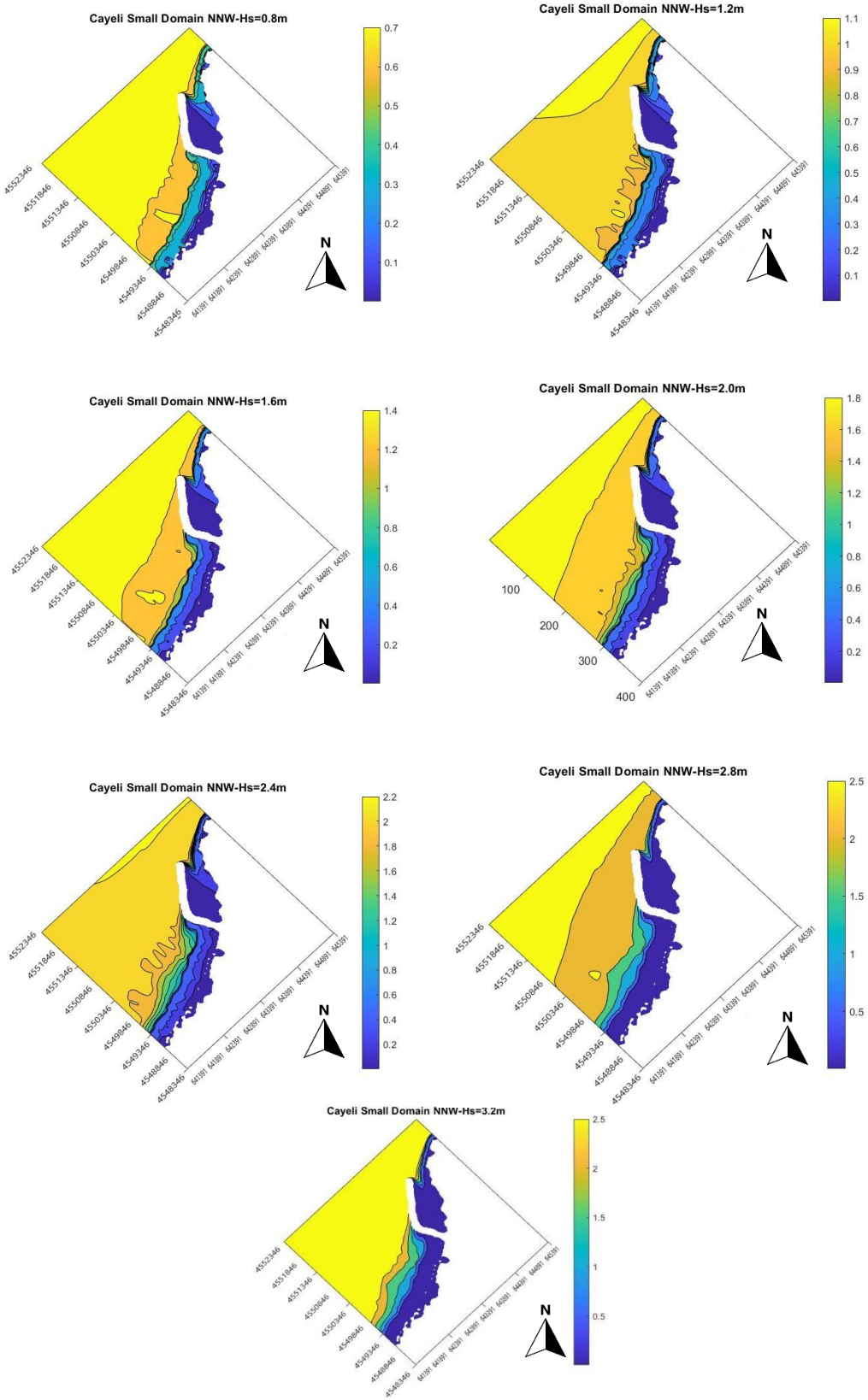

Figure A. 2 Cayeli Small Domain Model NNW Direction

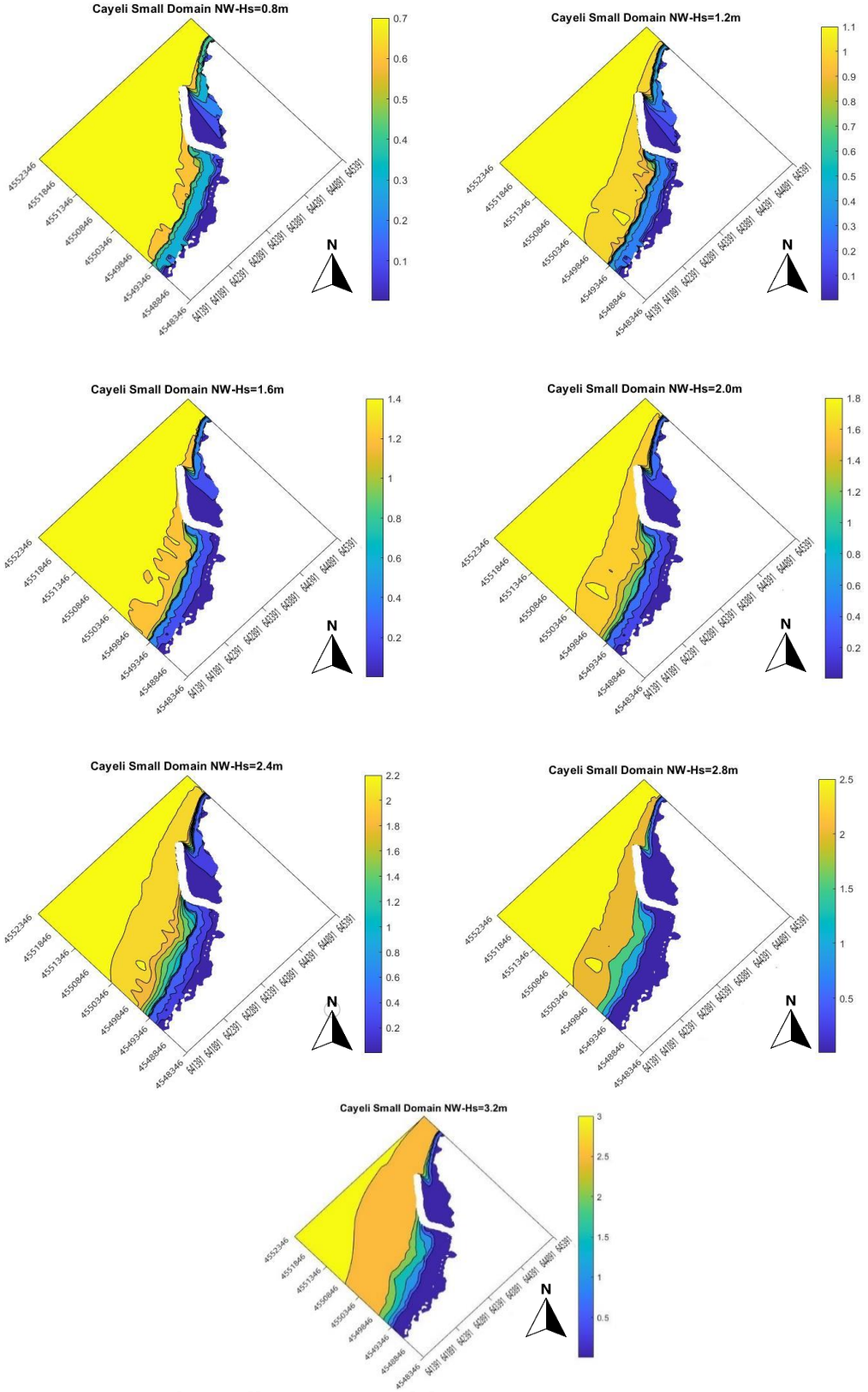

Figure A. 3 Cayeli Small Domain Model NW Direction

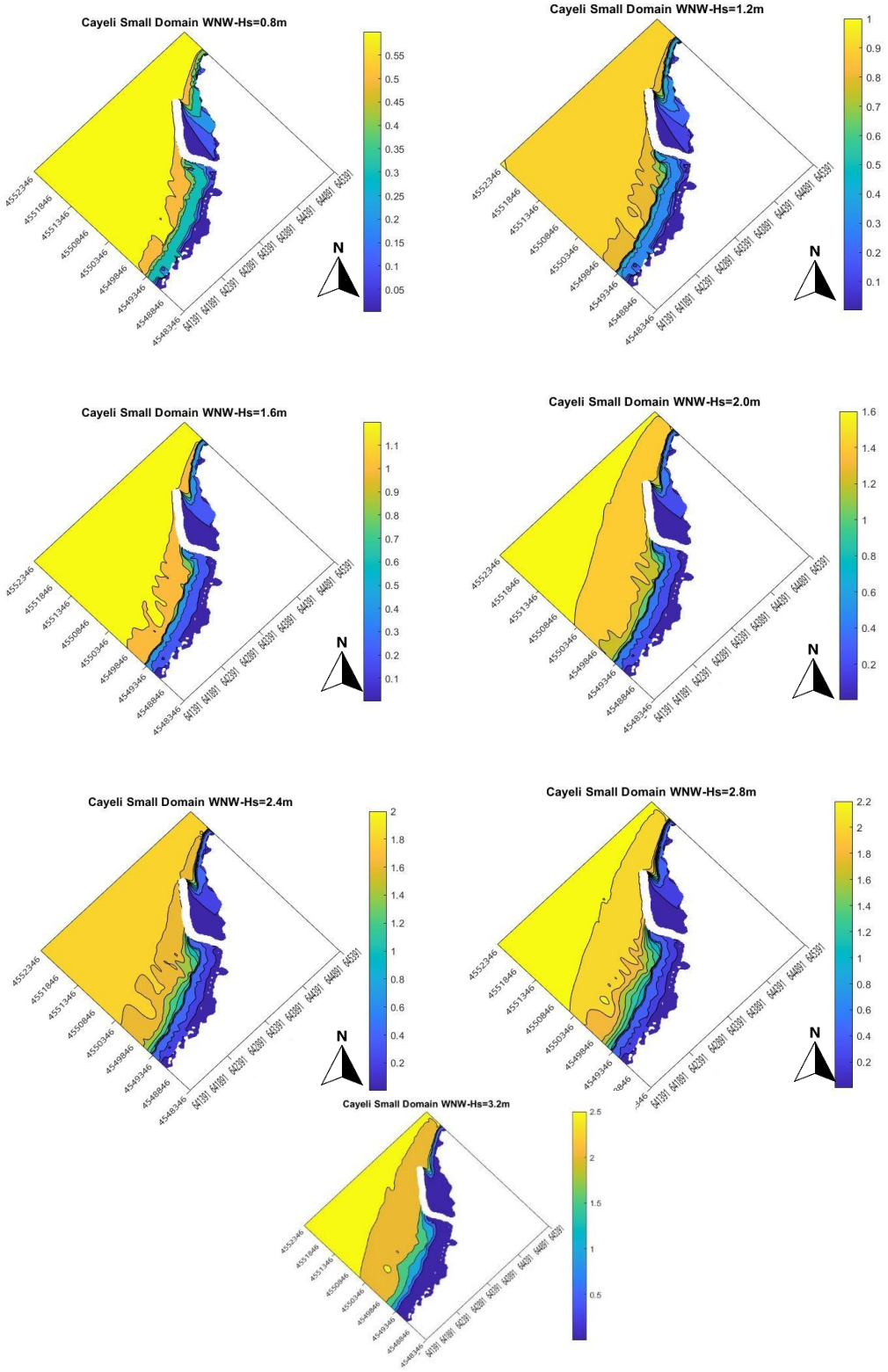

Figure A. 4 Cayeli Small Domain Model WNW Direction

B. Cide Small Domain, Wave Heights in SWAN Model Results

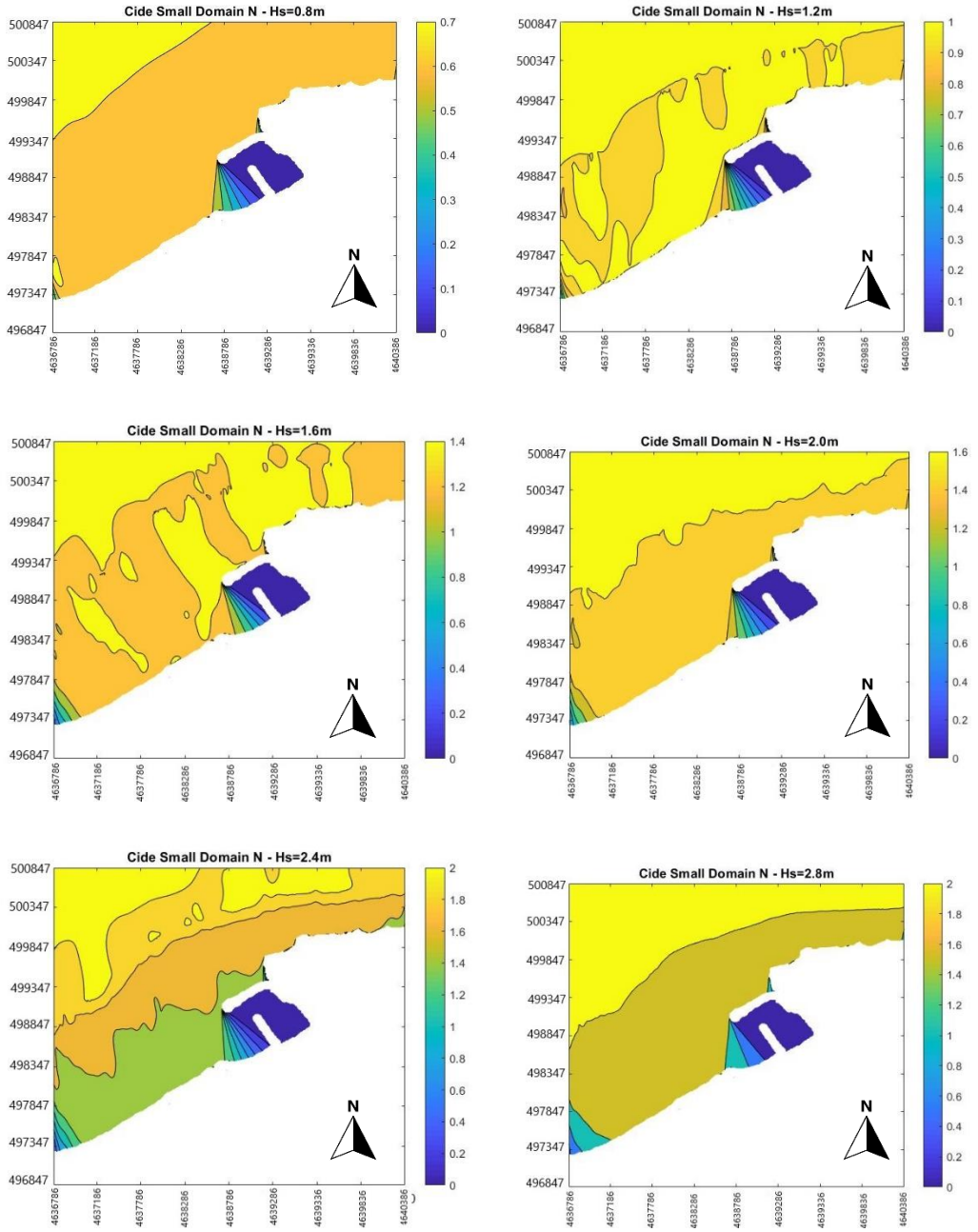

Figure B. 1 Cide Small Domain Model N Direction

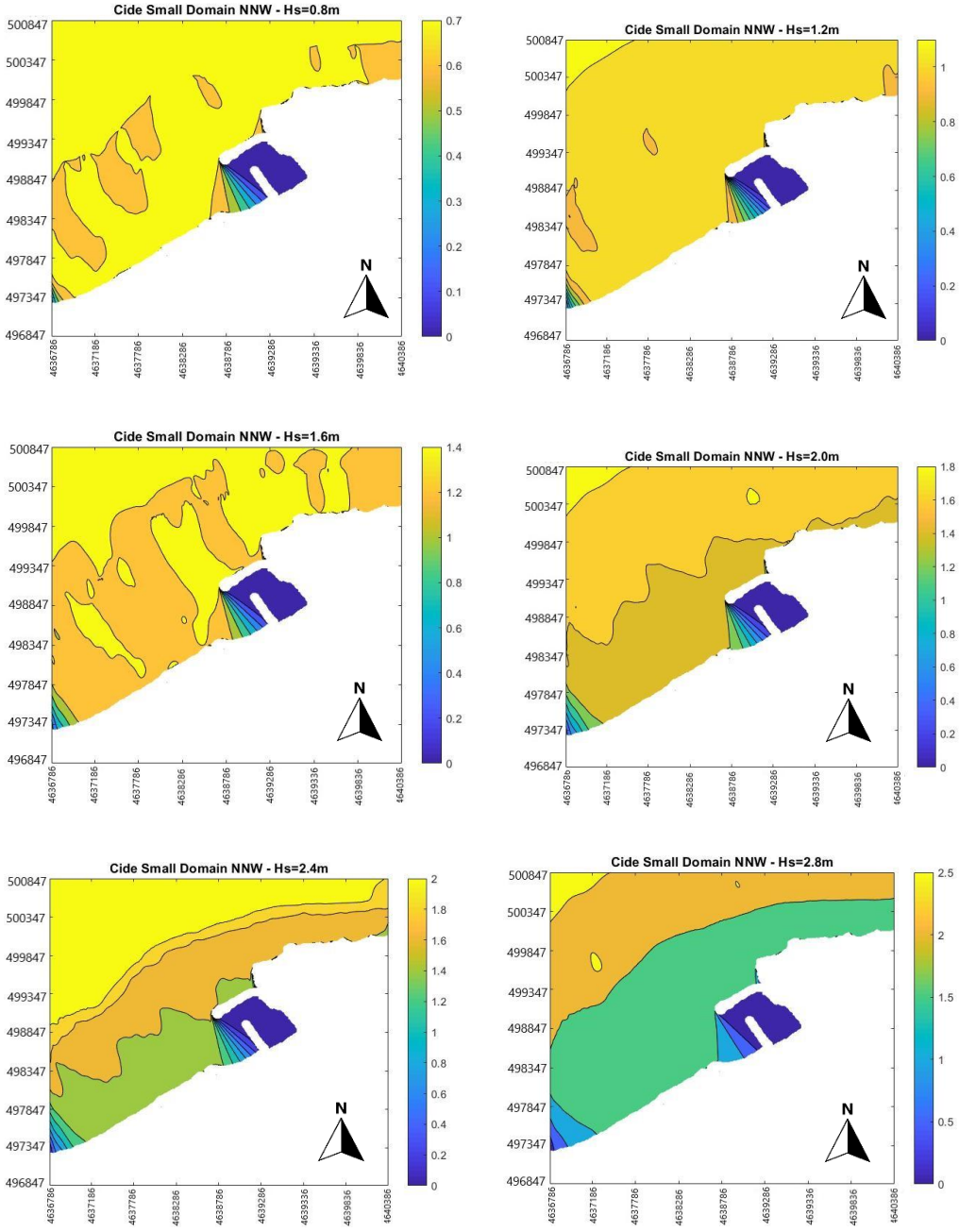

Figure B. 2 Cide Small Domain Model NNW Direction

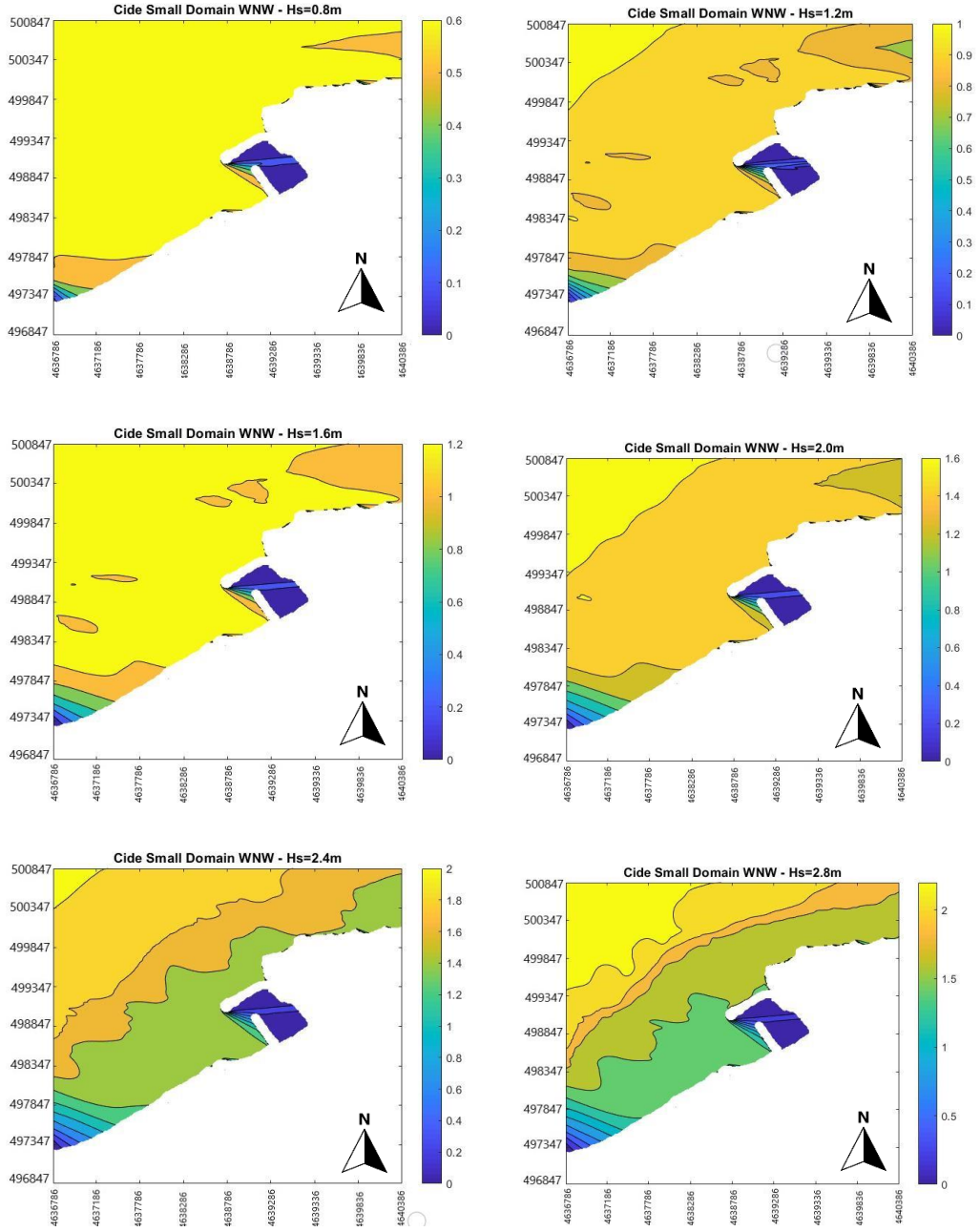

Figure B. 3 Cide Small Domain Model WNW Direction

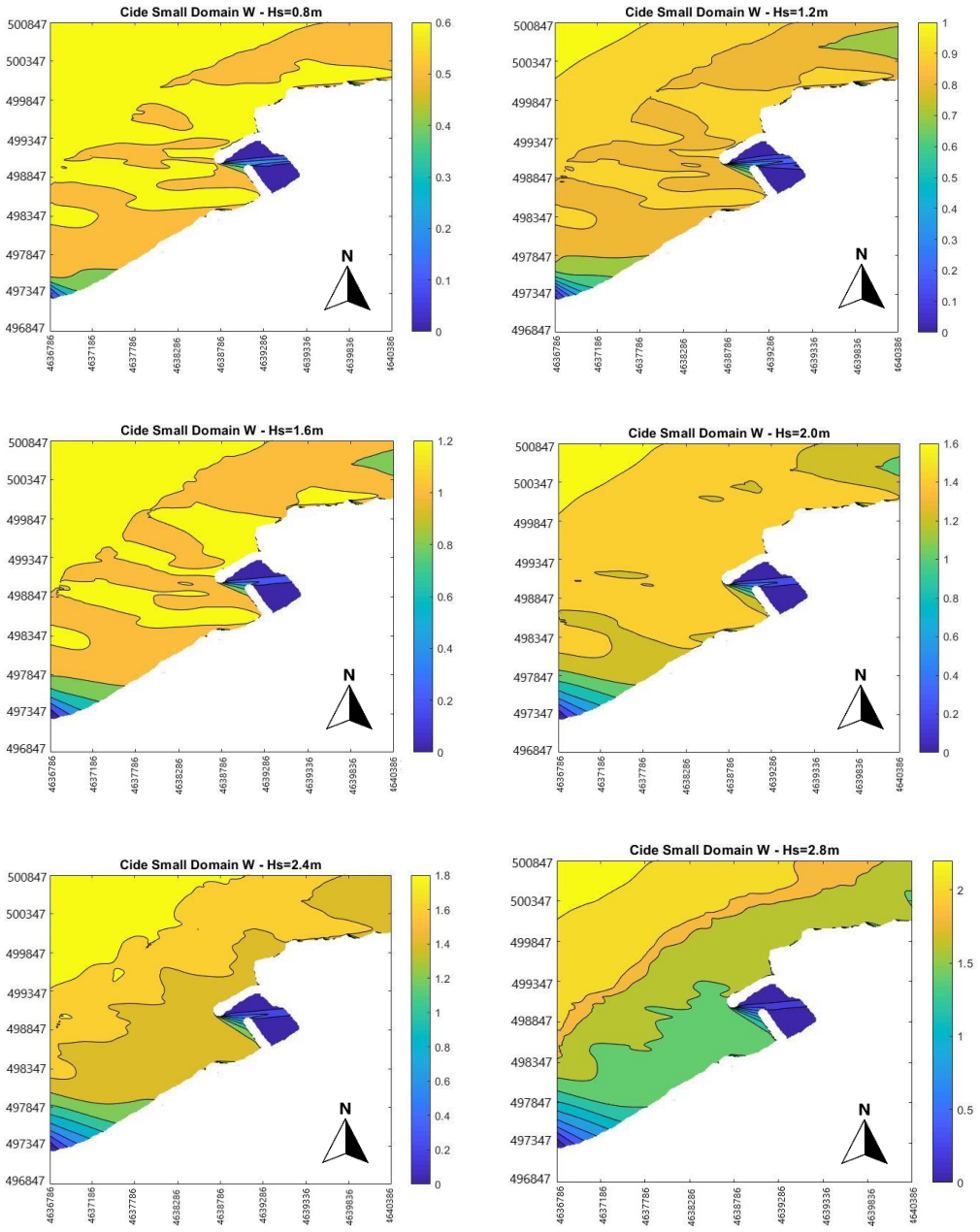

Figure B. 4 Cide Small Domain Model W Direction

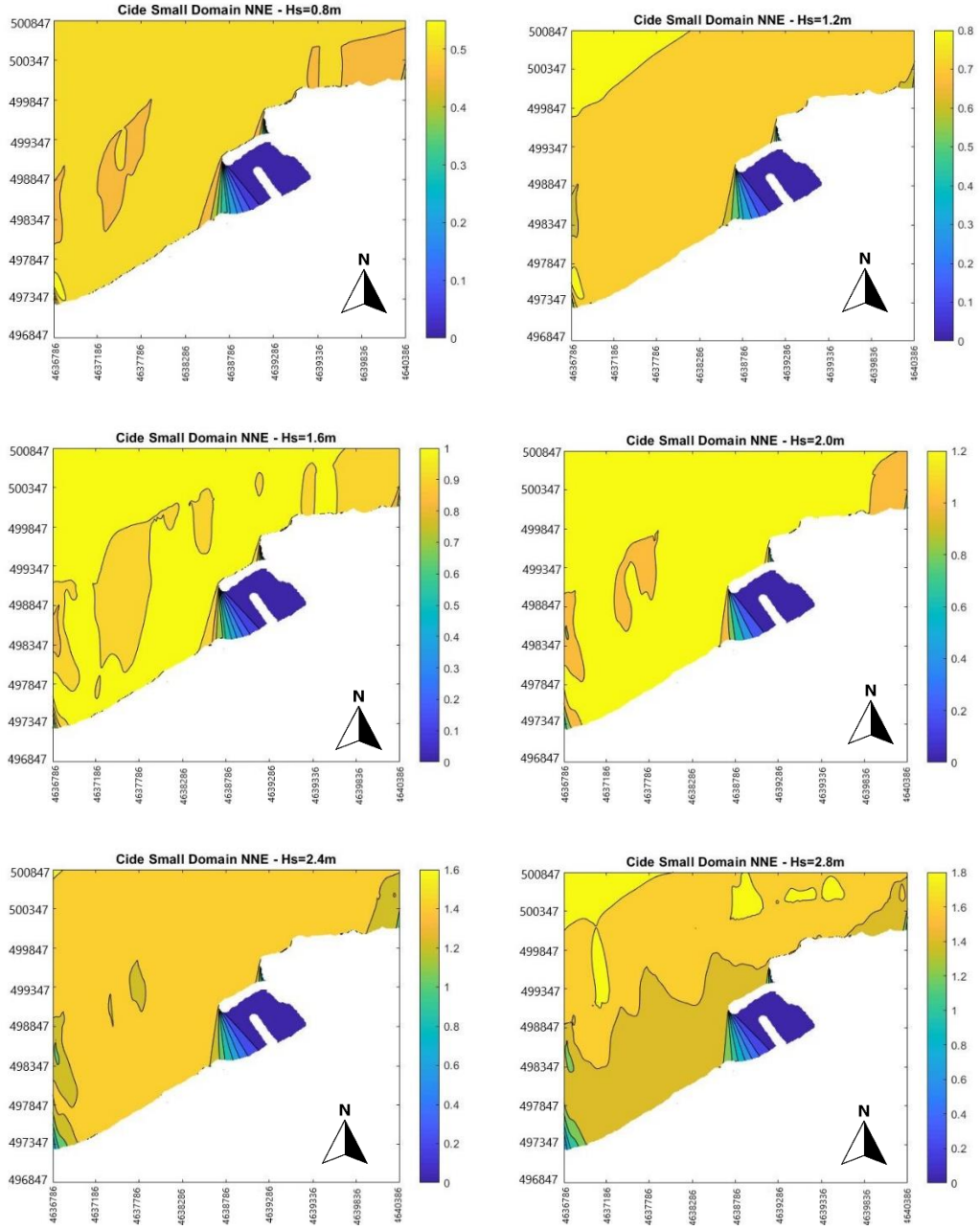

Figure B. 5 Cide Small Domain Model NNE Direction

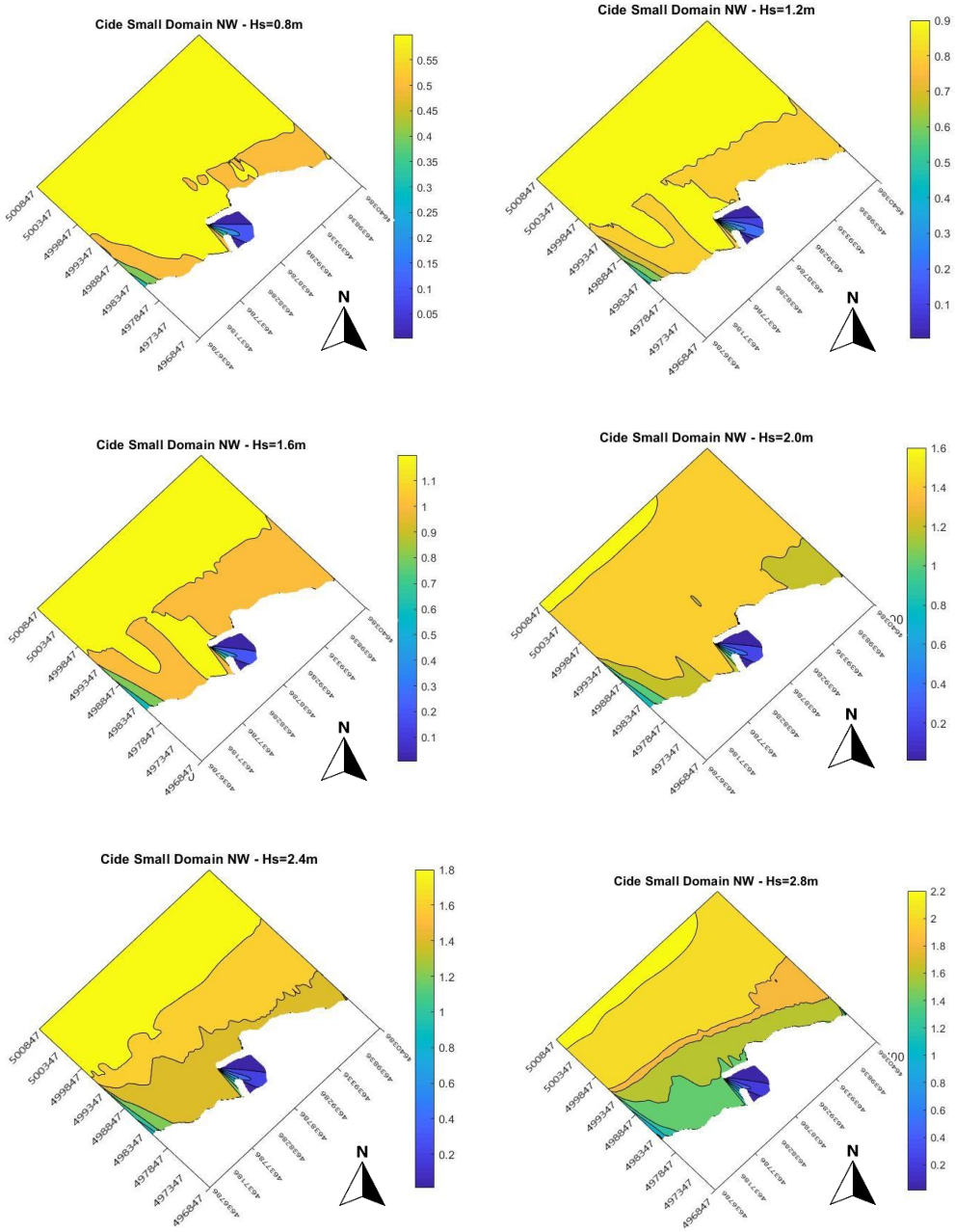

Figure B. 6 Cide Small Domain Model NW Direction

C. Amasra Small Domain, Wave Heights in SWAN Model Results

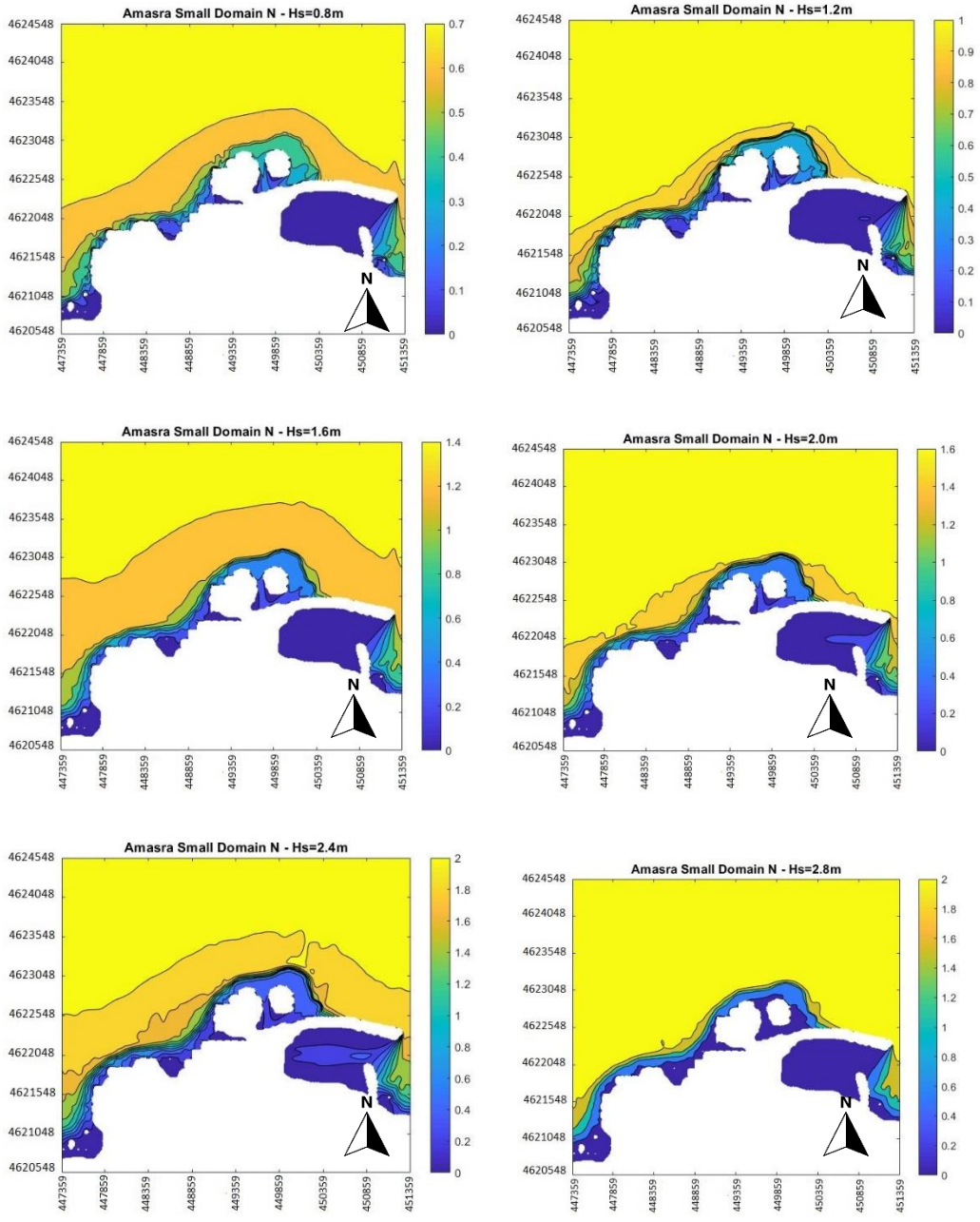

Figure C. 1 Amasra Small Domain Model N Direction

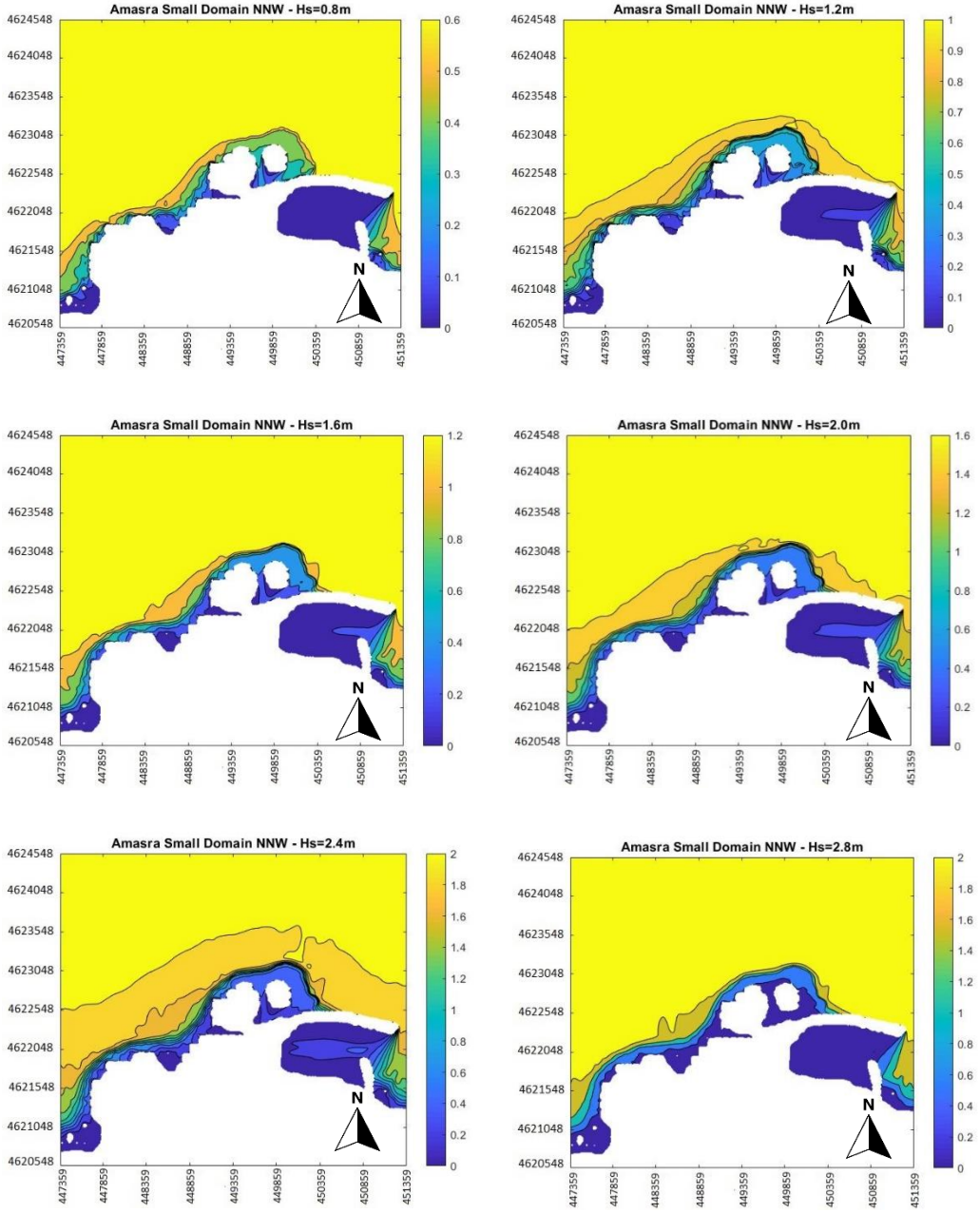

Figure C. 2 Amasra Small Domain Model NNW Direction

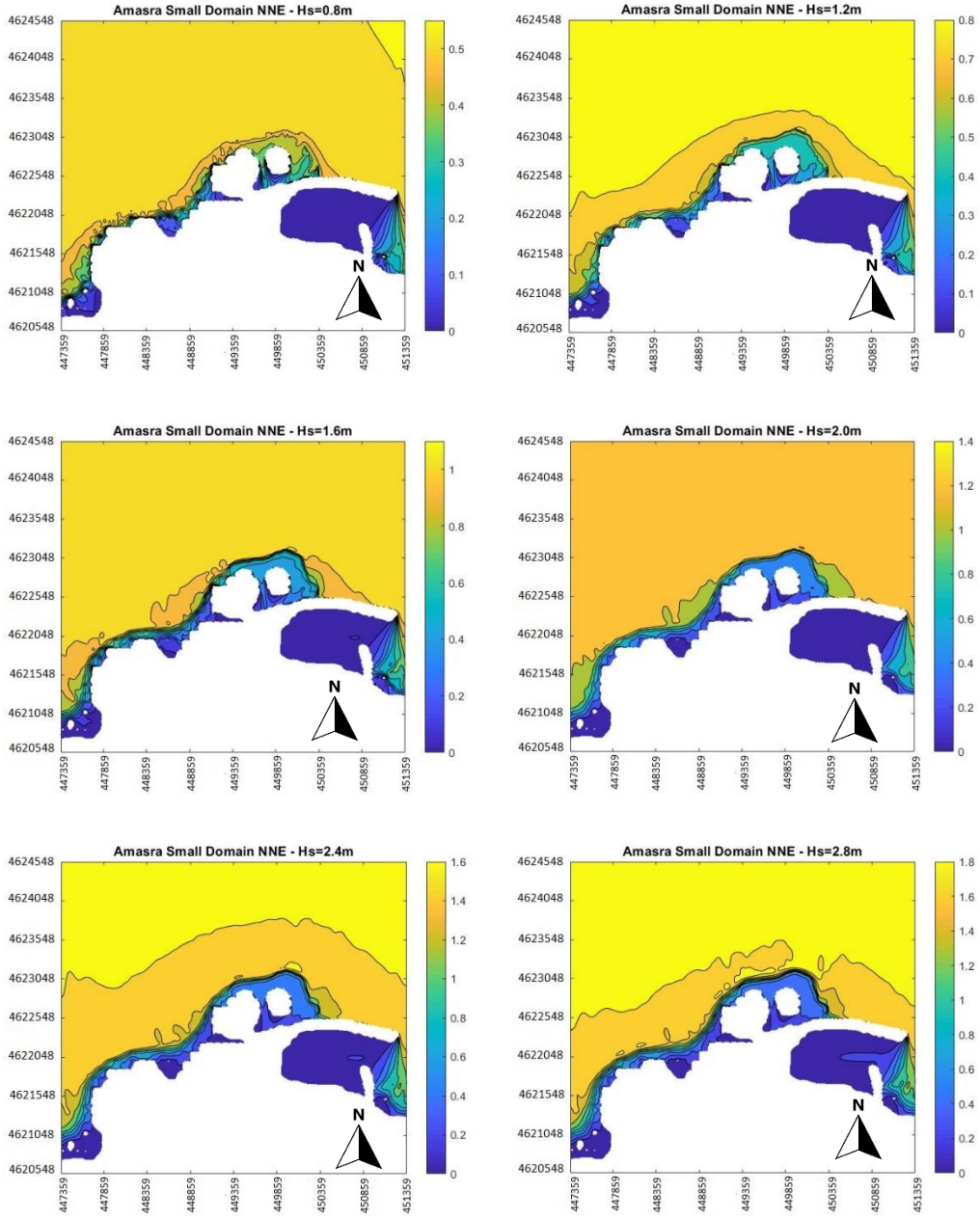

Figure C. 3 Amasra Small Domain Model NNE Direction

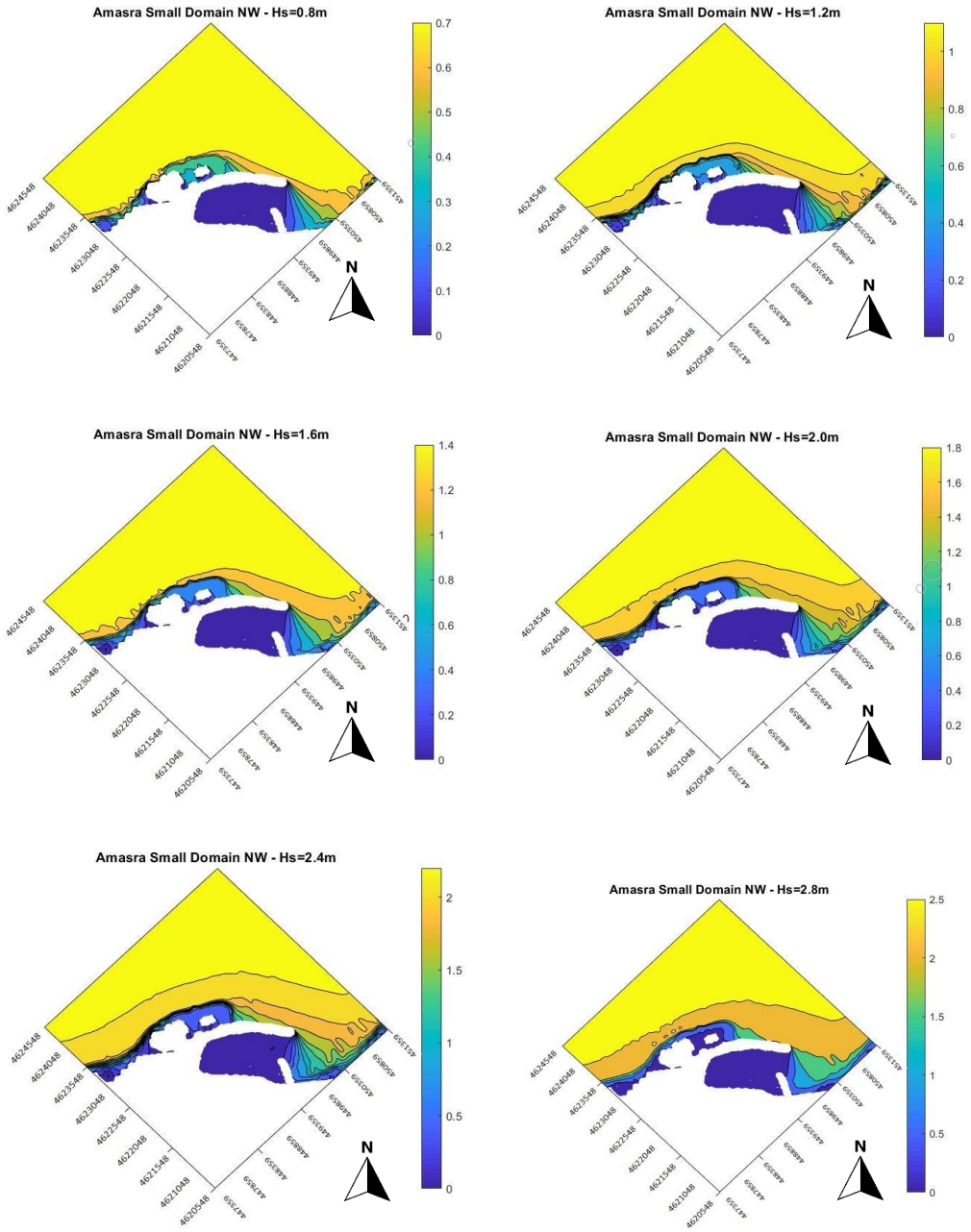

Figure C. 4 Amasra Small Domain Model NW Direction

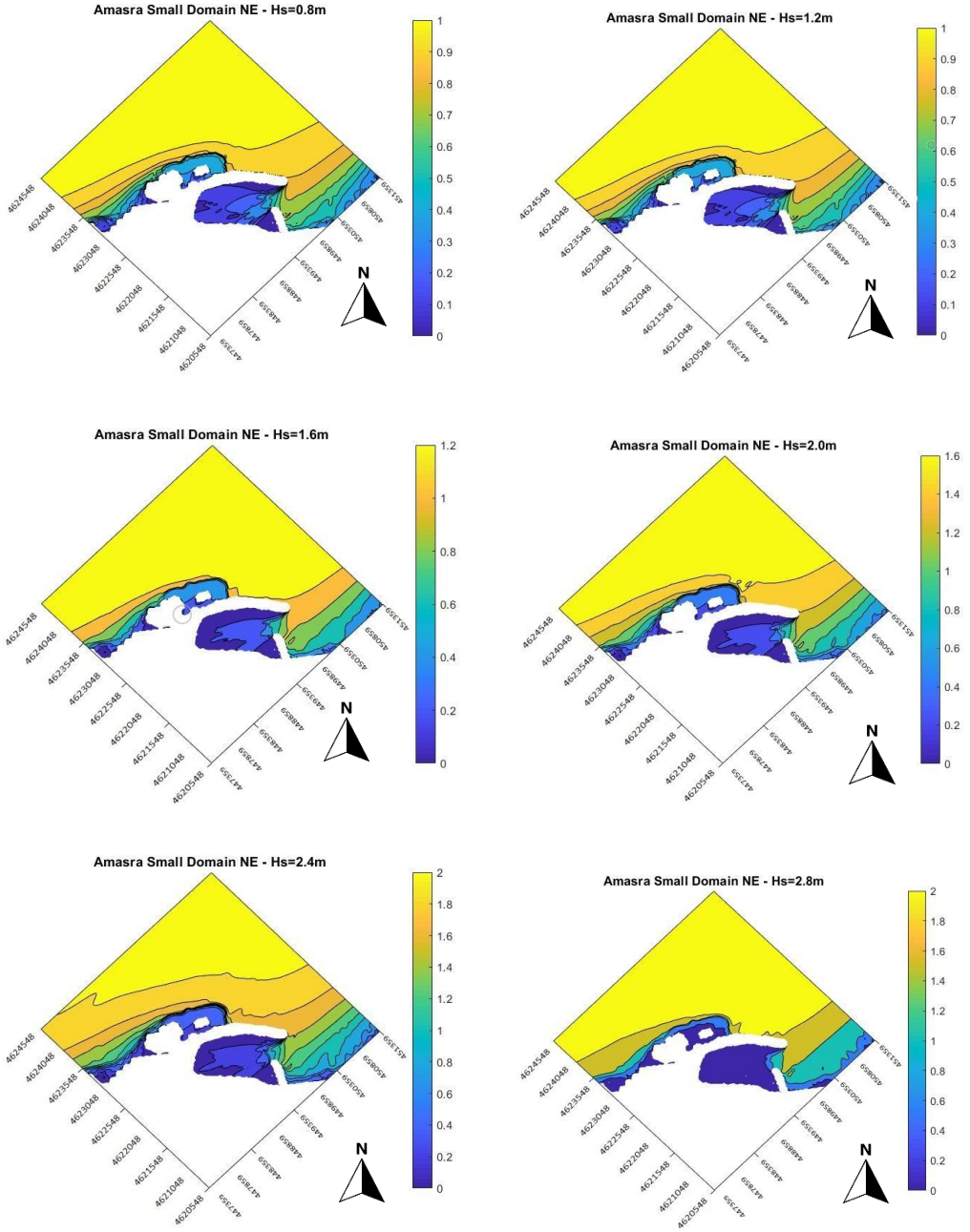

Figure C. 5 Amasra Small Domain Model NE Direction

D. Kiyikoy Small Domain, Wave Heights in SWAN Model Results

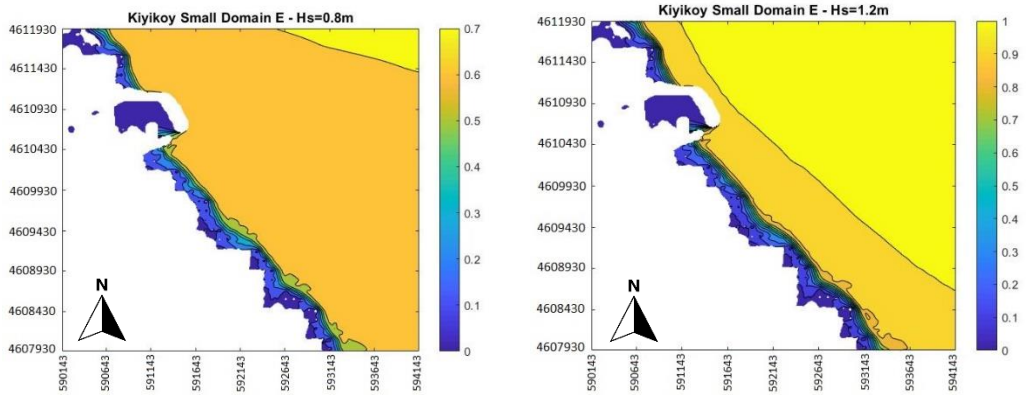

Figure D. 1 Kiyikoy Small Domain Model E Direction

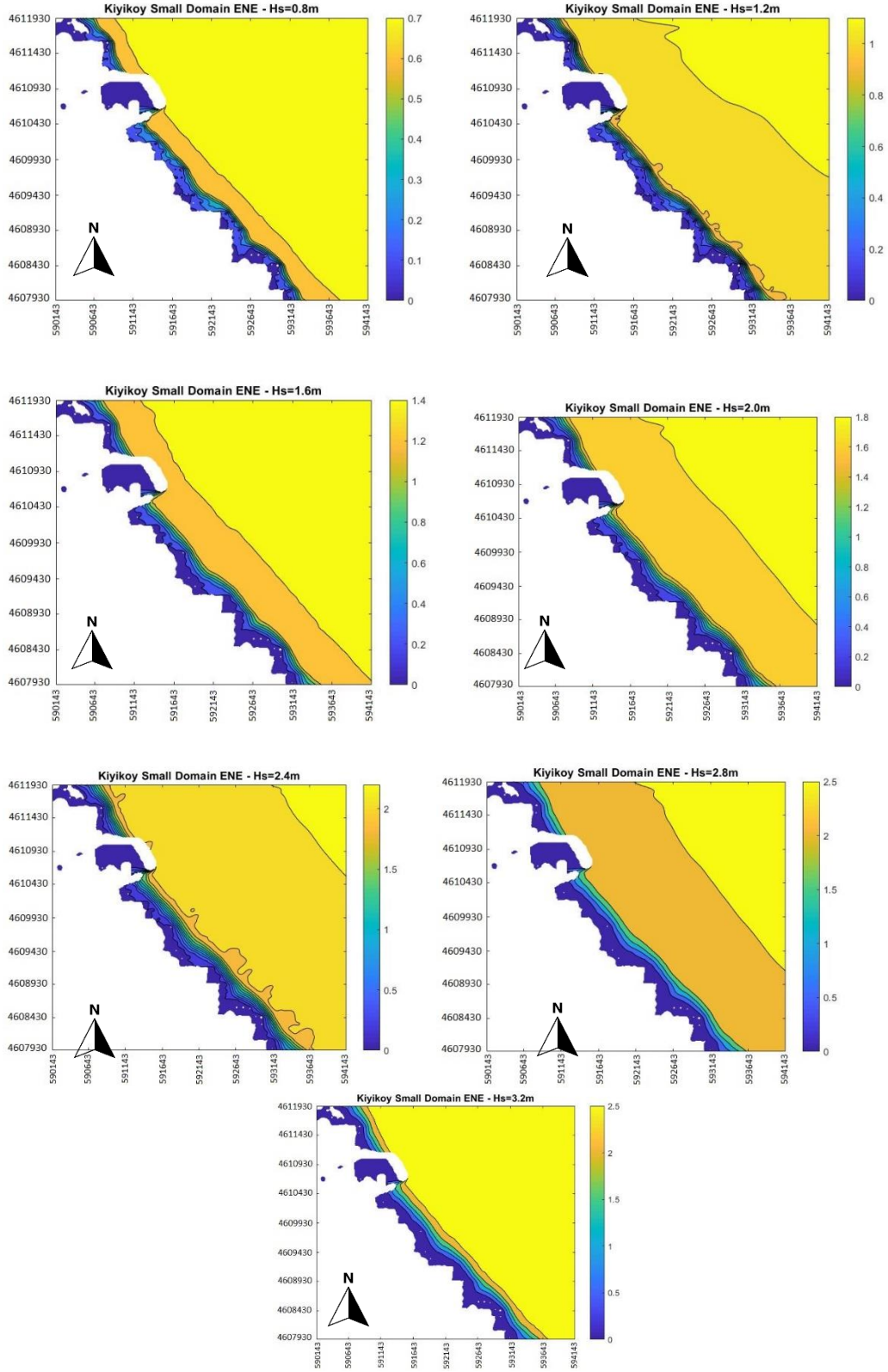

Figure D. 2 Kiyikoy Small Domain Model ENE Direction

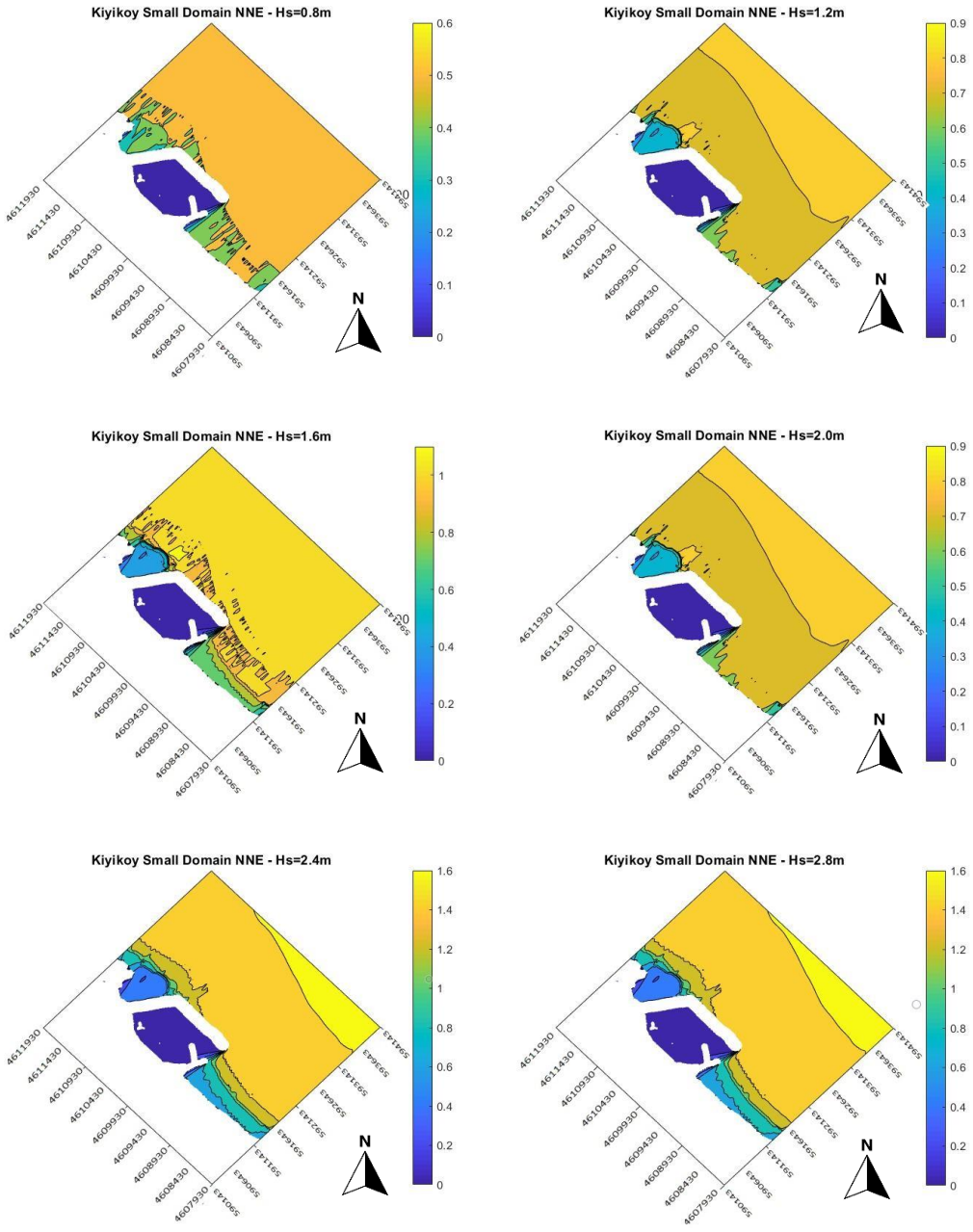

Figure D. 3 Kiyikoy Small Domain Model NNE Direction

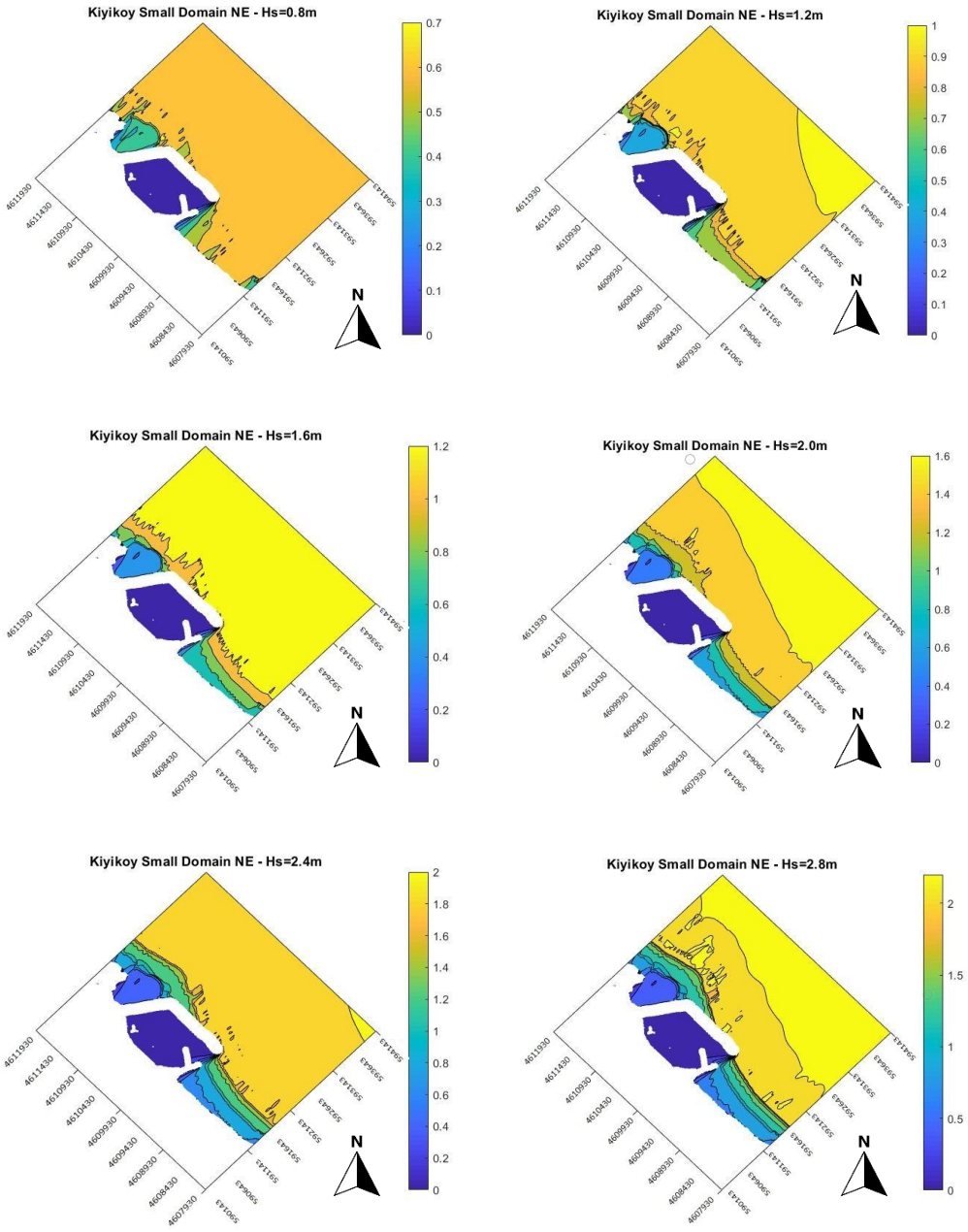

Figure D. 4 Kiyikoy Small Domain Model NE Direction

E. Cide Seasonal Wave Distribution

Table E. 1 Wave Height Distribution in Winter Seasons for 16 Directions in Hours, Cide (East Directions)

H / Dir	NNE	NE	ENE	E	ESE	SE	SSE	S
0	366	462	741	1132	387	160	116	84
0.4	1442	1862	2877	3256	973	542	541	494
0.8	1225	2234	2242	1713	167	148	184	217
1.2	720	1671	1575	739	25	21	27	72
1.6	507	1131	953	320	3	3	4	16
2	377	747	719	165	2	0	0	0
2.4	248	604	430	103	0	0	0	0
2.8	134	382	327	72	0	0	0	0
3.2	55	241	179	35	0	0	0	0
3.6	17	141	70	34	0	0	0	0
4	2	73	29	24	0	0	0	0
4.4	0	41	31	5	0	0	0	0
4.8	0	11	10	1	0	0	0	0
5.2	0	10	14	0	0	0	0	0
5.6	0	7	0	0	0	0	0	0
6	0	5	0	0	0	0	0	0
6.4	0	13	0	0	0	0	0	0
SUM	5093	9635	10197	7599	1557	874	872	883

Table E. 2 Wave Height Distribution in Winter Seasons for 16 Directions in Hours, Cide (West Directions)

H / Dir	SSW	SW	WSW	W	WNW	NW	NNW	N
0	145	243	307	304	232	316	333	302
0.4	541	816	2332	1982	1403	1483	1884	1752
0.8	297	603	2372	2098	1300	1558	1882	1630
1.2	104	330	1811	1624	822	1265	1447	947
1.6	21	75	1108	868	417	678	936	500
2	0	10	575	498	271	377	438	312
2.4	0	11	325	262	151	206	226	168
2.8	0	17	168	191	69	160	115	127
3.2	0	9	75	66	25	118	49	40
3.6	0	0	33	26	24	38	21	17
4	0	0	15	8	6	17	10	10
4.4	0	0	15	4	0	4	9	6
4.8	0	0	7	4	0	0	3	6
5.2	0	0	3	0	0	0	0	0
SUM	1108	2114	9146	7935	4720	6220	7353	5817

Table E. 3 Wave Height Distribution in Spring Seasons for 16 Directions in Hours, Cide (East Directions)

H / Dir	NNE	NE	ENE	E	ESE	SE	SSE	S
0	1522	2167	2378	2878	1028	344	193	199
0.4	1819	3352	4276	6096	985	310	252	211
0.8	978	1942	2579	3316	144	88	43	51
1.2	408	935	1423	1587	21	12	7	6
1.6	209	543	659	710	11	0	0	1
2	104	246	463	284	5	0	0	1
2.4	20	143	197	115	0	0	0	1
2.8	1	68	75	32	0	0	0	0
3.2	5	28	38	16	0	0	0	0
3.6	5	9	25	11	0	0	0	0
4	3	7	8	3	0	0	0	0
SUM	5074	9440	12121	15048	2194	754	495	470

Table E. 4 Wave Height Distribution in Spring Seasons for 16 Directions in Hours, Cide (West Directions)

H / Dir	SSW	SW	WSW	W	WNW	NW	NNW	N
0	216	351	1040	1385	1314	1221	1218	1076
0.4	239	660	2980	2604	1548	1565	1918	1633
0.8	68	265	1906	1617	876	931	1355	810
1.2	19	90	1079	782	373	437	626	403
1.6	7	26	495	298	166	193	280	219
2	0	8	245	94	52	122	86	77
2.4	0	10	128	68	44	20	43	33
2.8	0	9	22	17	12	2	24	15
3.2	0	11	12	6	7	3	14	7
3.6	0	0	11	2	4	2	5	4
4	0	0	5	15	11	2	0	2
4.4	0	0	0	0	2	0	0	0
SUM	549	1430	7923	6888	4409	4498	5569	4279

Table E. 5 Wave Height Distribution in Summer Seasons for 16 Directions in Hours, Cide (East Directions)

H / Dir	NNE	NE	ENE	E	ESE	SE	SSE	S
0	2607	2786	2248	1851	305	129	55	85
0.4	3780	5513	4547	3959	201	38	18	24
0.8	967	2648	2616	2709	24	7	7	8
1.2	168	785	924	1086	0	1	0	0
1.6	28	224	231	394	0	0	0	0
2	12	61	17	148	0	0	0	0
2.4	14	13	0	6	0	0	0	0
2.8	7	28	0	0	0	0	0	0
3.2	7	0	0	0	0	0	0	0
SUM	7590	12058	10583	10153	530	175	80	117

Table E. 6 Wave Height Distribution in Summer Seasons for 16 Directions in Hours, Cide (West Directions)

H / Dir	SSW	SW	WSW	W	WNW	NW	NNW	N
0	75	149	633	858	1391	1874	3156	2936
0.4	34	100	980	1927	2432	2995	4772	4172
0.8	9	26	472	1120	897	1169	1911	1427
1.2	0	7	270	363	386	432	830	469
1.6	0	9	89	133	179	205	261	63
2	0	0	36	86	60	86	57	10
2.4	0	0	8	24	27	37	12	3
2.8	0	0	12	20	16	16	3	0
3.2	0	0	4	16	27	13	2	0
3.6	0	0	1	12	19	6	1	0
4	0	0	0	6	2	5	0	0
4.4	0	0	0	5	5	5	0	0
4.8	0	0	0	2	0	0	0	0
SUM	118	291	2505	4572	5441	6843	11005	9080

Table E. 7 Wave Height Distribution in Fall Seasons for 16 Directions in Hours, Cide (East Directions)

H / Dir	NNE	NE	ENE	E	ESE	SE	SSE	S
0	883	1237	1622	2097	543	145	93	121
0.4	2077	3562	4184	4983	591	333	233	140
0.8	1344	2637	3335	3130	137	66	74	78
1.2	714	1919	2237	1538	12	3	9	21
1.6	298	1141	1527	680	1	0	0	4
2	150	489	798	339	0	0	0	1
2.4	127	355	402	148	0	0	0	0
2.8	27	165	258	81	0	0	0	0
3.2	18	117	84	32	0	0	0	0
3.6	8	39	57	12	0	0	0	0
4	0	19	28	2	0	0	0	0
4.4	0	1	0	0	0	0	0	0
SUM	5646	11681	14532	13042	1284	547	409	365

Table E. 8 Wave Height Distribution in Fall Seasons for 16 Directions in Hours, Cide (West Directions)

H / Dir	SSW	SW	WSW	W	WNW	NW	NNW	N
0	117	176	381	423	374	460	875	955
0.4	170	310	1429	1503	1055	1466	2490	2187
0.8	77	137	1148	1215	1030	1245	1991	1562
1.2	37	79	631	739	627	685	1311	867
1.6	8	34	365	490	341	494	569	409
2	4	11	193	281	213	317	321	163
2.4	0	5	115	185	119	153	200	74
2.8	0	2	60	109	50	78	80	39
3.2	0	0	39	66	18	23	48	9
3.6	0	0	26	17	9	10	21	0
4	0	0	9	12	10	3	7	0
4.4	0	0	14	7	1	3	9	0
4.8	0	3	5	2	2	4	4	0
5.2	0	0	3	1	4	0	0	0
5.6	0	0	0	1	1	0	0	0
6	0	0	0	5	2	0	0	0
6.4	0	0	0	3	0	0	0	0
SUM	413	757	4418	5059	3856	4941	7926	6265

F. Overtopping WEC Design Algorithm

```
%% Overtopping WEC Design

%Wave First Input
Hs=2.04;
Tp=5.80;
g=9.81;
ro=100;

%Dimensions of Overtopping WEC
tanAlpha=2/5;
n1=100;
n2=27; % total number of wave conditions
Rc=linspace(0.85,Hs+1,n1);
%h1 depth of the reservoir
hs=0.85; %water column inside the pipe above turbine
for i=1:n1
h1(i)=Rc(i)-hs;
H(i)=h1(i);%+hs
end
Total_nHydro=zeros(n1);
P_output=linspace(0,0,n1);

Hs=[0.63,0.93,1.21,1.5,1.79,2.16,2.6,3.0,3.4,0.70,1.04,1.37,1.68,2.02,2.33,2.59,3.0,
3.4,0.62,0.91,1.17,1.44,1.69,1.98,2.6,3.0,3.4];% Kiyikoy Hs
f=[8.3,4.6,2.8,1.6,1.0,1.2,0,0,0,4.9,2.0,0.9,0.4,0.2,0.1,0.1,0,0,0,0,0,0,0,0,0,0];%Ki
yikoy frequency of appearance
Steepness=0.040;
```

```
for i=1:n1
for ii=1:n2

Tp=((1/Steepness)*Hs/1.56).^0.5;
%% Overtopping discharge
c1=0.2;
c2=2.6;
GamaF=1; %friction factor, 1 for concrete and rock
GamaB=1; %berm factor, 1 in case of no berm
Beta=0; %approach angle at the toe of breakwater
GamaBeta=1-0.0022*Beta; %angle of wave attack factor
q(i,ii)=sqrt(g*Hs(ii)^3)*c1*exp(c2*(Rc(i)/Hs(ii))*(1/GamaF*GamaBeta*GamaB))
;

% Hydraulic Efficiency
Phydro(i,ii)=ro*g*q(i,ii)*Rc(i); %Power collected from waves (W/m)
Pwave(i,ii)=((ro*g^2)/(64*pi))*Hs(ii)^2*Tp(ii); %The initial wave power (W/m)

nHydro(i,ii)=Phydro(i,ii)/Pwave(i,ii); %Hydrodynamic efficiency

%The power of the water turbine
Pk(i,ii)=nHydro(i,ii)*ro*g*q(i,ii)*H(i); %The power of the water turbine (W/m)
%Pk(i,ii)=(Rc(i)*64*pi/(Hmo(ii)^2*Tp(ii)))*ro*q(i,ii)^2*(H(i));%The power of the
water turbine (W/m)

% Annual Energy Performance
n_gen=0.45; %Performance of the electric generator
P_output_matrix(i,ii)=n_gen*Pk(i,ii)*f(ii)*24*365; %Annual Energy
Output(MWh/m)
```

```
P_output(i)=P_output_matrix(i,ii)+P_output(i);
Total_nHydro(i)=nHydro(i,ii)+Total_nHydro(i);
Efficiency(i)=Total_nHydro(i)/n2;
ReservoirCapacity(i)=q(i); %for 1 meter length
B(i)=ReservoirCapacity(i)/h1(i)+h1(i)/(2*tanAlpha);
end
end

for i=1:n1
   if P_output(i)==max(P_output)
   DesignRc=Rc(i);
   DesignReservoirCapacity=ReservoirCapacity(i);
   Design_h1=h1(i);
   Design_B=DesignReservoirCapacity/Design_h1+Design_h1/(2*tanAlpha);
   end
end
Design_P_output_Annual=max(P_output); %W/m
Design_P_output_Hourly=Design_P_output_Annual/(24*365); %Wh/m
Design_P_output_Annual_100m=Design_P_output_Annual*100;
```